NASA CONTRACTOR REPORT

NASA CR-1313

THEORETICAL INVESTIGATION OF THE COMPOSITION AND LINE EMISSION CHARACTERISTICS OF ARGON-TUNGSTEN AND ARGON-URANIUM PLASMAS

by N. L. Krascella

Prepared by
UNITED AIRCRAFT CORPORATION
East Hartford, Conn.
for

NATIONAL AERONAUTICS AND SPACE ADMINISTRATION • WASHINGTON, D. C. • MARCH 1969

NASA CR-1313

THEORETICAL INVESTIGATION OF THE COMPOSITION AND LINE EMISSION CHARACTERISTICS OF ARGON-TUNGSTEN AND ARGON-URANIUM PLASMAS

By N. L. Krascella

Issued by Originator as Report No. G-910092-10

Prepared under Contract No. NASw-847 by
UNITED AIRCRAFT CORPORATION
East Hartford, Conn.

for

NATIONAL AERONAUTICS AND SPACE ADMINISTRATION

For sale by the Clearinghouse for Federal Scientific and Technical Information
Springfield, Virginia 22151 – CFSTI price $3.00

FOREWORD

An exploratory experimental and theoretical investigation of gaseous nuclear rocket technology is being conducted by the United Aircraft Research Laboratories under Contract NASw-847 with the joint AEC-NASA Space Nuclear Propulsion Office. The Technical Supervisor of the Contract for NASA is Captain C. E. Franklin (USAF). Results of portions of the investigation conducted during the period between September 15, 1967 and September 15, 1968 are described in the following five reports (including the present report) which comprise the required eighth Interim Summary Technical Report under the Contract:

1. Kendall, J. S., W. C. Roman, and P. G. Vogt: Initial Radio-Frequency Gas Heating Experiments to Simulate the Thermal Environment in a Nuclear Light Bulb Reactor. United Aircraft Research Laboratories Report G-910091-17, September 1968.

2. Mensing, A. E. and L. R. Boedeker: Theoretical Investigation of R-F Induction Heated Plasmas. United Aircraft Research Laboratories Report G-910091-18, September 1968.

3. Krascella, N. L.: Theoretical Investigation of the Composition and Line Emission Characteristics of Argon-Tungsten and Argon-Uranium Plasmas. United Aircraft Research Laboratories Report G-910092-10, September 1968. (present report)

4. Marteney, P. J., A. E. Mensing, and N. L. Krascella: Experimental Investigation of the Spectral Emission Characteristics of Argon-Tungsten and Argon-Uranium Induction Heated Plasmas. United Aircraft Research Laboratories Report G-910092-11, September 1968.

5. Latham, T. S.: Nuclear Studies of the Nuclear Light Bulb Rocket Engine. United Aircraft Research Laboratories Report G-910375-3, September 1968.

Theoretical Investigation of the Composition and Line Emission Characteristics of Argon-Tungsten and Argon-Uranium Plasmas

TABLE OF CONTENTS

Theoretical Investigation of the Composition and Line Emission Characteristics of Argon-Tungsten and Argon-Uranium Plasmas

SUMMARY

A theoretical investigation was conducted to determine the composition and integrated line emission characteristics of various ionization species of tungsten, uranium, and argon. The study was made to facilitate radiant heat transfer analysis in the seeded propellant and nuclear fuel regions of gaseous-core nuclear rocket engines and to provide a basis of comparison for a concurrent experimental program designed to examine line emission characteristics of gaseous tungsten and uranium over a wide spectral range.

Estimates were made of the composition as a function of temperature for mixtures of Ar with tungsten hexafluoride and uranium hexafluoride using an existing UARL machine composition program to ascertain the decomposition products of WF_6 and UF_6. For temperatures greater than 5000 deg K, a machine program was written to describe the concentrations of heavy-metal ionization species present based on the Saha equations. Calculations were made for mass ratios of W or U to Ar of 1.0×10^{-3}, 1.0×10^{-5}, and 1.0×10^{-7} for a total pressure of 1.0 atm and for temperatures in the range from 3000 deg K to 10,000 deg K.

Data generated with the composition routines were used as input to a line intensity machine program designed to compute the integrated line intensities for classified W, U, and Ar spectral lines of known or estimated oscillator strength. Lines from two ionization species of Ar (neutral argon and singly ionized argon) as well as the corresponding species in W and U were considered in the line intensity program. Integrated line intensities summed over wavelength intervals of 100 Å were calculated in the spectral region between wavelengths of 1700 Å and 10,000 Å. W-to-Ar or U-to-Ar mass ratios of 1.0×10^{-3}, 1.0×10^{-5}, and 1.0×10^{-7} were considered at temperatures of 5000, 7000, and 9000 deg K. The total pressure in all cases was 1.0 atm.

CONCLUSIONS

1. Ionization of argon in an Ar-WF_6 or Ar-UF_6 system tends to suppress ionization of the heavy-metal species.

2. At temperatures up to 9000 deg K, lines from neutral argon (ArI) are the principal contributors to line emission in Ar.

3. At a temperature of 5000 deg K and for heavy metal-to-Ar mass ratios less than 1.0×10^{-3}, WI and UI lines are the principal contributors to line emission in Ar-WF_6 and Ar-UF_6 systems. At temperatures greater than 5000 deg K and for mass ratios greater than 1.0×10^{-3}, WII and UII lines tend to dominate emission in W and U.

4. Total emission from all W lines exceeds that for all U lines at fixed temperatures and mass ratios of heavy metal-to-Ar in Ar-WF_6 and Ar-UF_6 systems. In addition total emission from all lines in Ar, W, or U increases with an increase in temperature.

INTRODUCTION

Radiation of energy in gaseous media and control of such energy is of general interest for many engineering and scientific problems and is of particular interest in gaseous-core nuclear rocket engine concepts such as those described in Refs. 1 and 2. The functioning of such engines depends upon the generation of energy by nuclear fission and the radiative transfer of the fission energy to a surrounding propellant, usually hydrogen seeded with carbon or a heavy-atom metal. In feasibility studies of these engine concepts, knowledge of the composition and spectral emission and absorption characteristics of the various gases present is required in order to estimate the effectiveness of the radiative transfer process (Refs. 3 and 4).

A number of analytical studies have been conducted at UARL to ascertain the emission and absorption properties of hydrogen (Refs. 5 and 6) and various heavy-atom metal gases used as nuclear fuel or seeding agents (Refs. 6, 7, and 8). In early studies of the spectral properties of the heavy-atom metals, the bound-bound regions of the spectra were considered as continua or broad bands. Detailed computation of the spectral distribution of energy for classified lines of the heavy-atom metals was not made. In addition, no estimates were made in these preliminary studies of the integrated line intensities for classified lines of heavy-atom metals (because of the complexity of the spectra).

In view of the foregoing discussion, the objective of this study was to calculate the integrated line intensities of classified lines of known transition probabilities for two heavy-atom gases, tungsten and uranium. This information is of use in determining radiation characteristics of gaseous nuclear rockets and also serves as a basis for comparison with concurrent experimentally determined line intensity distributions of Ar, W, and U measured in RF-heated, argon-heavy metal hexafluoride systems (Ref. 9).

COMPOSITION OF ARGON-HEAVY METAL HEXAFLUORIDES

A prerequisite to the examination of the spectral properties of any atomic species is a knowledge of the number density of absorbing species in various quantum states as a function of temperature. Estimates of these number density distributions were made for each of the constituents in mixtures of argon and tungsten or uranium hexafluoride. Composition calculations were made for these systems in order to provide a basis of comparison for a concurrent experimental study of line emission characteristics of different ionization species of tungsten and uranium. An existing UARL machine program (Ref. 10) was used to compute the decomposition products of the heavy-metal hexafluorides in an argon matrix as a function of temperature for various heavy metal-to-argon mass ratios. Calculations using this machine program were carried out for a number of mass ratios and for temperatures up to approximately 5000 deg K. The UARL composition routine, previously mentioned, included only the first two ionization species of tungsten and uranium; however, preliminary estimates indicated that WIII (doubly ionized tungsten) was evident in quantities comparable to WI and WII at a temperature greater than approximately 8000 deg K. Similar preliminary estimates for uranium indicated that UIII (doubly ionized uranium) became evident in quantities comparable to UI and UII at a temperature greater than approximately 4000 deg K; therefore a separate composition program was written to describe the ionization of tungsten and uranium mixed with argon in terms of the first three ionization species of each heavy metal.

Partition Functions

Calculation of ionization processes in atomic species requires knowledge of the partition functions of each ionization species as a function of temperature. While Ref. 11 contains the partition functions for WI, WII, UI, and UII for a temperature of 5100 deg K, data of this type are not generally available over the extended temperature range considered in this report. The partition functions of WI, WII, UI, and UII were estimated using the following equation by direct summation of the exponential functions at various temperatures:

$$Z_i = \sum_n g_{i,n} \exp -(E_{i,n}/kT) \qquad (1)$$

where Z_i is the partition function for a given ionization species i, $g_{i,n}$ is the statistical weight of level n, $E_{i,n}$ is the energy of level n, k is the Boltzmann constant, and T is the absolute temperature. The number of energy levels considered for each ionization species is listed together with the corresponding reference in Table I. Insufficient energy level data were

available to justify calculation of the partition function of WIII and UIII by direct summation of the exponential function defined in Eq. (1); therefore it was assumed in subsequent calculations that the partition functions for WIII and UIII were identical to WII and UII, respectively. The calculated partition functions for WI and WII are plotted in Fig. 1 and for UI and UII in Fig. 2 as a function of temperature. The partition functions reported in Ref. 11 at a temperature of 5100 deg K are indicated on Fig. 1 for WI and WII and on Fig. 2 for UI and UII. The agreement between calculated values of the partition function and those reported in Ref. 11 is very good. Partition functions for ArI and ArII were obtained from current literature and are listed as a function of temperature in Table II.

Ionization in Argon, Tungsten and Uranium

The basic reactions describing the ionization in an Ar-W or Ar-U systems are:

$$\mathrm{ArI} = \mathrm{ArII} + e^- \tag{2}$$

$$\mathrm{BI} = \mathrm{BII} + e^- \tag{3}$$

$$\mathrm{BII} = \mathrm{BIII} + e^- \tag{4}$$

where BI represents WI or UI; BII represents WII or UII; and BIII represents WIII or UIII.

The total pressure is given by Dalton's law of partial pressures:

$$P_{TOTAL} = P_{ArI} + P_{ArII} + P_{BI} + P_{BII} + P_{BIII} + P_{e^-} \tag{5}$$

where P_{e^-} is the electron partial pressure. Electricity neutrality is described by the following equation:

$$P_{e^-} = P_{ArII} + P_{BII} + 2P_{BIII} \tag{6}$$

The pertinent Saha equations are:

$$\frac{P_{ArII}\,P_{e^-}}{P_{ArI}} = 2\,\frac{(2\pi m_e)^{3/2}}{h^3}\,(kT)^{5/2}\,\frac{Z_{ArII}}{Z_{ArI}}\,\exp -(I'_{ArI}/kT) \tag{7}$$

$$\frac{P_{BII}\,P_{e^-}}{P_{BI}} = 2\,\frac{(2\pi m_e)^{3/2}}{h^3}\,(kT)^{5/2}\,\frac{Z_{BII}}{Z_{BI}}\,\exp -(I'_{BI}/kT) \tag{8}$$

$$\frac{P_{B\,III}\,P_{e^-}}{P_{B\,II}} = 2\,\frac{(2\pi m_e)^{3/2}}{h^3}\,(kT)^{5/2}\,\frac{Z_{B\,III}}{Z_{B\,II}}\,\exp-(I'_{B\,II}/kT) \qquad (9)$$

where the subscripted P's represent the partial pressures of the different ionization species. The subscripted (I')'s represent the ionization potentials of the indicated ionization species. Values of the ionization potentials used in the machine program are listed together with the corresponding references in Table III. The quantity m_e is the mass of an electron; other symbols have been previously defined.

If the mass ratio is defined as follows:

$$F_B = \frac{MW_B\,(P_{B\,I} + P_{B\,II} + P_{B\,III})}{MW_{Ar}\,(P_{Ar\,I} + P_{Ar\,II})} \qquad (10)$$

the six equations necessary to determine the six unknown partial pressures, Eqs. (5) through (10), may be solved simultaneously for a fixed temperature, total pressure, and mass ratio. These equations were programmed for machine computation and were used to generate ionization composition data at temperatures greater than 5000 deg K. Below a temperature of 5000 deg K, the UARL composition machine program described in Ref. 10 was used to compute the decomposition of WF_6 and UF_6 in Ar. Typical composition data generated by these machine programs are graphically illustrated in Figs. 3 through 7 for Ar-WF_6 systems at temperatures between 3000 deg K and 10,000 deg K and for W-to-Ar mass ratios of 1.0×10^{-2} to 1.0×10^{-7}. Similar data were computed for Ar-UF_6 systems in the same temperature range and for the same mass ratios. The Ar-UF_6 data are shown in Figs. 8 through 12. All composition data were calculated for a total pressure of 1.0 atm.

Argon-Tungsten Hexafluoride Composition

In Fig. 3, it should be noted that tungsten exists as a condensed phase up to a temperature of approximately 3900 deg K in a system in which the mass ratio of W-to-Ar is 1.0×10^{-3}. Figures 3 through 7 show that the quantity of WIII present is small and becomes appreciable only at temperatures in excess of 8000 deg K. At a temperature of 10,000 deg K the partial pressures of WI and WIII are about equal but less than the partial pressure of WII by more than an order of magnitude. Since the ionization potential of ArI is 15.755 eV as compared to 7.98 eV for WI (see Table III) one would expect that the ionization of WI would control the partial pressure of electrons in the system up to that temperature at which the WI is almost completely ionized. This is in fact

demonstrated in Figs. 3 through 7. Ar does not significantly contribute to the electron partial pressure until near the completion of the first ionization in W. Subsequent increased ionization of ArI to ArII with increasing temperature causes a rise in the electron density and a consequent repression of the ionization of WI. This effect is shown in Figs. 3 through 7 by a marked decrease in the rate at which the partial pressure of WI decreases with increasing temperature. It also should be noted that the neutral fluorine atom, FI, is the principal fluorine component in the decomposition of WF_6.

Argon-Uranium Hexafluoride Composition

Details of the decomposition of UF_6 in Ar and subsequent ionization of U and Ar are shown graphically in Figs. 8 through 12. Comments similar to those for the Ar-WF_6 systems apply to the Ar-UF_6 systems; however, no condensed phase of U appears in any of the figures. In addition a small but relatively negligible contribution to the composition is made by the negative fluorine ion, F^- (see Figs. 8 and 9). Because the first ionization potential of UI (6.1 eV) is lower than that of WI (7.98 eV) (see Table III), the suppression of UI ionization by ionization of ArI is more pronounced than in W as indicated by the subsequent increase in the partial pressure of UI as the temperature increases. In contrast to W, the doubly ionized species UIII, is present in large amounts and is approximately a factor of 50 greater than that of UI at a temperature of 10,000 deg K.

Degree of Ionization in Tungsten and Uranium

The degree of ionization in W as a function of temperature is shown in Fig. 13 for various W-to-Ar mass ratios. Comparable data are present in Fig. 14 for U. It should be noted in both W and U that decreasing the amount of heavy metal (reducing the mass ratio) promotes ionization of the heavy metal; that is, ionization of WI or UI is complete at increasingly lower temperatures as the mass ratio is decreased from a value of 1.0×10^{-3} to 1.0×10^{-6}. This is a result of the solution of the composition equations which show that the degree of ionization is inversely dependent upon the total mass of heavy metal present.

INTEGRATED LINE INTENSITIES IN ARGON, TUNGSTEN, AND URANIUM

Detailed mathematical analysis of the intensity of all significant emission lines of material such as W or U is not possible at present because of the lack of adequate knowledge of line profiles and line half-widths. Similarly, exact knowledge of prerequisite data such as energy levels and transition probabilities is usually lacking except for a relatively small fraction of the total number of lines attributed to a given ionization species. However, lines of known wavelength, energy levels, and transition probability generally represent a major fraction of the energy emitted in the bound-bound region of the spectrum of a given species. Although details of the spectral distribution of emitted energy for these lines are not readily calculable, knowledge of the wavelength, energy levels and transition probabilities does allow estimation of integrated line intensities. Thus, analysis of the integrated intensities for such lines does give considerable insight into the spectral distribution of emitted energy in the bound-bound spectral region.

Mathematical Analysis

The total power radiated by a single line per unit volume, per unit solid angle and per unit wavelength interval is given by (Ref. 22):

$$I_\lambda = \frac{hc}{4\pi} \phi_\lambda A_{n,m} N_n \tag{11}$$

where I_λ is the emitted intensity or power radiated; $A_{n,m}$, the spontaneous emission probability for the transition from level n to level m; N_n, the number density of emitting atoms or ions in the upper state n; λ, the wavelength of the radiation and ϕ_λ the shape function or line profile. The quantities h and c are the usual physical constants. The line profile is normalized to unity, such that:

$$\int_{\text{line}} \phi_\lambda \, d\lambda \equiv 1 \tag{12}$$

Thus, the total power radiated by a line per unit volume and per unit solid angle, (the integrated intensity of a line), is given by the integral of Eq. (11):

$$I = \int I_\lambda \, d\lambda = \frac{hc \, A_{n,m} \, N_n}{4\pi\lambda} \tag{13}$$

If the system is in thermodynamic equilibrium then Boltzmann statistics apply and the density of emitters in the upper state, N_n, is given by:

$$N_n = \frac{N_i}{Z_i} g_{i,n} \exp -(E_{i,n}/kT) \tag{14}$$

Thus, the final expression for integrated line intensities is:

$$I = \int I_\lambda \, d\lambda = \frac{hc}{4\pi} \frac{g_{i,n} A_{n,m}}{\lambda} \frac{N_i}{Z_i} \exp -(E_{i,n}/kT) \tag{15}$$

where $g_{i,n}$ is the statistical weight of the upper level, n; N_i, the number density of ionization species i in all quantum states; Z_i, the corresponding partition function; $E_{i,n}$, the energy of the upper level, n, for the transition; and T, the absolute temperature. The Boltzmann constant is represented by k. Equation (15) was programmed for machine computation and subsequently summed for all lines in wavelength intervals of 100 Å as indicated by the following equation:

$$I_{\Delta\lambda} = \sum_{100\text{Å}} \int I_\lambda \, d\lambda \tag{16}$$

The computer program for integrated line intensities, summarized mathematically by Eqs. (15) and (16), required as input the number density and partition functions for the ionization species of interest. These input quantities were derived from the composition routines previously discussed. In addition, the integrated line intensity program required a listing of energy levels, wavelengths, statistical weights and transition probabilities. These data were provided for ArI, ArII, WI, WII, UI, and UII. Since little or no data for WIII or UIII were available in the current literature, these species were not included in the machine program. Table I summarizes the wavelength regions covered for each ionization species studied as well as the total number of lines and energy levels used in the program. Also indicated in Table I are the numerous references from which the significant spectroscopic data were obtained.

The standard source of spectroscopic quantities for non-gaseous elements, Ref. 11, lists transition probabilities for 108 classified lines of WII and 326 classified lines of UI. Experimental intensity results reported in Ref. 14 for WII lines and in Ref. 15 for UI lines were used to estimate transition probabilities for 1961 additional lines in WII and 833 additional lines in UI. Thus, the line intensity program ultimately included a total of 2069 classified lines of WII and 1159 classified lines of UI.

Integrated line intensities, summed over wavelength intervals of 100 Å were computed for ArI, ArII, WI, WII, UI, and UII at temperatures of 5000, 7000, and 9000 deg K at a total pressure of 1.0 atm. W-to-Ar and U-to-Ar mass ratios considered were 1.0×10^{-3}, 1.0×10^{-5}, and 1.0×10^{-7}.

Line Density Distributions

The total number of classified lines with known or estimated transition probabilities used for each ionization species studied are listed in Table I as previously indicated. The number distribution of these lines with wavelength is illustrated in Fig. 15 as the number of lines in wavelength intervals of 100 Å as a function of the wavelength at the center of the interval for ArI and ArII. Examination of Fig. 15 shows that the distribution of lines for ArI is essentially symmetrical and centered at a wavelength of approximately 6000 Å. No line data are available for wavelengths less than approximately 3500 Å or for wavelengths greater than 9800 Å. Figure 15 also indicates that only 23 lines of ArII have been assessed for transition probabilities. Similar data are represented in Fig. 16 for WI and WII classified lines of measured or estimated transition probabilities. The distribution curves for WI and WII tend to rise sharply from wavelengths between 1000 to 2000 Å, peak at approximately 2500 Å, and diminish slowly beyond a wavelength of approximately 4000 Å to a terminal value in the infrared at approximately 9000 Å. It should be noted that the data for WII represent the results obtained after estimating transition probabilities for about 2000 lines as discussed previously.

In Fig. 17, comparable results are presented for UI and UII line data. As in the case of WII, the UI line data are the result of estimating transition probabilities for approximatly 800 classified lines.

Integrated Line Intensity Results

Integrated line intensities were calculated for ArI, ArII, WI, WII, UI, and UII and subsequently summed over wavelength intervals of 100 Å. These data were computed at temperatures of 5000, 7000, and 9000 deg K and for W-to-Ar and U-to-Ar mass ratios of 1.0×10^{-3}, 1.0×10^{-5}, and 1.0×10^{-7}. All line intensity data were calculated for a pressure of 1.0 atm.

Argon

The integrated line intensity data for ArI, summed over wavelength intervals of 100 Å, are graphically illustrated in Figs. 18, 19, and 20 for temperatures of 5000, 7000, and 9000 deg K respectively. Similar results are shown for the limited number of ArII lines in Fig. 21, 22, and 23. Since the Ar composition is essentially independent of the heavy metal-to-argon mass ratio, the results in Figs. 18 through 23 are representative of ArI or ArII integrated intensities for any heavy atom-to-Ar mass ratio.

Figures 18, 19, and 20 show the relative increase in intensity of the ArI lines with increasing wavelength. Also exhibited on each figure is the total intensity of all lines calculated for ArI. The total intensity of all lines in ArI increases from a value of 1.48×10^{-6} watt/cm^3 - sr at a temperature of 5000 deg K to a value of 6.89×10^{-1} watt/cm^3 - sr at a temperature of 9000 deg K. This enhancement in total intensity of all lines is attributable to the increased population of various quantum states of ArI as the temperature is raised.

Although much less line data are represented in Figs. 21, 22, and 23 for ArII lines, the same trends are observed as in the ArI data. In ArII, the total intensity of all lines increases markedly from a value of 1.92×10^{-20} watt/cm^3 - sr at a temperature of 5000 deg K to a value of 1.85×10^{-6} watt/cm^3 - sr at a temperature of 9000 deg K. The very pronounced increase in total intensity is primarily the result of ionization of ArI to ArII.

Tungsten

The integrated line intensities, summed over wavelength intervals of 100 Å, for WI and WII are shown in Figs. 24, 25, and 26 (at temperatures of 5000, 7000, and 9000 deg K respectively) as a function of the wavelength at the center of the 100 Å interval. These results are for a W-to-Ar mass ratio of 1.0×10^{-3}. Similar results are plotted in Figs. 27, 28, and 29 for a W-to-Ar mass ratio of 1.0×10^{-5} and in Figs. 30, 31, and 32 for a W-to-Ar mass ratio of 1.0×10^{-7}. The total of all integrated line intensities of each ionization species of W is also presented on each figure.

A number of trends is apparent in Figs. 24 through 32. The integrated line intensities of WI for any particular 100 Å wavelength interval tend to predominate at large W-to-Ar mass ratios (1.0×10^{-3}) and at a temperature of 5000 deg K. As the W-to-Ar mass ratio decreases, the WII integrated intensities predominate at a temperature of 5000 deg K, particularly for wavelength intervals less than about 4000 Å. Since the integrated intensity of any line is a function of the amount of emitter present, reference to the composition results in Figs. 3, 5, and 7 show that the quantity of WII relative to WI increases with a decrease in the W-to-Ar mass ratio at a temperature of 5000 deg K. An increase in temperature from 5000 to 9000 deg K at any given W-to-Ar mass ratio results in an enhancement of the WII integrated line intensities with respect to WI; thus, at a temperature of 9000 deg K, WII integrated line intensities predominate. This effect is primarily due to increased ionization of WI to WII at the higher temperatures; therefore less WI, relative to WII, is present in the system at temperatures of 7000 and 9000 deg K. At temperatures in excess of 7000 deg K, WI is at least 80 percent ionized. Furthermore, examination of the tabulated data for the total of all integrated line intensities for either WI or WII shown on each figure indicates an increase in total intensity

as the temperature is increased from 5000 to 9000 deg K. This increase in total integrated line intensity is attributable to the exponential dependence of line intensity on temperature as exemplified by Eq. (15). The more marked increase in total integrated intensity for all the lines in WII with temperature (as compared to WI) is a result of the increased ionization of WI to WII as shown in the composition results (see Figs. 3 through 7).

Uranium

The integrated line intensities, summed over wavelength intervals of 100 Å, for UI and UII are graphically illustrated in Figs. 33, 34 and 35 (at temperatures of 5000, 7000, and 9000 deg K) as a function of the wavelength at the center of the 100 Å interval. The results in Figs. 33, 34, and 35 are for a U-to-Ar mass ratio of 1.0×10^{-3}. Additional results are shown at the same temperatures in Figs. 36, 37, and 38 for a mass ratio of 1.0×10^{-5} and in Figs. 39, 40, and 41 for a mass ratio of 1.0×10^{-7}. The total of all integrated line intensities for both UI and UII are tabulated on each figure as in the case of the W results. In general, the same trends are observed in the U data as were observed in the W data.

Total Integrated Line Intensities

The separate results obtained for WI and WII integrated line intensities in wavelength intervals of 100 Å were combined to give the sum of integrated line intensities for W in 100 Å wavelength intervals. These data are shown for W-to-Ar mass ratios of 1.0×10^{-3}, 1.0×10^{-5}, and 1.0×10^{-7} as a function of the wavelength at the center of the 100 Å interval for a temperature of 5000 deg K in Fig. 42, 7000 deg K in Fig. 43, and 9000 deg K in Fig. 44. Also presented on each figure is the sum of all integrated line intensities at each mass ratio studied. Similar data are exhibited for combined UI and UII integrated line intensities in 100 Å wavelength intervals for a temperature of 5000 deg K in Fig. 45, 7000 deg K in Fig. 46, and 9000 deg K in Fig. 47. These figures summarize the data presented in the preceding curves.

In the case of Ar, the integrated line intensities in 100 Å intervals for ArII are always orders of magnitude less than the corresponding results calculated for ArI. Thus, Figs. 18, 19 and 20, which were calculated for ArI alone, also effectively represent the combined results for ArI and ArII integrated line intensities.

The total emission from Ar, W, U, W combined with Ar, and U combined with Ar are shown as a function of temperature in Fig. 48 for a heavy metal-to-Ar mass ratio of 1.0×10^{-3}; in Fig. 49, for a mass ratio of 1.0×10^{-5}; and in Fig. 50, for a mass ratio of 1.0×10^{-7}. A number of trends is evident upon examination of these figures. In all cases the total intensity of all lines

increases with an increase in temperature; the most marked increase with temperature occurs in Ar, the least marked increase with temperature occurs in U. At a mass ratio of 1.0×10^{-3} (see Fig. 48), the total intensity of all lines in Ar is considerably less than in W or U. As shown in Fig. 49 (mass ratio of 1.0×10^{-5}), the total line emission from Ar exceeds that from U at temperatures greater than approximately 7500 deg K, but is less than the emission from all lines in W at any temperature. Similarly, Fig. 50 shows that the line emission in Ar exceeds that from U at all temperatures in excess of approximately 6000 deg K; the Ar line emission exceeds that for W line emission at temperatures greater than 6700 deg K.

In order to facilitate comparison of the calculated line intensity data for Ar, W, and U with that of a black body, the intensity of a black body over wavelength intervals of 100 Å was calculated and is plotted as a function of the wavelength at the center of the 100 Å interval in Fig. 51 for temperatures of 5000, 7000, and 9000 deg K (Ref. 18). To illustrate the use of this figure, consider an Ar-W plasma with a mass ratio of 1.0×10^{-7} at a temperature of 7000 deg K. In the wavelength region between 2200 and 2300 Å the emission from all WI and WII lines is given as approximately 2.2×10^{-4} watt/cm^3 - sr (see Fig. 43). If the path length in the emitting gas is 0.1 cm, the emitted intensity is 2.1×10^{-5} watt/cm^2 - sr for all lines in WI and WII as compared to approximately 2.3×10^{0} watt/cm^2 - sr for a black body at the same temperature and in the same wavelength interval (see Fig. 51). Therefore, at a temperature of 7000 deg K, the ratio of radiation from tungsten to that from a black body is approximately 1.0×10^{-5} in the wavelength region between 2200 and 2300 Å. This ratio is sufficiently low that there is almost certainly no self absorption in the gases. It should be noted, however, that integrated intensity data do not take into account actual line shapes or line half-widths, and peak line intensities will be much closer to black body radiation than indicated in the example. If the ratio of line radiation to black-body radiation approaches unity, a separate determination must be made of the shape of key lines to determine if their peaks are low enough above the average to approach the black body radiation in local parts of the spectrum.

REFERENCES

1. Weinstein, H. and R. Ragsdale: The Coaxial Flow Reactor - A Gaseous Nuclear Rocket Concept. ARS Reprint 1518-60, presented at the ARS 15th Annual Meeting, Washington, D. C., December 1960.

2. McLafferty, G. H. and H. E. Bauer: Preliminary Conceptual Design Study of a Specific Vortex-Stabilized Gaseous Nuclear Rocket Engine. UARL Report E-910093-29, September 1966.

3. Kesten, A. S. and R. B. Kinney: Theoretical Effect of Changes in Constituent Opacities on Radiant Heat Transfer in Vortex-Stabilized Gaseous Nuclear Rocket. UARL Report D-910092-5, September 1965.

4. Kesten, A. S. and N. L. Krascella: Theoretical Investigation of Radiant Heat Transfer in the Fuel Region of a Gaseous Nuclear Rocket Engine. UARL Report E-910092-9, September 1966. Also issued as NASA CR-695.

5. Krascella, N. L.: Tables of the Composition, Opacity and Thermodynamic Properties of Hydrogen at High Temperatures. UARL Report B-910168-1, September 1963. Also issued as NASA SP-3005.

6. Krascella, N.L.: Theoretical Investigation of the Spectral Opacities of Hydrogen and Nuclear Fuel. Air Force Systems Command Report RTD-TDR-63-1101, November 1963.

7. Krascella, N. L.: Theoretical Investigation of the Opacity of Heavy-Atom Gases. UARL Report D-910092-4, September 1965.

8. Krascella, N. L.: Theoretical Investigation of the Absorptive Properties of Small Particles and Heavy-Atom Gases. UARL Report E-910092-7, September 1966.

9. Marteney, P. J., A. E. Mensing, and N. L. Krascella: Experimental Investigation of the Spectral Emission Characteristics of Argon-Tungsten and Argon-Uranium Induction Heated Plasmas. UARL Report G-910092-11, September 1968.

10. McMahon, D. G. and R. Roback: Machine Computation of Chemical-Equilibria in Reacting Systems. In Kinetics, Equilibria, Performance of High Temperature Systems. Proceedings of the First Conference Western States Section of the Combustion Institute, Los Angeles, California, November 1959, edited by G. S. Bahn and E. E. Zukoski, Butterworths, Washington, 1960.

11. Corliss, C. H. and W. R. Bozman: Experimental Transition Probabilities for Spectral Lines of Seventy Elements. NBS Monograph 53, Washington 25, D. C., July 20, 1962.

12. Corliss, C. H. and J. B. Shumaker, Jr.: Transition Probabilities in Argon I. Journal of Research of the National Bureau of Standards Vol. 71A, No. 6, November-December 1967.

13. Adcock, B. D. and W. E. G. Plumtree: On Excitation Temperature Measurements in a Plasma-Jet, and Transition Probabilities for Argon Lines. Journal of Quantitative Spectroscopy and Radiative Transfer, Vol. 4, 1964.

14. Laun, D. D.: Second Spectrum of Tungsten (WII). Journal of Research of the National Bureau of Standards, Vol. 68A, No. 2, March-April 1964.

15. Kiess, C. C., C. J. Humphreys, and D. D. Laun: Preliminary Description and Analysis of the First Spectrum of Uranium. Journal of Research of the National Bureau of Standards, Research Paper RP 1729, Vol. 27, July 1946.

16. Moore, C. E.: Atomic Energy Levels, Circular of the National Bureau of Standards, Vol. I, June 1949; Vol. III, May 1958.

17. Olsen, H. N.: The Electric Arc as a Light Source for Quantitative Spectroscopy. Journal of Quantitative Spectroscopy and Radiative Transfer, Vol. 3, 1963.

18. Allen, C. W.: "Astrophysical Quantities". University of London, The Athlone Press, 1955.

19. Mann, J. B.: Ionization of U, UO, and UO_2 by Electron Impact. Journal of Chemical Physics, Vol. 40, March-April 1964.

20. Waber, J. T., D. Liberman and D. T. Cromer: Private communication, Los Alamos Scientific Laboratory, Los Alamos, New Mexico, June 1966.

21. Williamson, H. A., H. H. Michels, and S. B. Schneiderman: Theoretical Investigation of the Lowest Five Ionization Potentials of Uranium. UARL Report D-910099-2, September 1965.

22. Cooper, J.: Plasma Spectroscopy. Reports on Progress in Physics, Vol. XXIX, Part I, 1966.

23. Pivovonsky, M. and M. R. Nagel: "Tables of Blackbody Radiation Functions", The Macmillian Company, New York, 1961.

LIST OF SYMBOLS

α	Degree of ionization
$A_{n,m}$	Spontaneous transition probability, sec^{-1}
Ar	Argon
ArI, ARI	Neutral argon atom
ArII, ARII	Singly ionized argon ion
ArIII, ARIII	Doubly ionized argon ion
BI, BII, BIII	Denotes an ionization species of W or U
e^-	Electron
$E_{i,n}$	Energy of n^{th} level in ionization species i, cm^{-1}
F_B, F	Mass ratio defined by Eq. (10)
FI	Neutral fluorine atom
F^-	Negative fluorine ion
$g_{i,n}$	Statistical weight of n^{th} level in ionization species i
h	Planck constant, 6.6237×10^{-27} erg-sec
i	Denotes an ionization species
I	Integrated line intensity, watt/cm^3 - sr
I_i'	Ionization potential of ionization species i, ev
I_t	Total intensity of all lines, watt/cm^3 - sr
I_λ	Line intensity or radiated power, watt/cm^3 - Å - sr
$I_{\Delta\lambda}$	Integrated line intensities summed over wavelength intervals of 100 Å, watt/cm^3 - sr - 100 Å
$I^B_{\Delta\lambda}$	Intensity of a black body in wavelength intervals of 100 Å, watt/cm^2 - sr - 100 Å

k	Boltzmann constant, 1.3802×10^{-16} erg/K
m	Quantum number of an upper level
m_e	Electron mass, 9.11×10^{-28} g
M_i	Weight, mols
MW_B	Molecular weight
n	Quantum number of lower level
N_i	Number density of ionization species i, cm^{-3}
$N_{i,n}$	Number density of ionization species i in the n^{th} level, cm^{-3}
P_i	Partial pressure of ionization species i, atm
SR, sr	Steradian
T	Absolute temperature, deg K
U	Uranium
UI	Neutral uranium atom
UII	Singly ionized uranium ion
UIII	Doubly ionized uranium ion
UF_4	Decomposition product of UF_6
UF_6	Uranium hexafluoride
W	Tungsten
WI	Neutral tungsten atom
WII	Singly ionized tungsten ion
WIII	Doubly ionized tungsten ion
WF	Decomposition product of WF_6
WF_6	Tungsten hexafluoride

Z_i	Partition function for ionization species i
ϕ_λ	Shape function or line profile, Å^{-1}
λ	Wavelength, Å
λ_c	Wavelength at center of a wavelength interval of 100 Å, Å
$\Delta\lambda$	Wavelength interval, Å

TABLE I

Spectral Region, Number of Lines
and Number of Energy Levels Used
In Integrated Line Intensity
Program

Ionization Species	Spectral Region Å	Spectral Lines		Energy Levels		Refs. for Transition Probabilities
		Number	Refs. for λ	Number	Refs. for $E_{i,n}$	
ARI	3400 - 9800	278	12, 13	113	16	12, 13
ARII	3500 - 5100	23	13	15	16	13
WI	2100 - 8900	1019	11	353	11, 16	11
WII	1700 - 6300	2069	11, 14	194	14, 16	11, 14*
UI	2900 - 10,000	1159	11, 15	293	11, 15	11, 15*
UII	2500 - 8600	315	11	254	11	11

*Estimated values derived from indicated references.

TABLE II

Partition Functions for Argon
(Ref. 17)

Temperature (°K)	Partition Functions	
	ARI	ARII
1,000	1.000×10^{0}	5.1949×10^{0}
2,000	1.000×10^{0}	5.1949×10^{0}
3,000	1.000×10^{0}	5.1949×10^{0}
4,000	1.000×10^{0}	5.1949×10^{0}
5,000	1.000×10^{0}	5.3245×10^{0}
6,000	1.000×10^{0}	5.4187×10^{0}
7,000	1.000×10^{0}	5.4900×10^{0}
8,000	1.000×10^{0}	5.5459×10^{0}
9,000	1.0001×10^{0}	5.5908×10^{0}
10,000	1.6003×10^{0}	5.6276×10^{0}

TABLE III

Ionization Potentials

Ionization Species	Ionization Potential (eV)	Reference
ARI	15.755	18
WI	7.98	18
WII	14.0	18
UI	6.1	19
UII	12.0	20, 21

EFFECT OF TEMPERATURE ON THE PARTITION FUNCTIONS OF TUNGSTEN I AND TUNGSTEN II

$$Z_i = \sum_n g_{i,n} e^{-E_{i,n}/KT}$$

$E_{i,n}$ AND $g_{i,n}$ FROM REFS. 11 AND 15

$I'_{W\,I} = 7.98$ ev

$I'_{W\,II} = 14.0$ ev

O $-Z_{WI}$ □ $-Z_{WII}$ FROM REF. 11

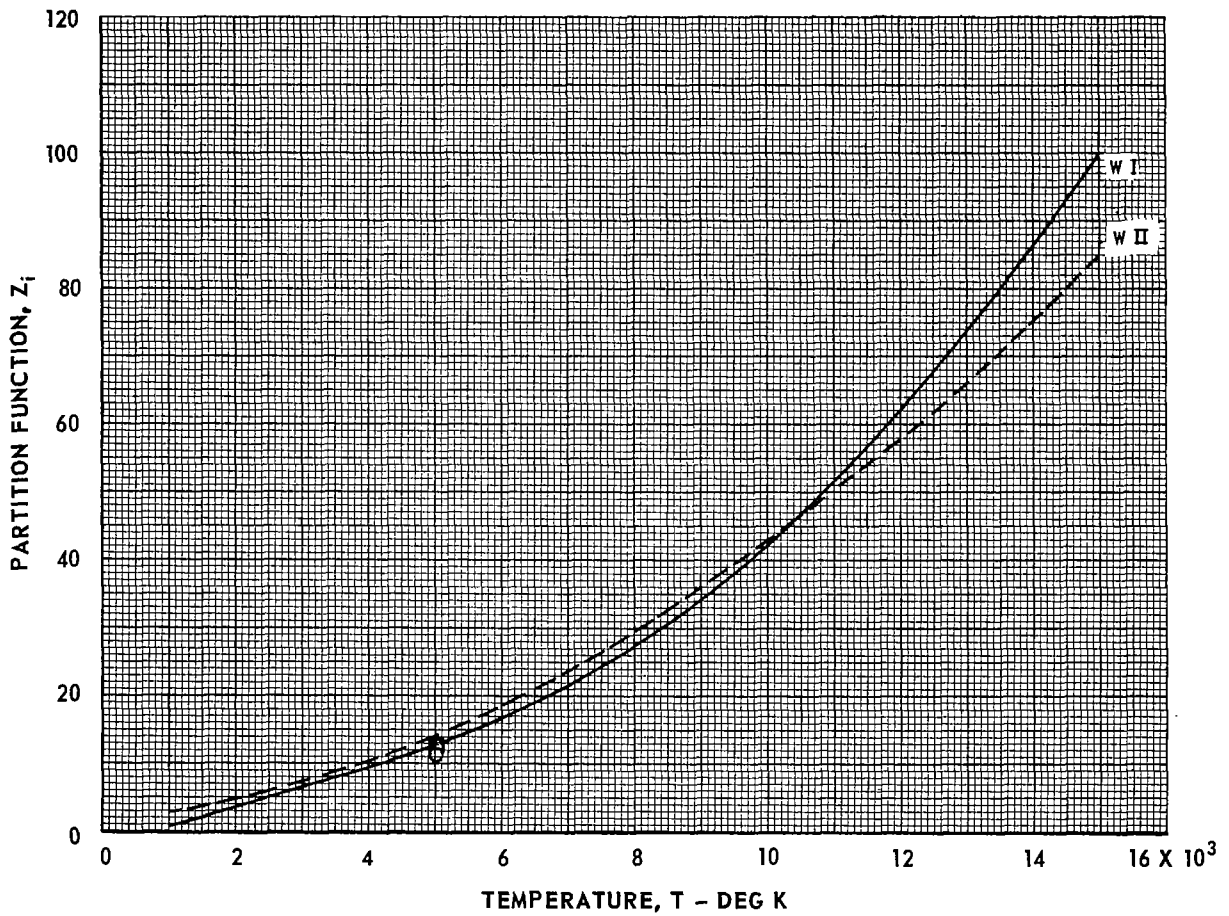

FIG. 1

EFFECT OF TEMPERATURE ON THE PARTITION FUNCTIONS OF URANIUM I AND URANIUM II

$$Z_i = \sum_n g_{i,n} e^{-E_{i,n}/KT}$$

$E_{i,n}$ AND $g_{i,n}$ FROM REFS. 11, 14 AND 16

$I'_{UI} = 6.1$ ev

$I'_{UII} = 12.0$ ev

○ $-Z_{UI}$ □ $-Z_{UII}$ FROM REF. 11

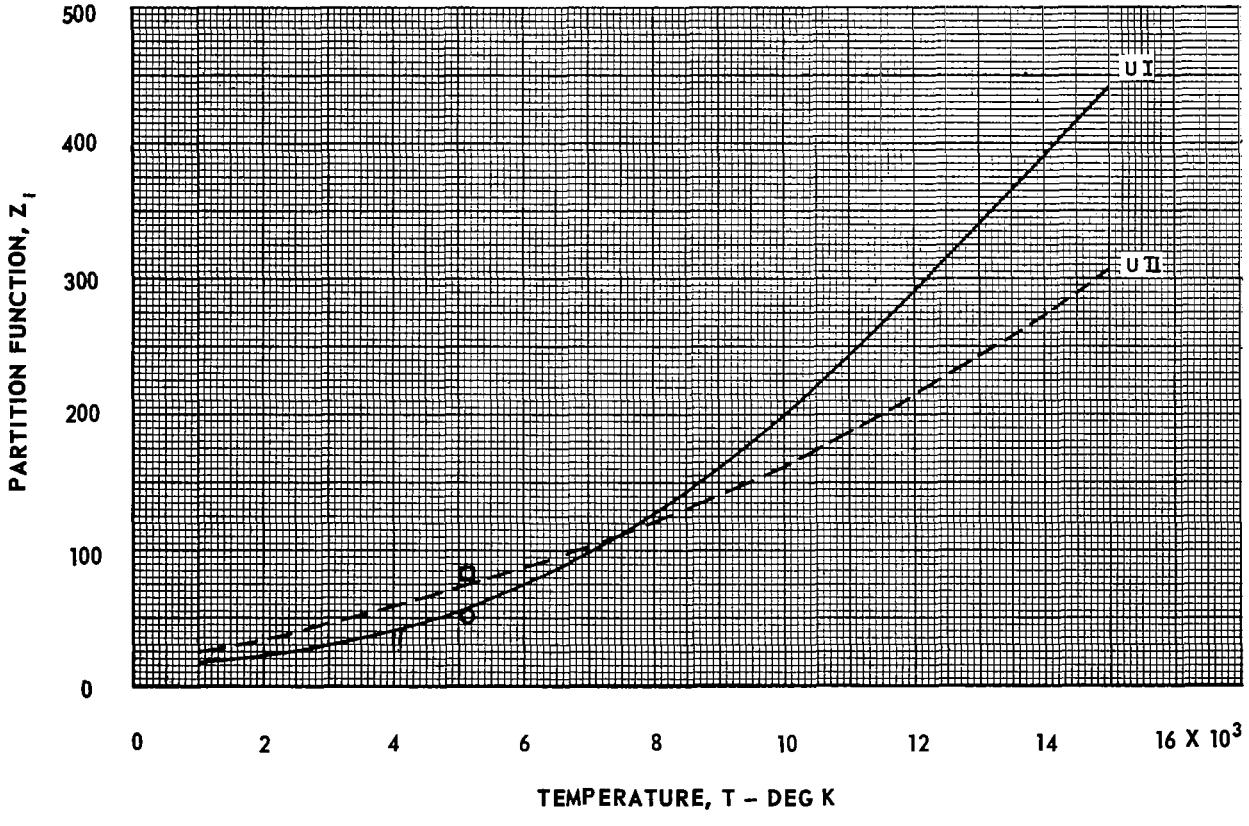

FIG. 2

FIG. 3

COMPOSITION OF AN ARGON – TUNGSTEN HEXAFLUORIDE PLASMA AS A FUNCTION OF TEMPERATURE FOR TUNGSTEN TO ARGON MASS RATIO OF 1.0×10^{-3}

TOTAL PRESSURE = 1.0 ATM
(REMAINING PARTIAL PRESSURE IS AR I)

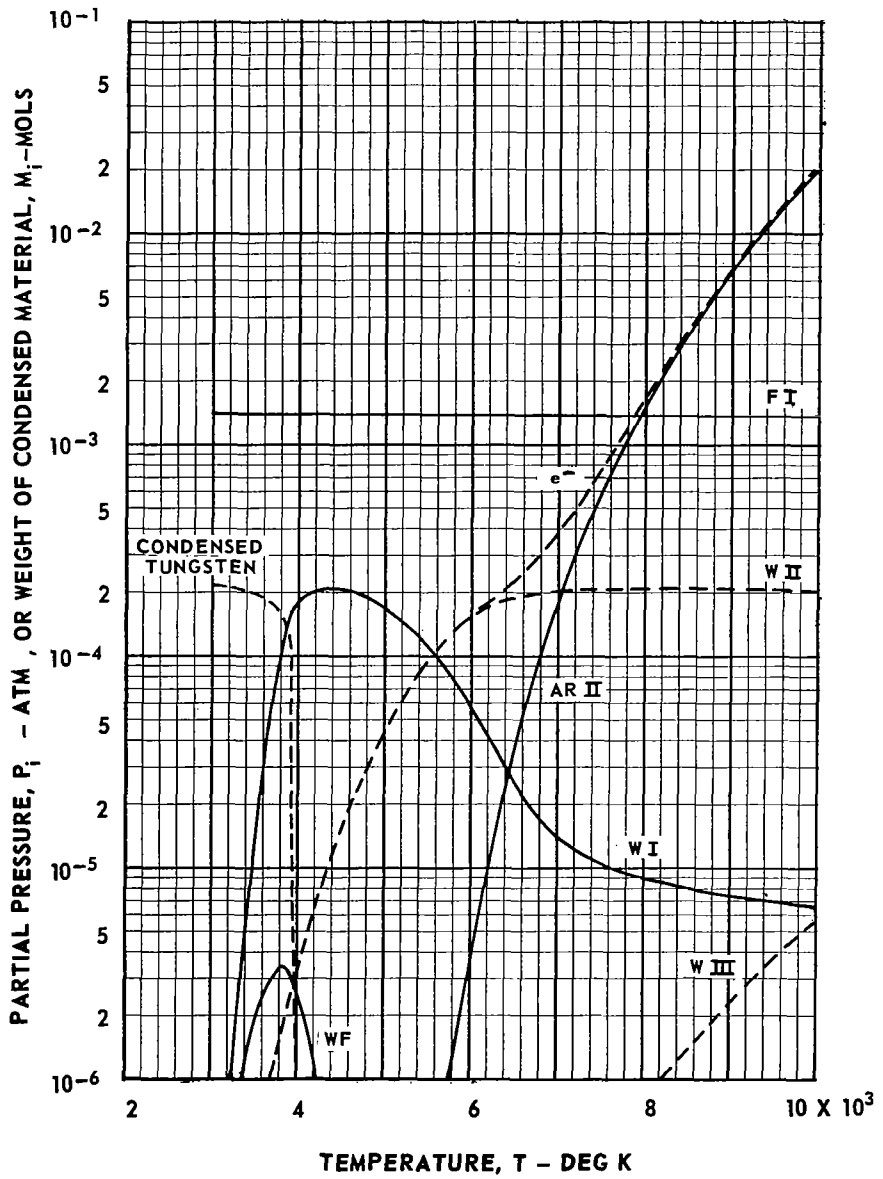

FIG. 4

COMPOSITION OF AN ARGON – TUNGSTEN HEXAFLUORIDE PLASMA AS A FUNCTION OF TEMPERATURE FOR TUNGSTEN TO ARGON MASS RATIO OF 1.0×10^{-4}

TOTAL PRESSURE = 1.0 ATM
(REMAINING PARTIAL PRESSURE IS AR I)

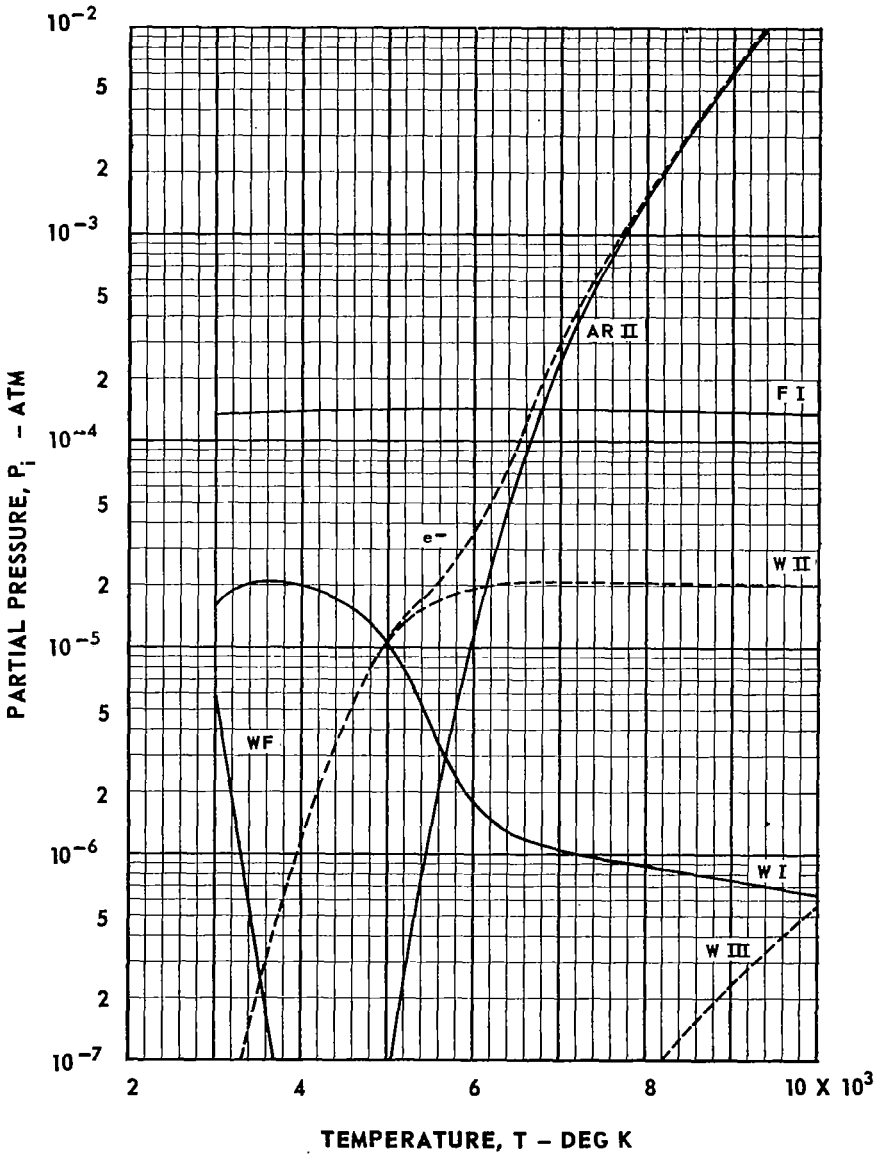

FIG. 5

COMPOSITION OF AN ARGON – TUNGSTEN HEXAFLUORIDE PLASMA AS A FUNCTION OF TEMPERATURE FOR TUNGSTEN TO ARGON MASS RATIO OF 1.0×10^{-5}

TOTAL PRESSURE = 1.0 ATM

(REMAINING PARTIAL PRESSURE IS AR I)

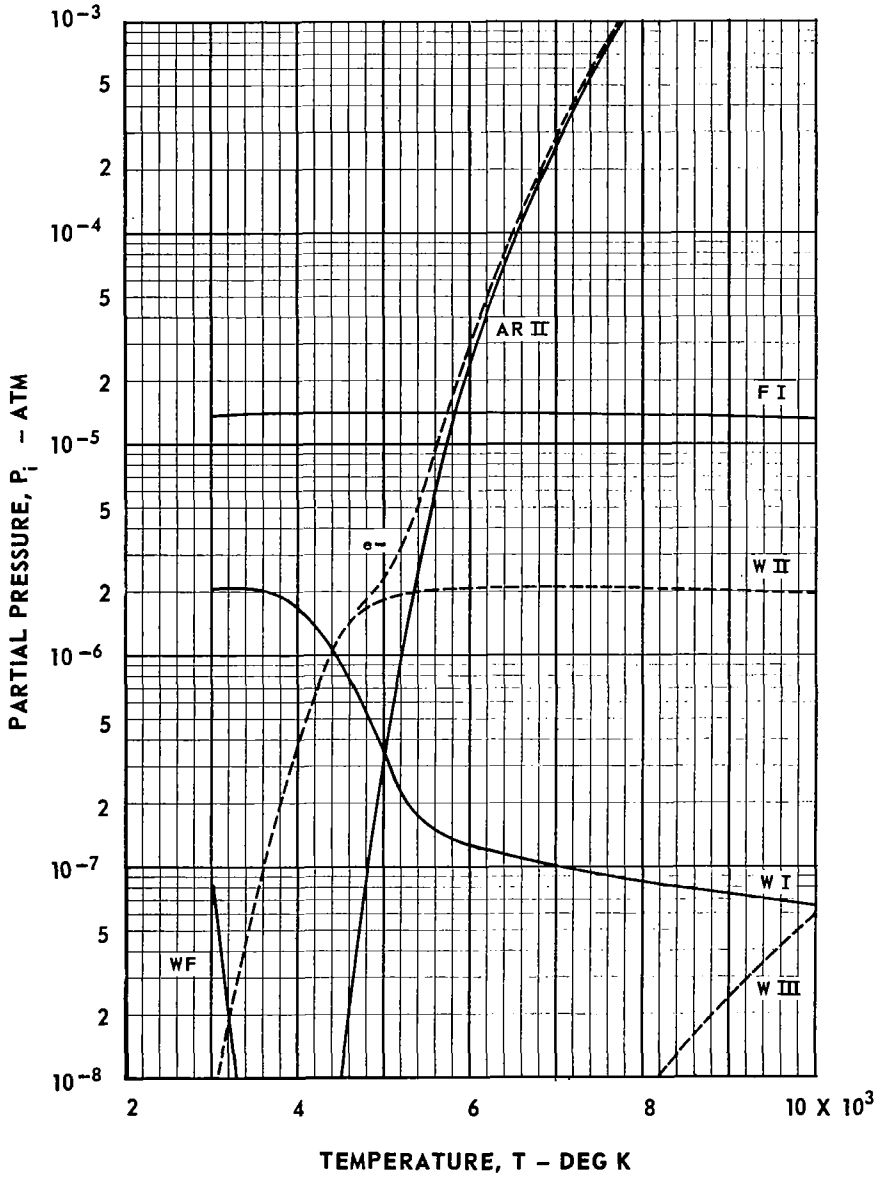

FIG. 6

COMPOSITION OF AN ARGON – TUNGSTEN HEXAFLUORIDE PLASMA AS A FUNCTION OF TEMPERATURE FOR TUNGSTEN TO ARGON MASS RATIO OF 1.0×10^{-6}

TOTAL PRESSURE = 1.0 ATM

(REMAINING PARTIAL PRESSURE IS AR I)

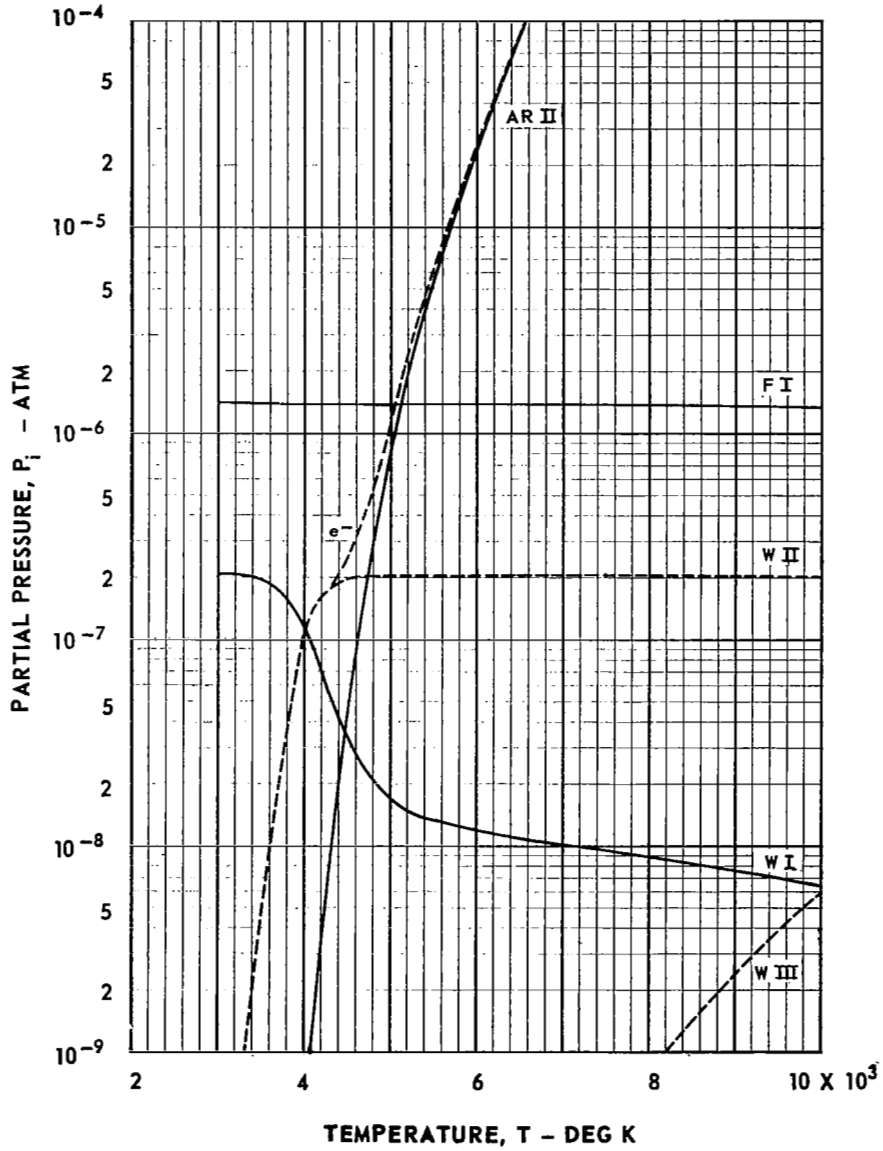

FIG. 7

COMPOSITION OF AN ARGON – TUNGSTEN HEXAFLUORIDE PLASMA AS A FUNCTION OF TEMPERATURE FOR TUNGSTEN TO ARGON MASS RATIO OF 1.0×10^{-7}

TOTAL PRESSURE = 1.0 ATM
(REMAINING PARTIAL PRESSURE IS AR I)

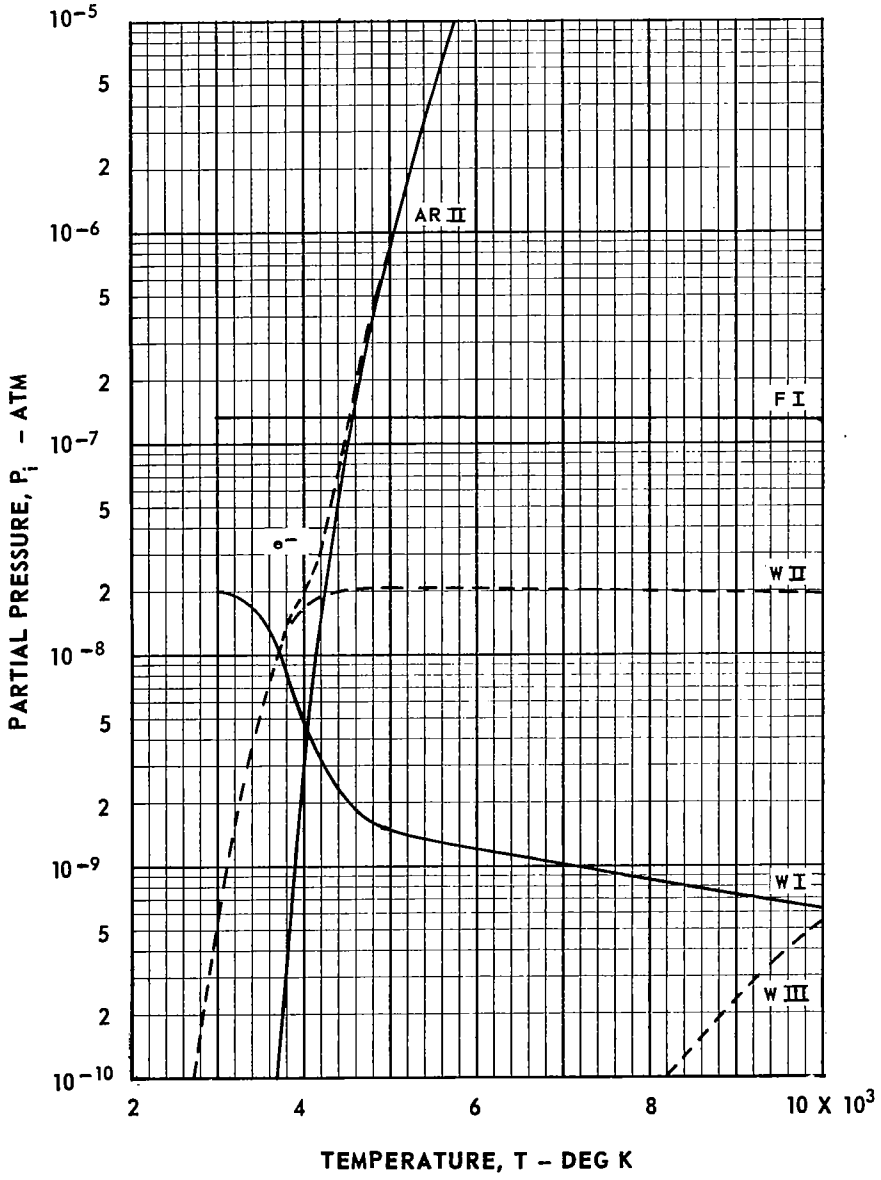

FIG. 8

COMPOSITION OF AN ARGON – URANIUM HEXAFLUORIDE PLASMA AS A FUNCTION OF TEMPERATURE FOR URANIUM TO ARGON MASS RATIO OF 1.0×10^{-3}

TOTAL PRESSURE = 1.0 ATM
(REMAINING PARTIAL PRESSURE IS AR I)

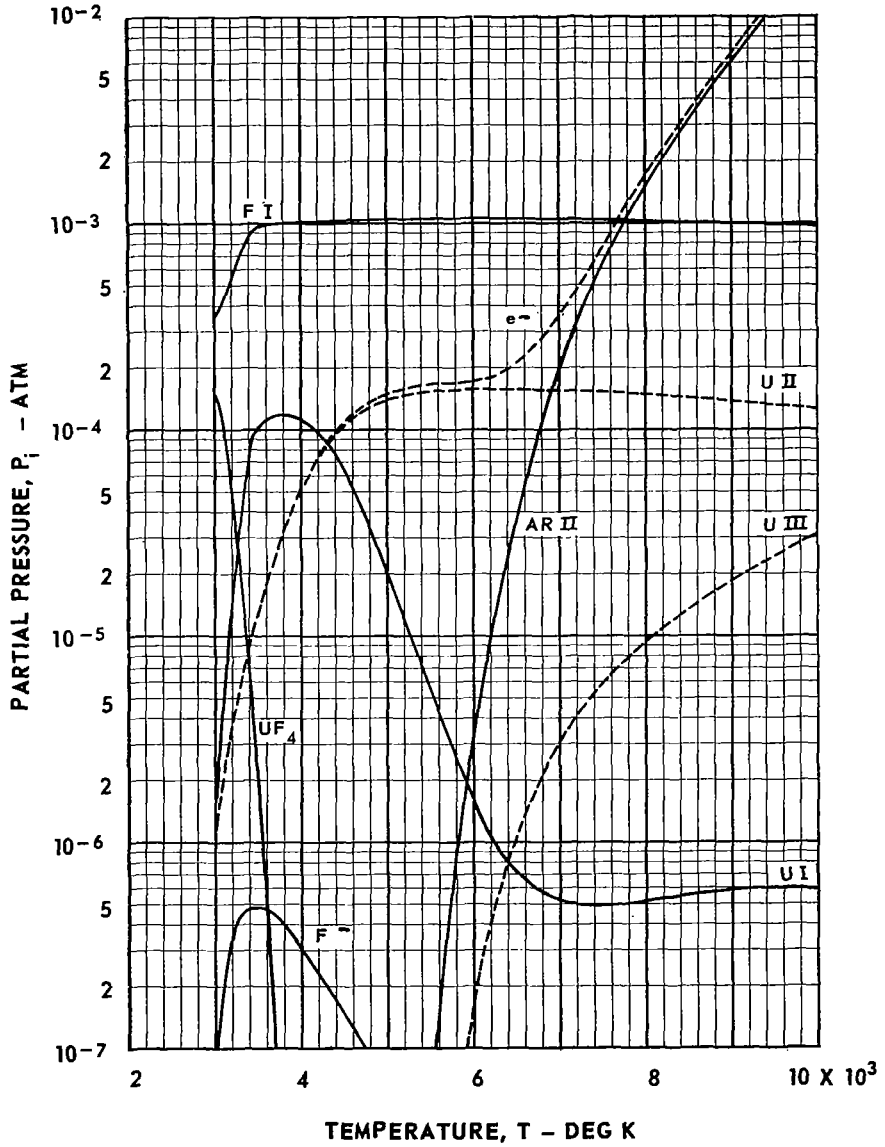

FIG. 9

COMPOSITION OF AN ARGON – URANIUM HEXAFLUORIDE PLASMA AS A FUNCTION OF TEMPERATURE FOR URANIUM TO ARGON MASS RATIO OF 1.0×10^{-4}

TOTAL PRESSURE = 1.0 ATM
(REMAINING PARTIAL PRESSURE IS AR I)

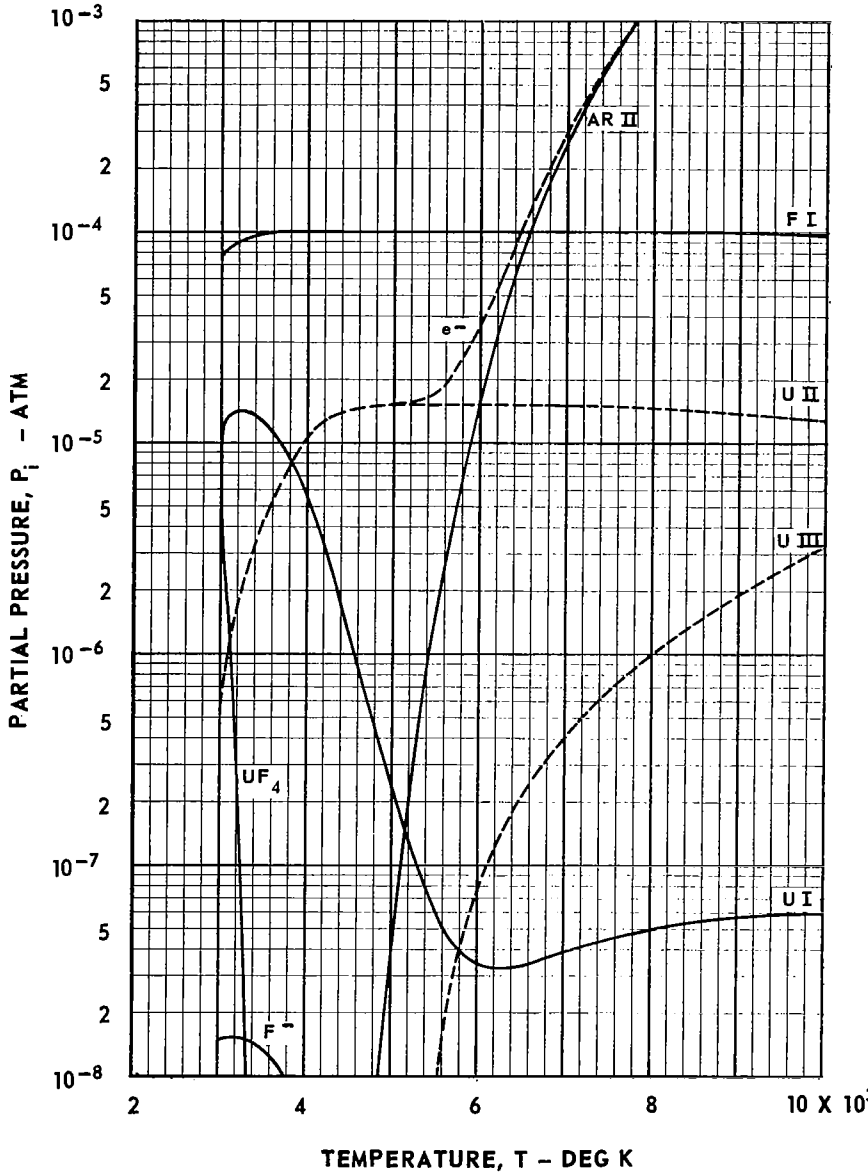

FIG. 10

COMPOSITION OF AN ARGON – URANIUM HEXAFLUORIDE PLASMA AS A FUNCTION OF TEMPERATURE FOR URANIUM TO ARGON MASS RATIO OF 1.0×10^{-5}

TOTAL PRESSURE = 1.0 ATM
(REMAINING PARTIAL PRESSURE IS AR I)

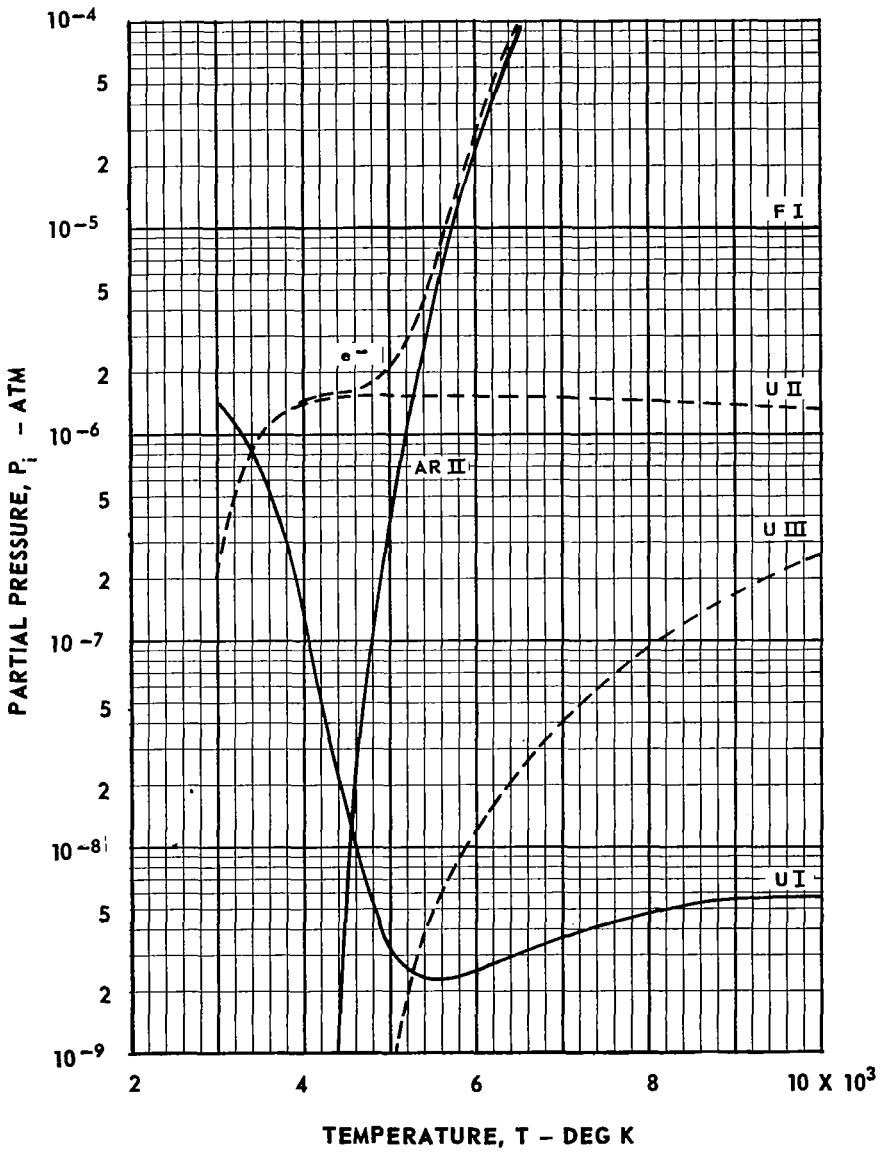

FIG. 13

DEGREE OF IONIZATION OF TUNGSTEN IN AN ARGON–TUNGSTEN HEXAFLUQRIDE PLASMA AS A FUNCTION OF TEMPERATURE FOR VARIOUS TUNGSTEN TO ARGON MASS RATIOS

TOTAL PRESSURE = 1.0 ATM

$$\alpha = \frac{P_{W II} + P_{W III}}{P_{W I} + P_{W II} + P_{W III}}$$

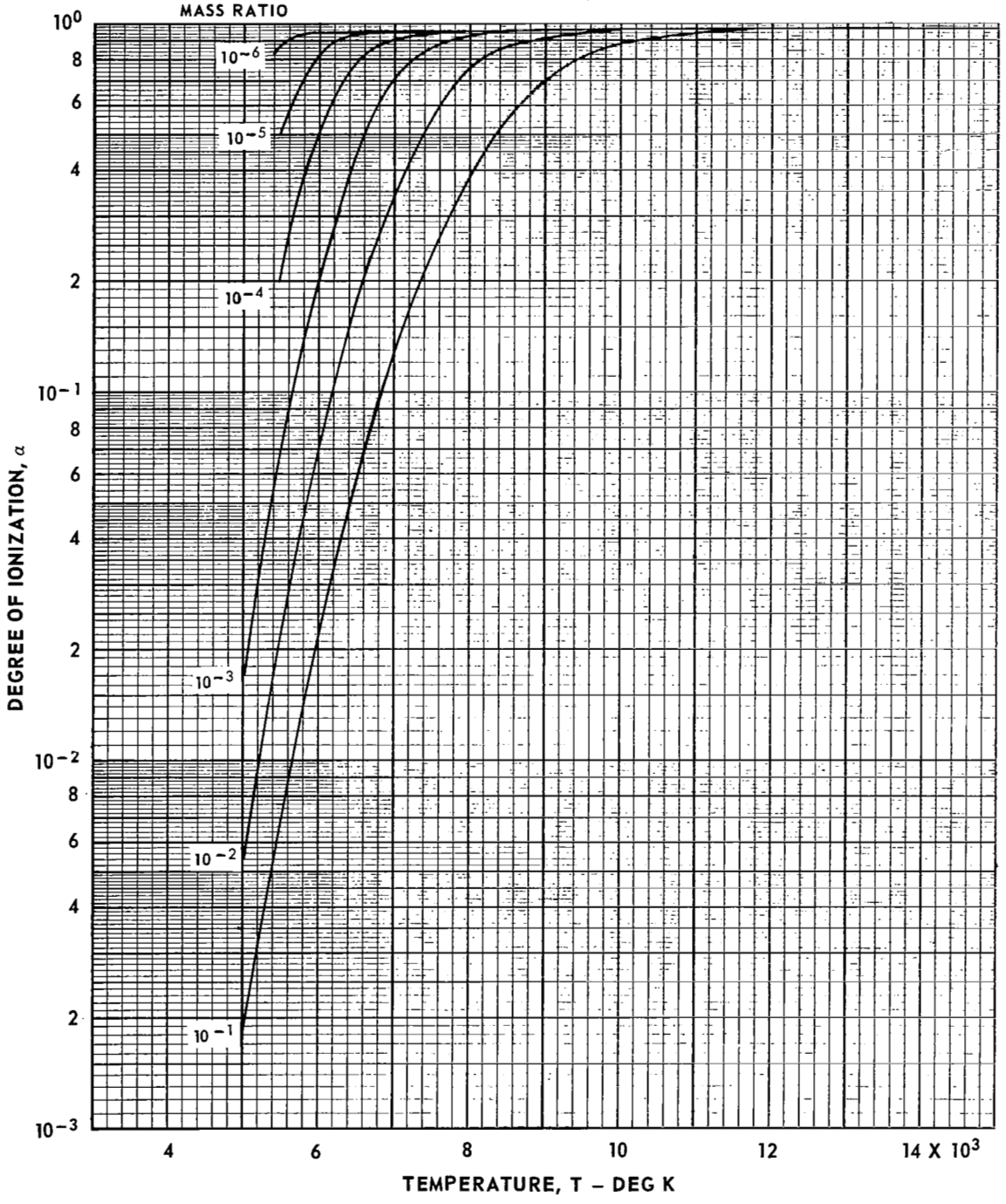

FIG. 14

DEGREE OF IONIZATION OF URANIUM IN AN ARGON – URANIUM HEXAFLUORIDE PLASMA AS A FUNCTION OF TEMPERATURE FOR VARIOUS URANIUM TO ARGON MASS RATIOS

TOTAL PRESSURE = 1.0 ATM

$$\alpha = \frac{P_{UII} + P_{UIII}}{P_{UI} + P_{UII} + P_{UIII}}$$

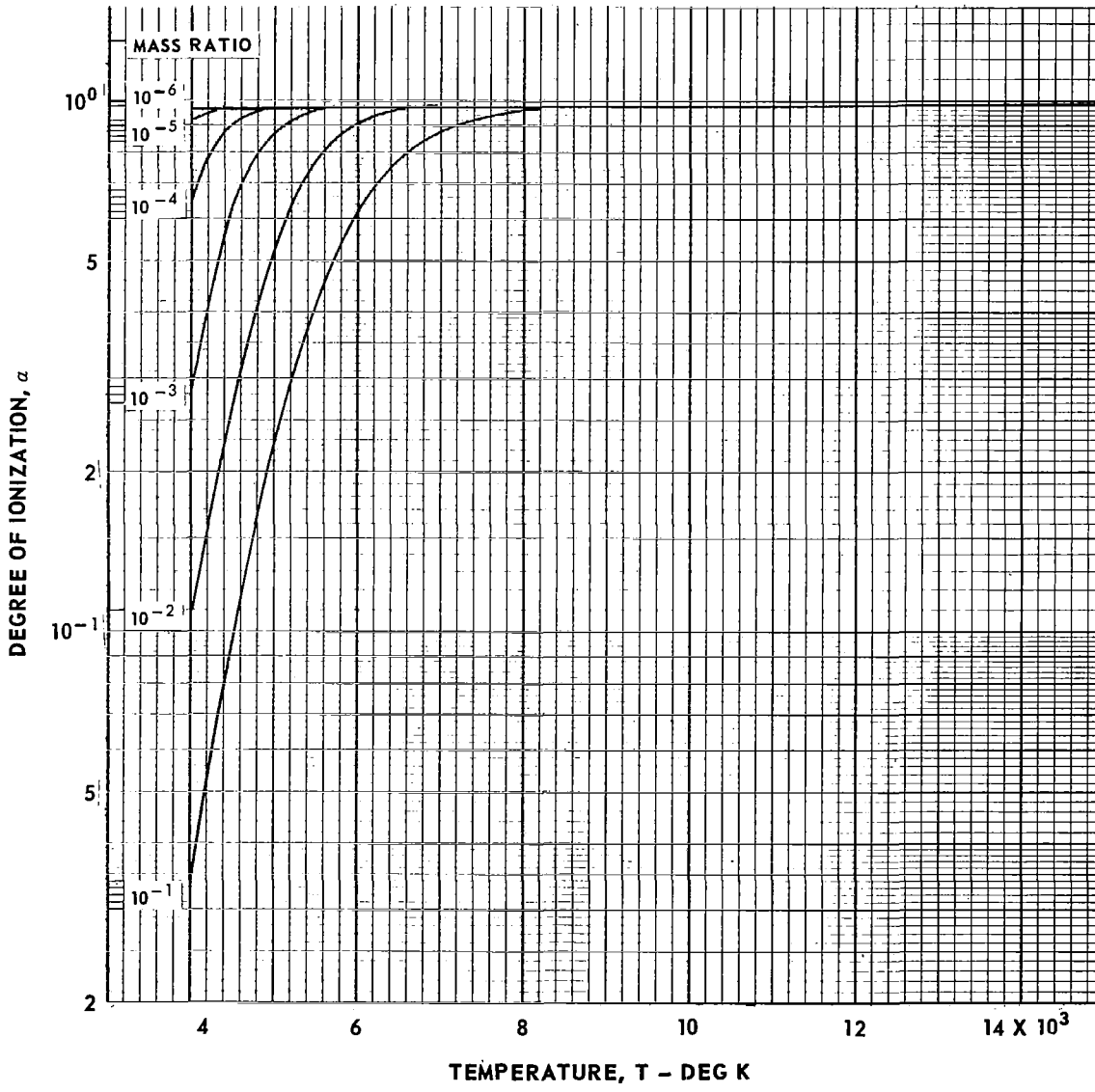

FIG. 15

LINE DENSITY IN ARGON I AND ARGON II

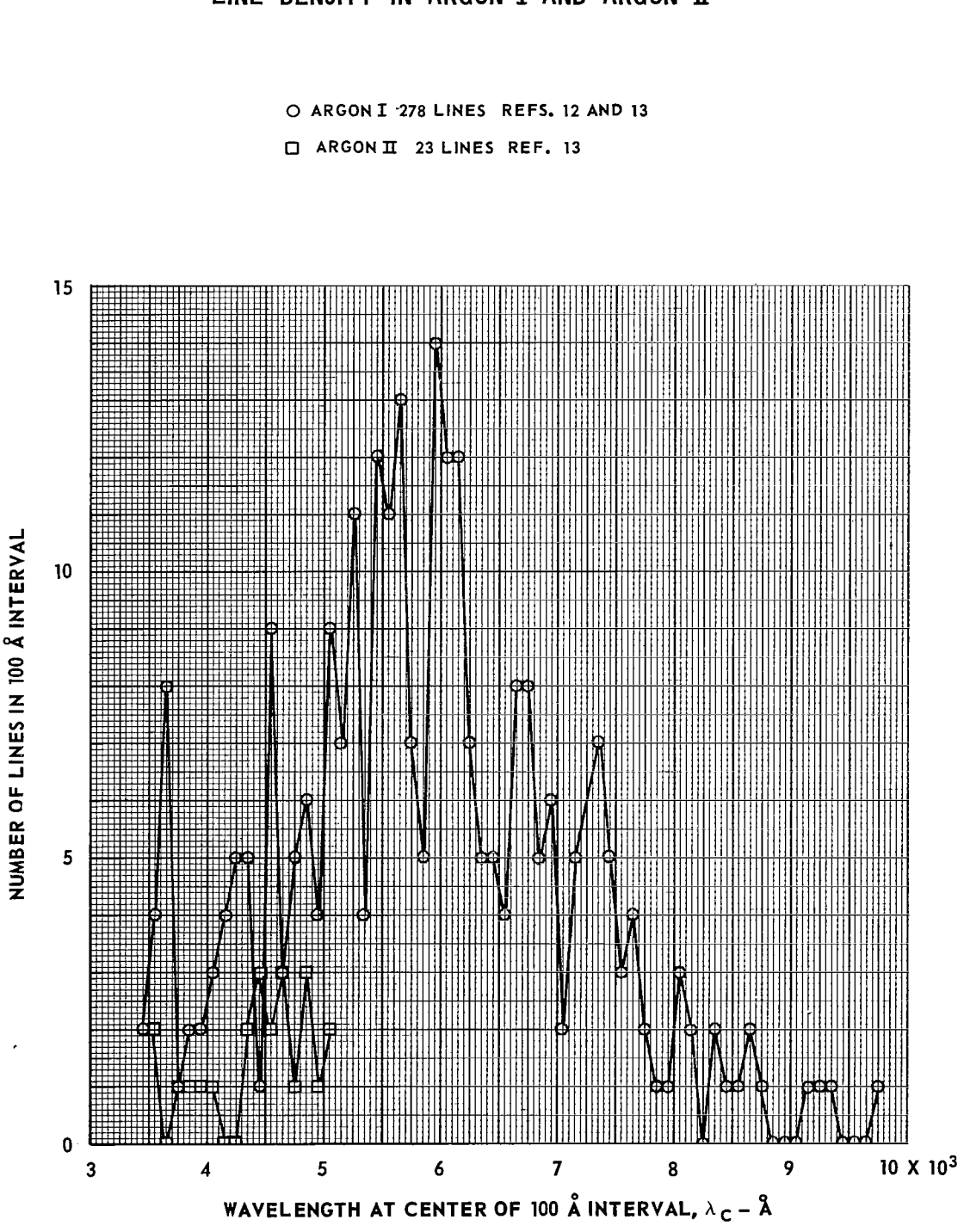

FIG. 16

LINE DENSITY IN TUNGSTEN I AND TUNGSTEN II

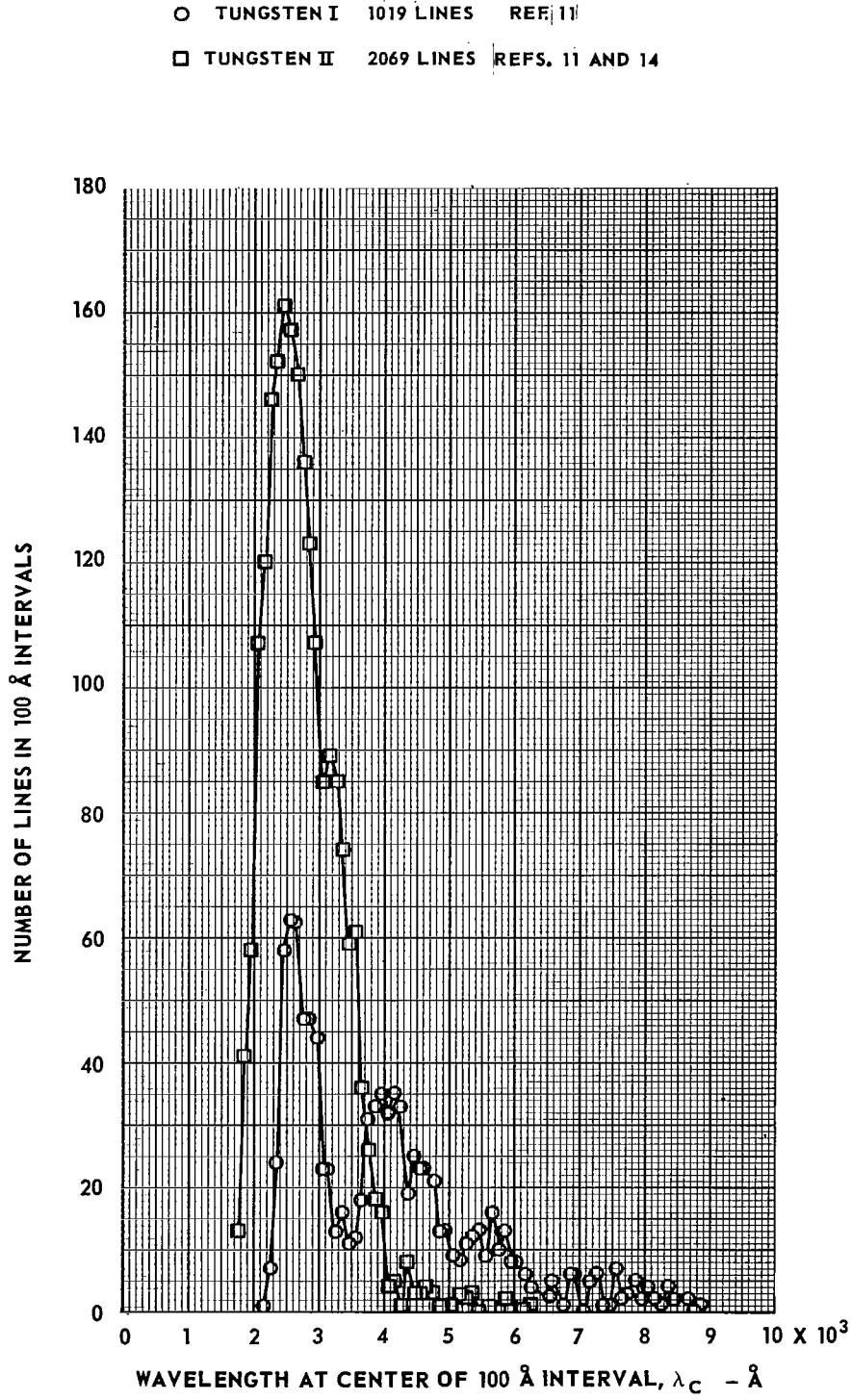

LINE DENSITY IN URANIUM I AND URANIUM II

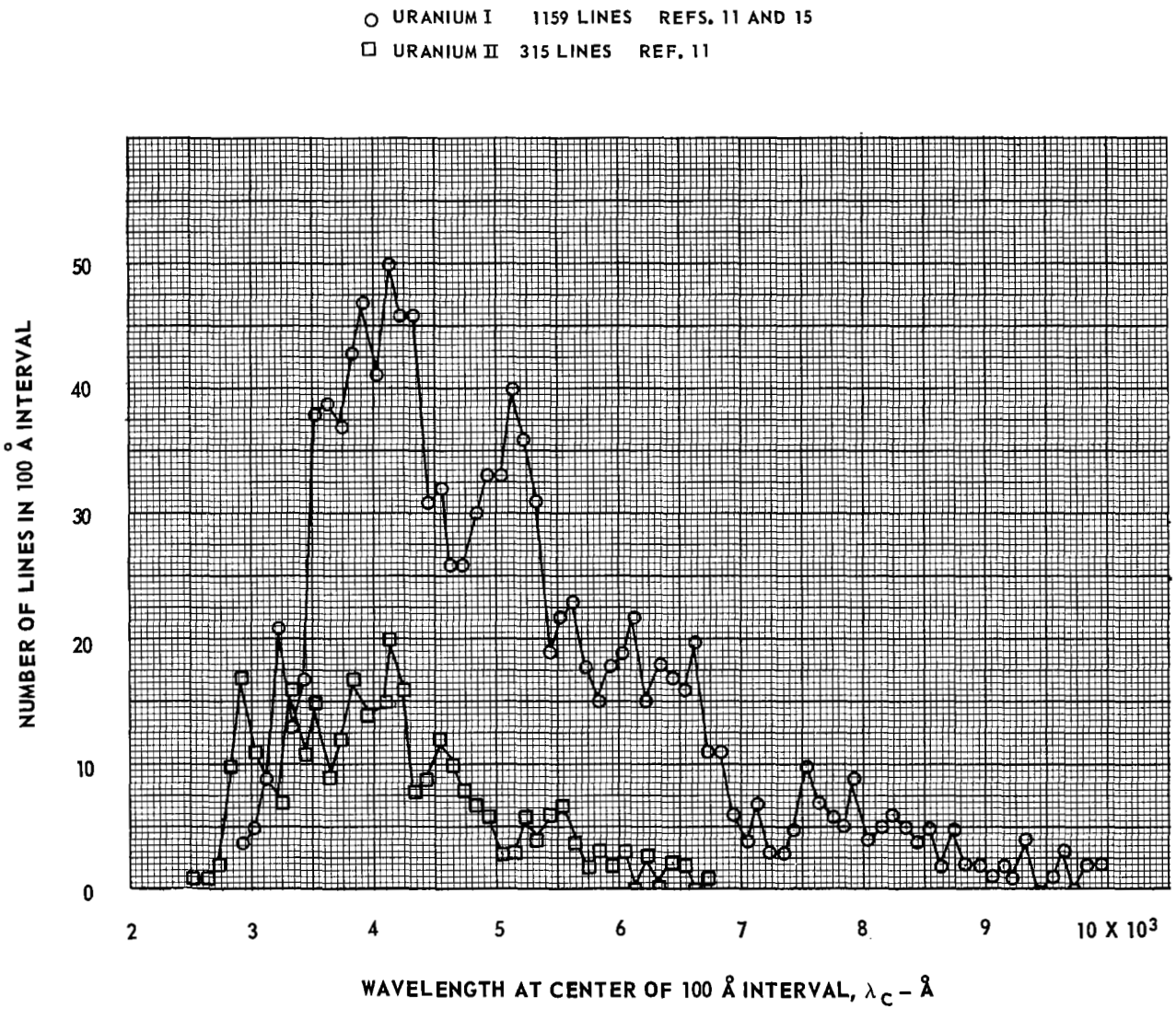

FIG. 17

FIG. 18

TOTAL INTEGRATED LINE INTENSITY IN 100 Å WAVELENGTH INTERVALS FOR ARGON I AT A TEMPERATURE OF 5000 DEG K

INTENSITY OF ALL LINES = 1.48×10^{-6} WATT/CM^3 - SR

——— NO LINES IN INTERVENING INTERVAL

$$I_{\Delta\lambda} = \sum_{100\ \text{Å}} \int I_\lambda \, d\lambda$$

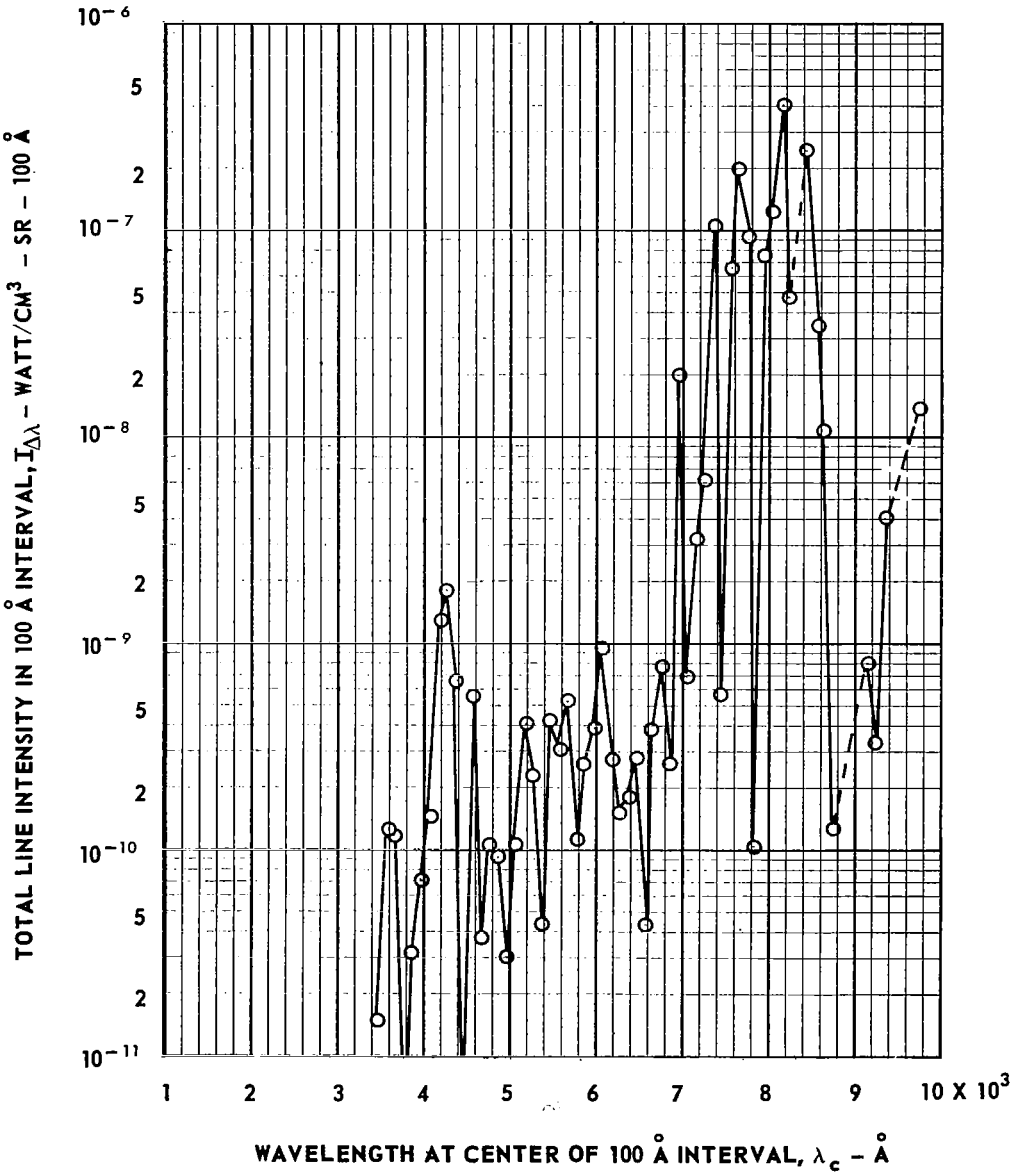

FIG. 19

TOTAL INTEGRATED LINE INTENSITY IN 100 Å WAVELENGTH INTERVALS FOR ARGON I AT A TEMPERATURE OF 7000 DEG K

INTENSITY OF ALL LINES = 6.77×10^{-3} WATT/CM^3 – SR

——— NO LINES IN INTERVENING INTERVAL

$$I_{\Delta\lambda} = \sum_{100\ \text{Å}} \int I_\lambda \, d\lambda$$

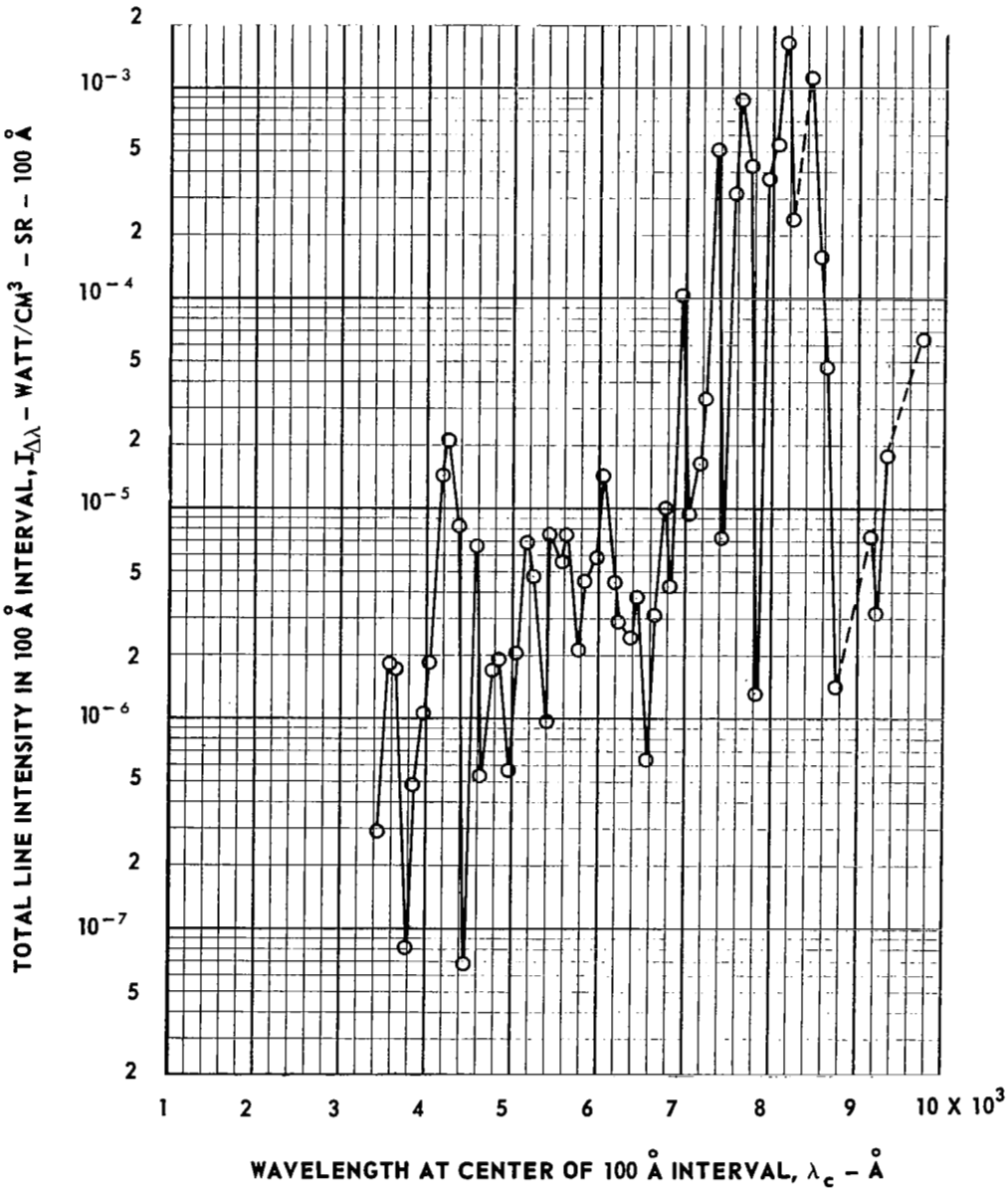

TOTAL INTEGRATED LINE INTENSITY IN 100 Å WAVELENGTH INTERVALS FOR ARGON I AT A TEMPERATURE OF 9000 DEG K

INTENSITY OF ALL LINES = 6.89×10^{-1} WATT/CM^3 – SR

——— NO LINES IN INTERVENING INTERVAL

$$I_{\Delta\lambda} = \sum_{100\ \text{Å}} \int I_\lambda \, d\lambda$$

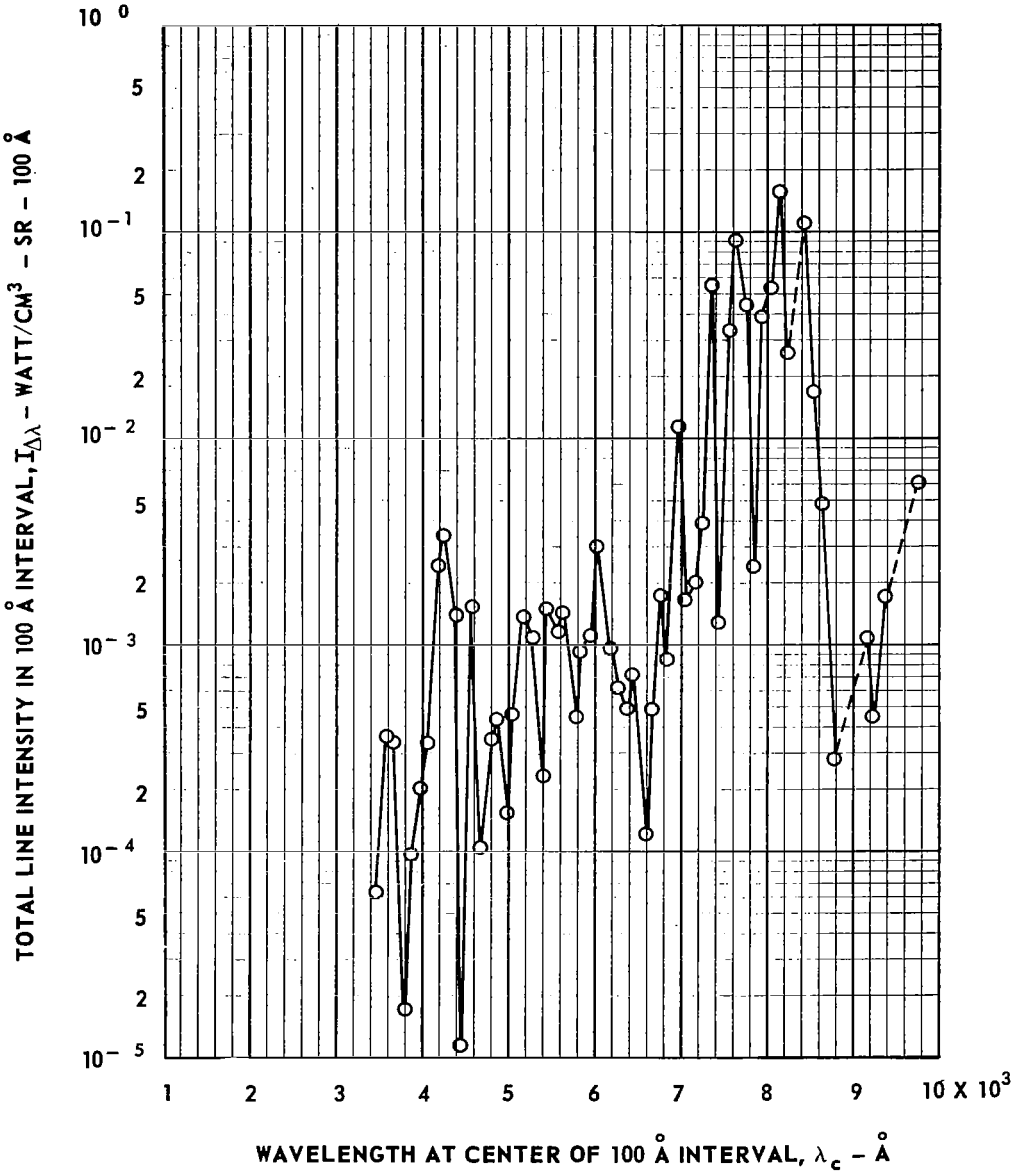

FIG. 21

TOTAL INTEGRATED LINE INTENSITY IN 100 Å WAVELENGTH INTERVALS FOR ARGON II AT A TEMPERATURE OF 5000 DEG K

INTENSITY OF ALL LINES = 1.92×10^{-20} WATT/CM^3 – SR

– – – NO LINES IN INTERVENING INTERVAL

$$I_{\Delta\lambda} = \sum_{100\ \text{Å}} \int I_\lambda \, d\lambda$$

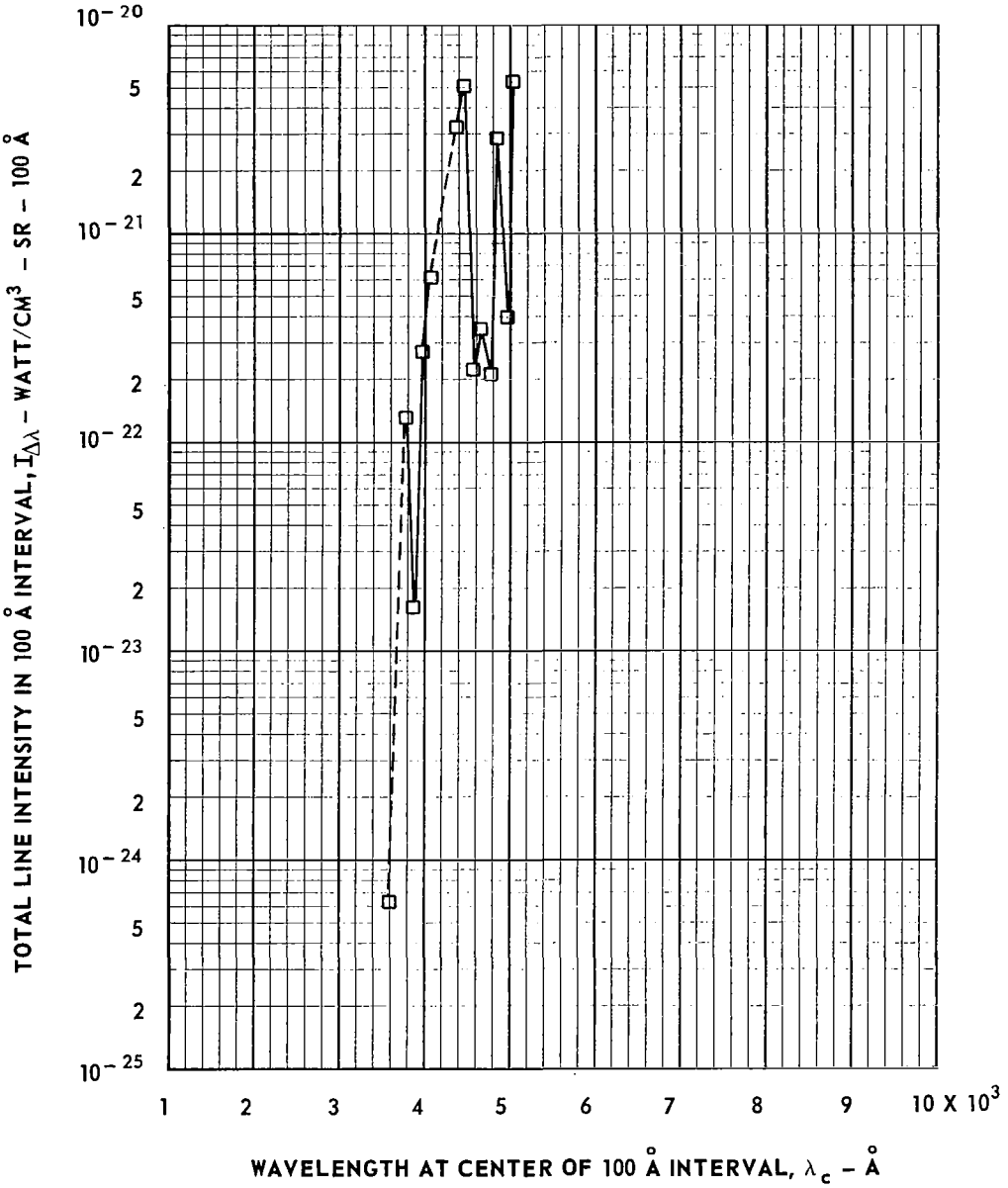

FIG. 22

TOTAL INTEGRATED LINE INTENSITY IN 100 Å WAVELENGTH INTERVALS FOR ARGON II AT A TEMPERATURE OF 7000 DEG K

INTENSITY OF ALL LINES = 5.07×10^{-11} WATT/CM^3 – SR

——— NO LINES IN INTERVENING INTERVAL

$$I_{\Delta\lambda} = \sum_{100\ \text{Å}} \int I_\lambda \, d\lambda$$

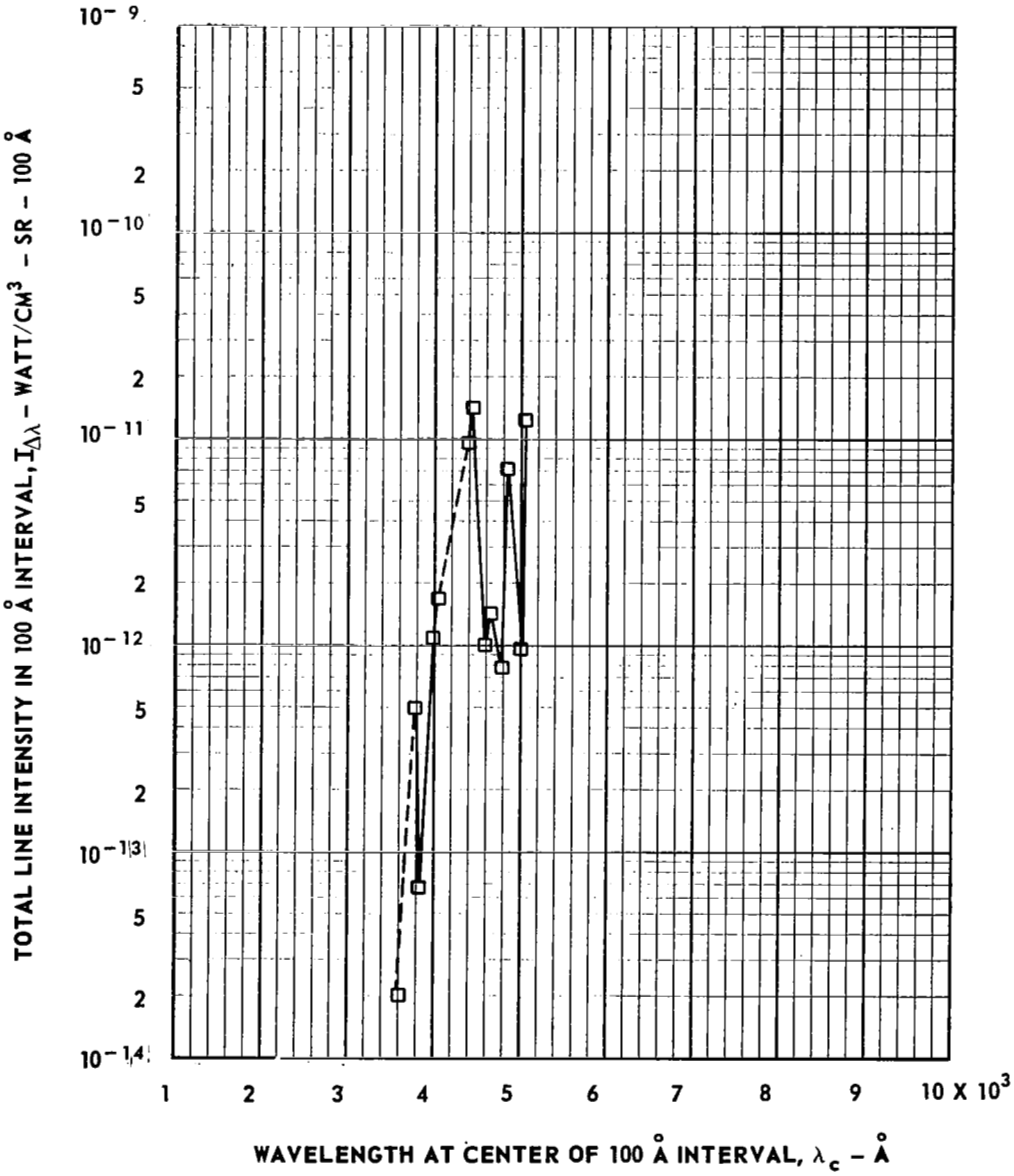

FIG. 23

TOTAL INTEGRATED LINE INTENSITY IN 100 Å WAVELENGTH INTERVALS FOR ARGON II AT A TEMPERATURE OF 9000 DEG K

INTENSITY OF ALL LINES = 1.83 X 10^{-6} WATT/CM^3 – SR

– – – NO LINES IN INTERVENING INTERVAL

$$I_{\Delta\lambda} = \sum_{100\ \text{Å}} \int I_\lambda \, d\lambda$$

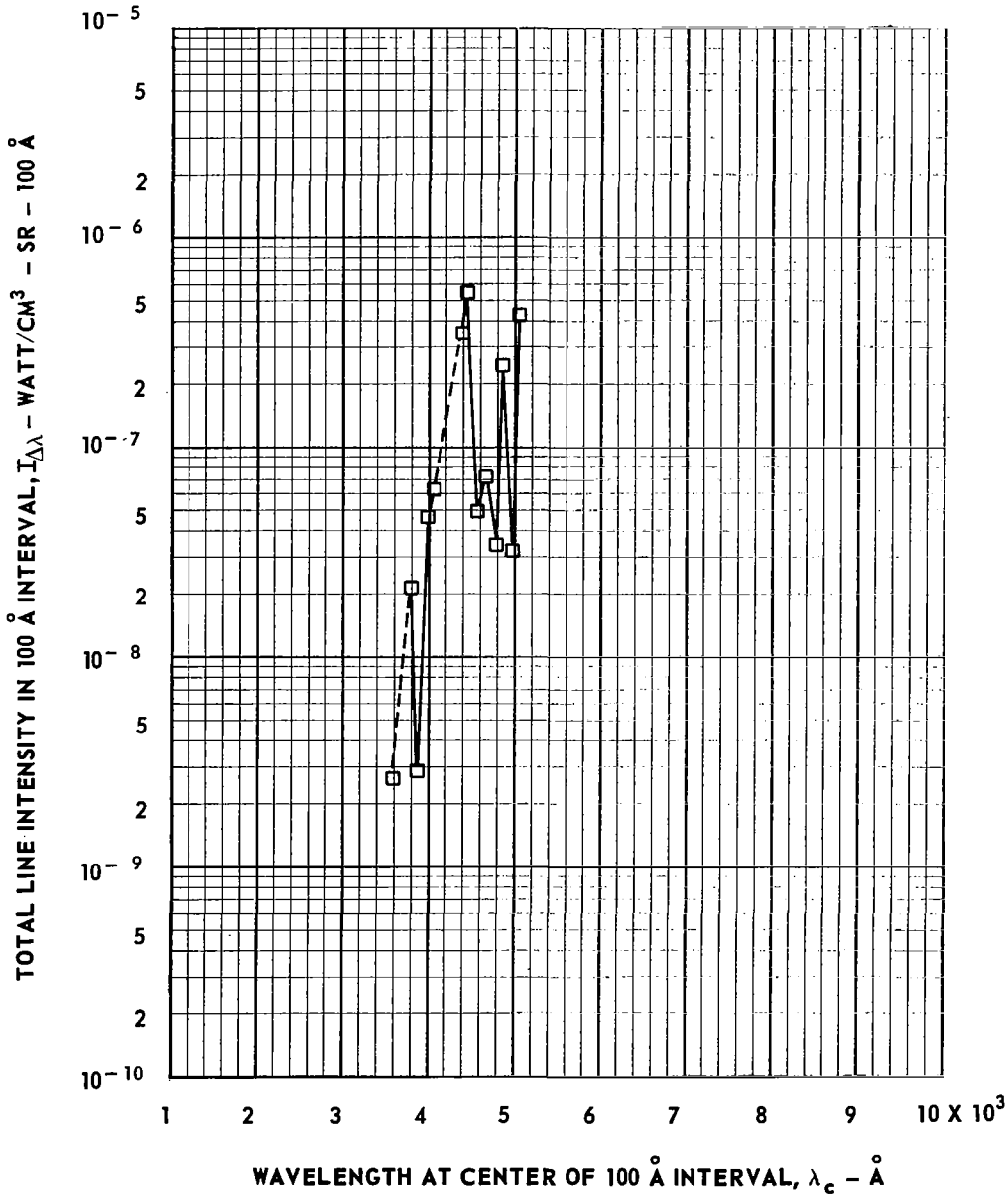

FIG. 24

TOTAL INTEGRATED LINE INTENSITY IN 100 Å WAVELENGTH INTERVALS FOR TUNGSTEN I AND II AT A TEMPERATURE OF 5000 DEG K FOR TUNGSTEN TO ARGON MASS RATIO OF 1.0×10^{-3}

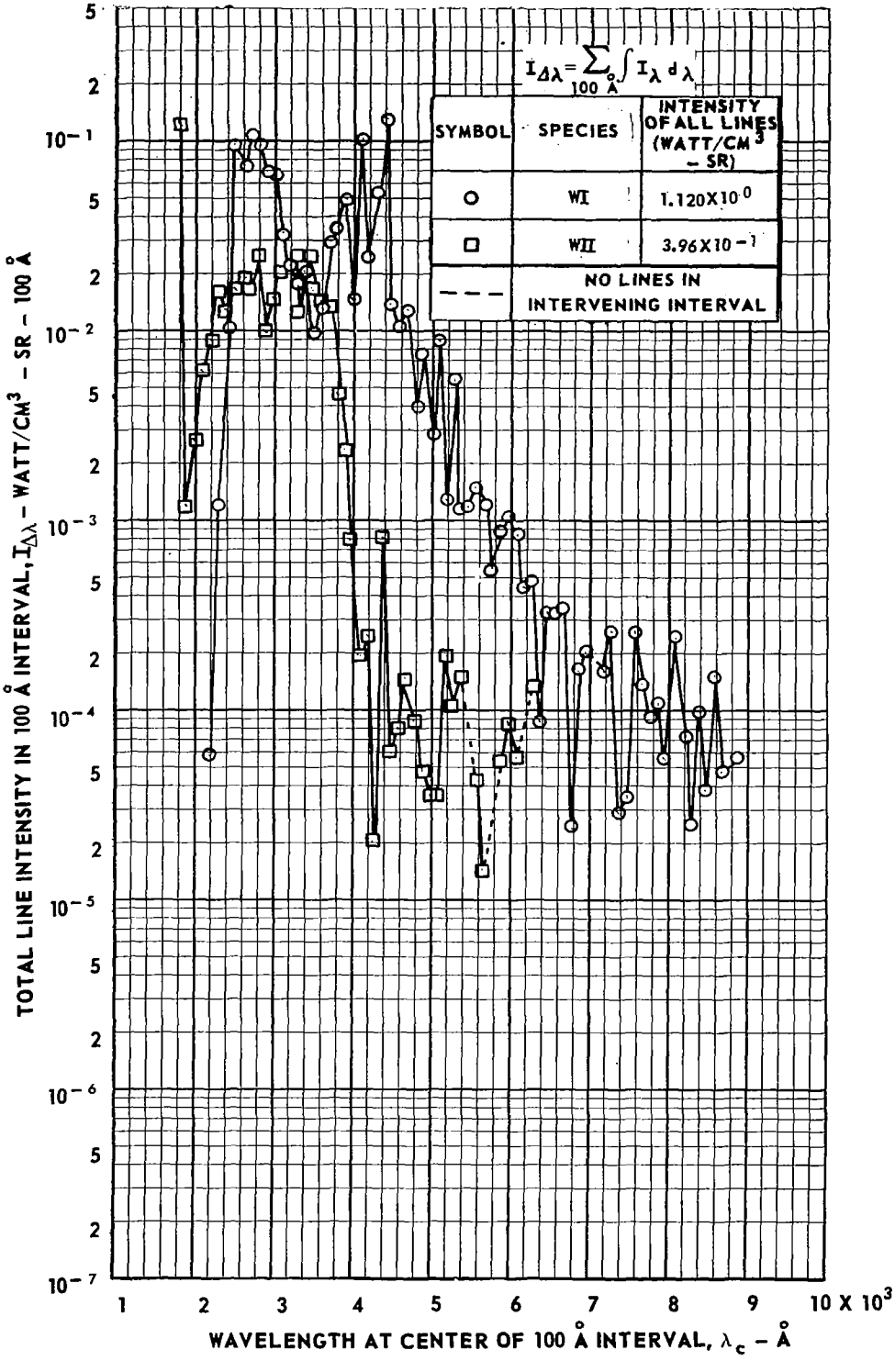

FIG. 25

TOTAL INTEGRATED LINE INTENSITY IN 100 Å WAVELENGTH INTERVALS FOR TUNGSTEN I AND II AT A TEMPERATURE OF 7000 DEG K FOR TUNGSTEN TO ARGON MASS RATIO OF 1.0×10^{-3}

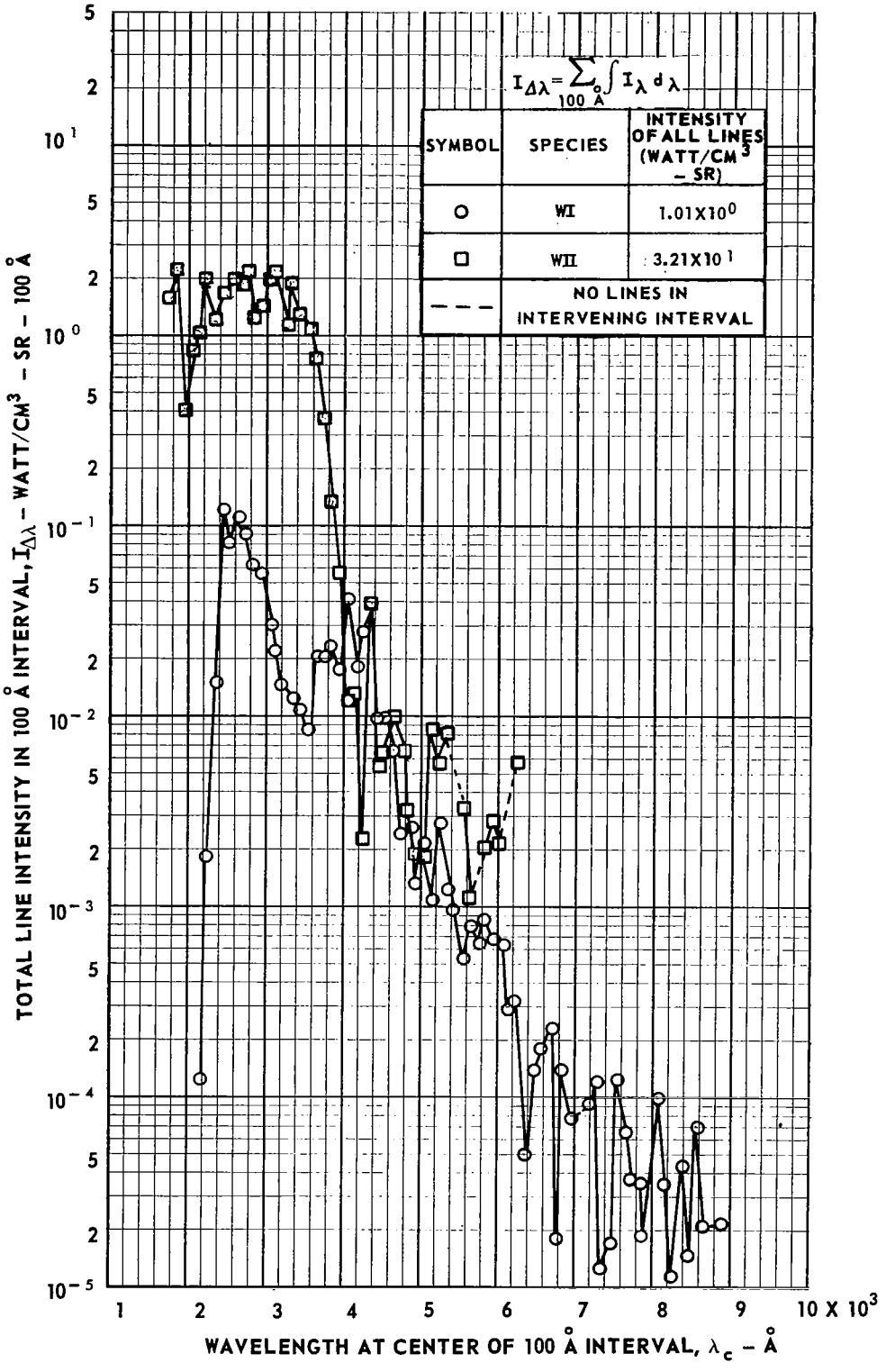

FIG. 26

TOTAL INTEGRATED LINE INTENSITY IN 100 Å WAVELENGTH INTERVALS FOR TUNGSTEN I AND II AT A TEMPERATURE OF 9000 DEG K FOR TUNGSTEN TO ARGON MASS RATIO OF 1.0×10^{-3}

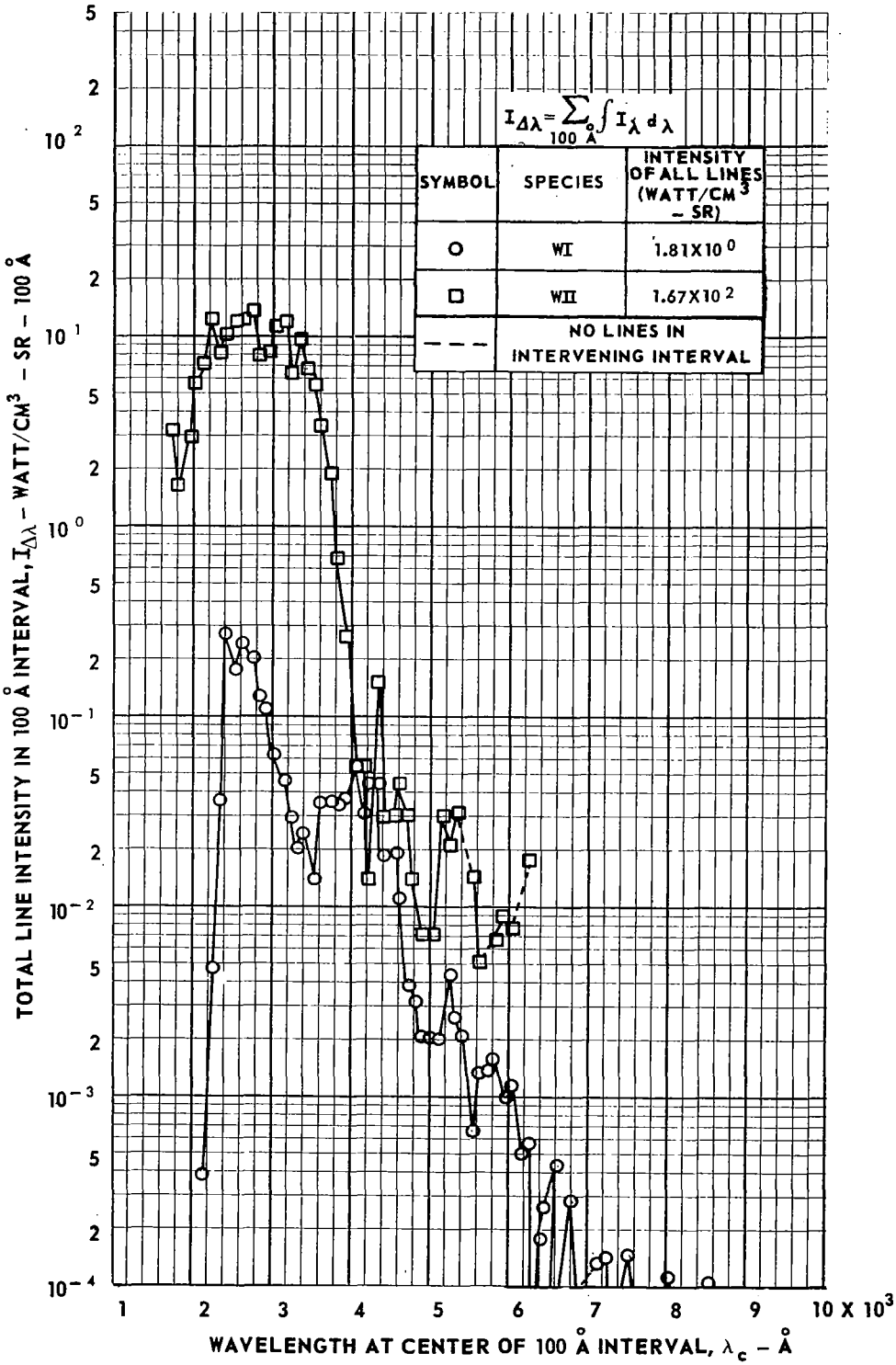

FIG. 27

TOTAL INTEGRATED LINE INTENSITY IN 100 Å WAVELENGTH INTERVALS FOR TUNGSTEN I AND II AT A TEMPERATURE OF 5000 DEG K FOR TUNGSTEN TO ARGON MASS RATIO OF 1.0×10^{-5}

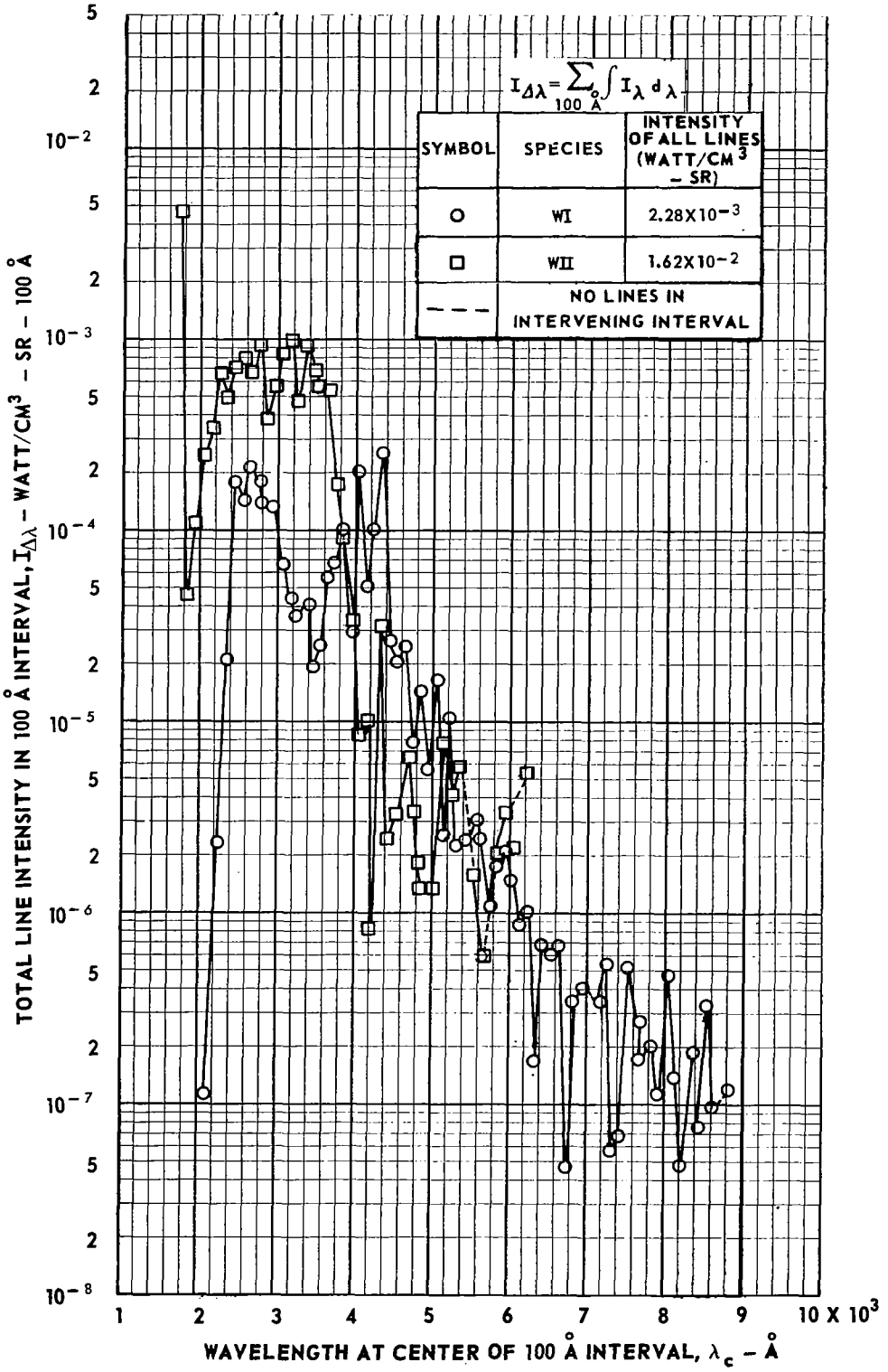

FIG. 28

TOTAL INTEGRATED LINE INTENSITY IN 100 Å WAVELENGTH INTERVALS FOR TUNGSTEN I AND II AT A TEMPERATURE OF 7000 DEG K FOR TUNGSTEN TO ARGON MASS RATIO OF 1.0×10^{-5}

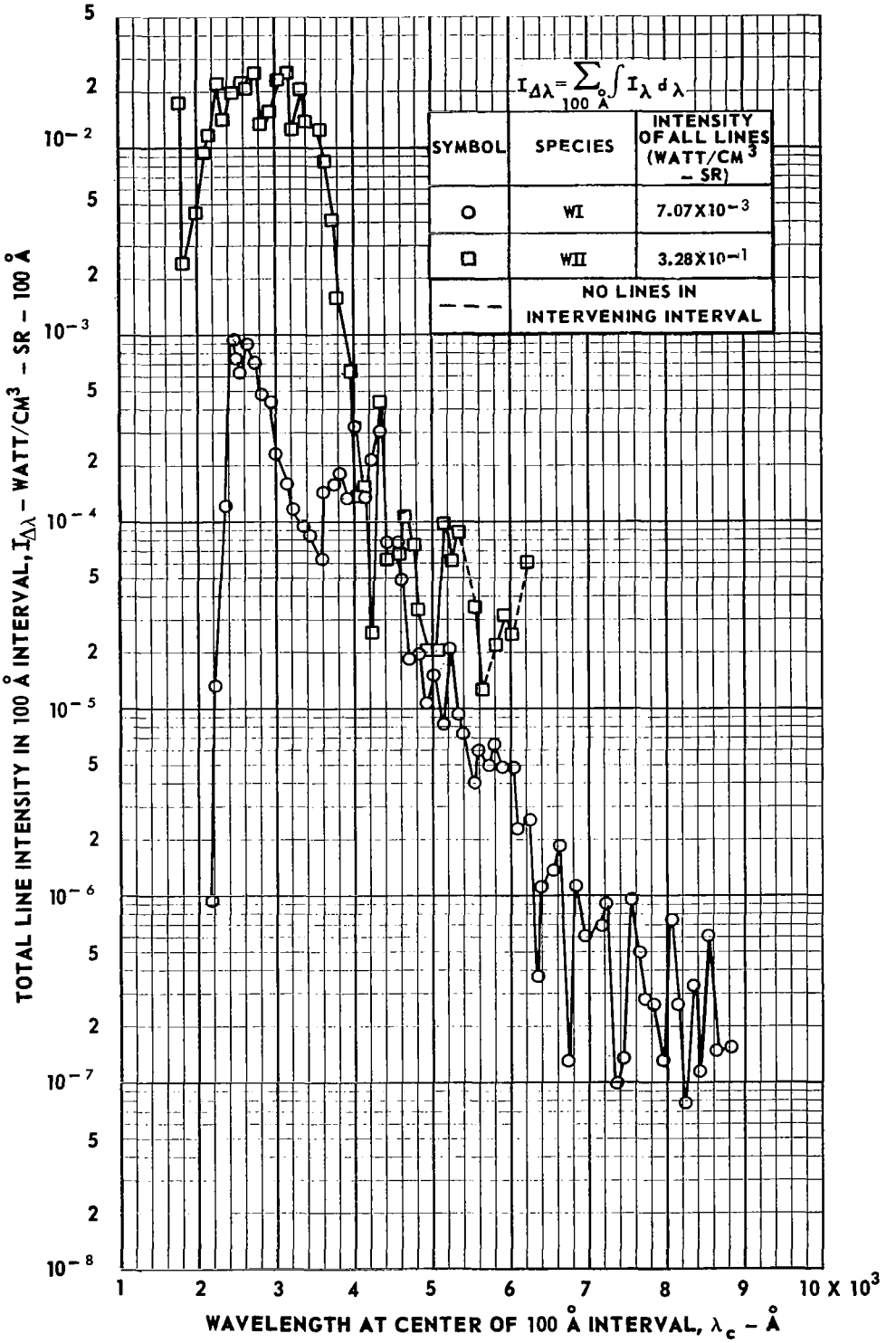

FIG. 29

TOTAL INTEGRATED LINE INTENSITY IN 100 Å WAVELENGTH INTERVALS FOR TUNGSTEN I AND II AT A TEMPERATURE OF 9000 DEG K FOR TUNGSTEN TO ARGON MASS RATIO OF 1.0×10^{-5}

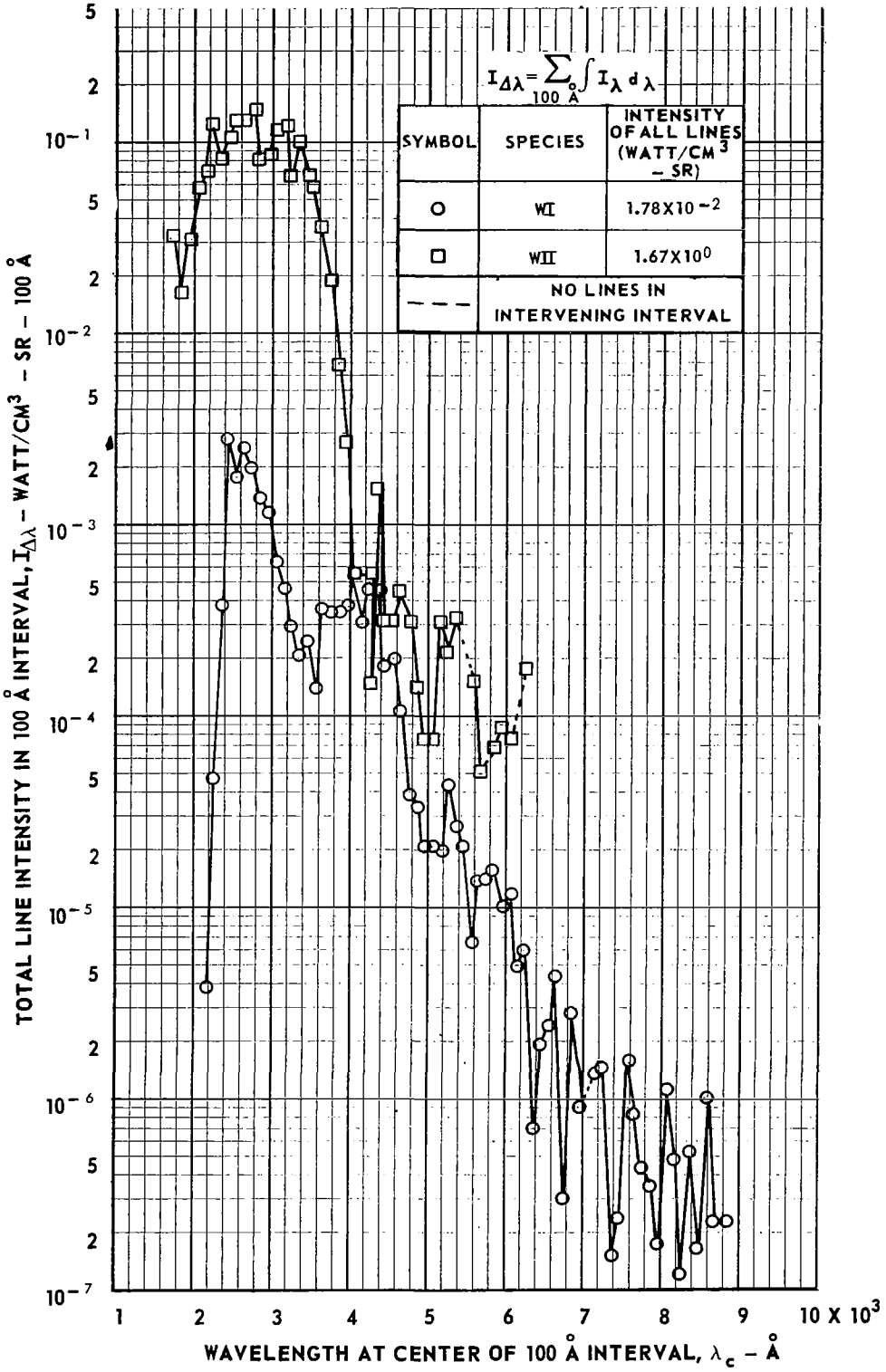

FIG. 30

TOTAL INTEGRATED LINE INTENSITY IN 100 Å WAVELENGTH INTERVALS FOR TUNGSTEN I AND II AT A TEMPERATURE OF 5000 DEG K FOR TUNGSTEN TO ARGON MASS RATIO OF 1.0×10^{-7}

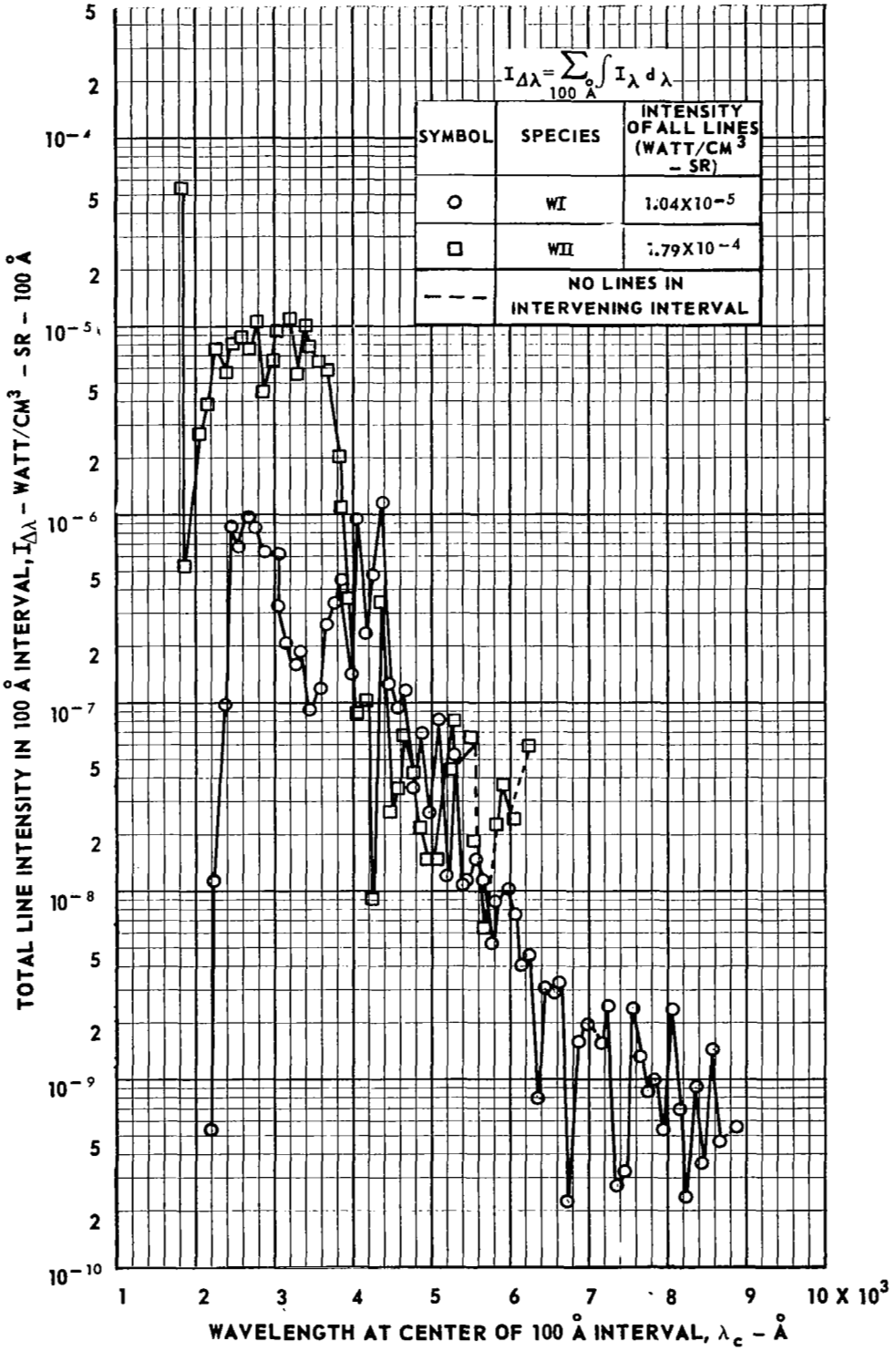

FIG. 31

TOTAL INTEGRATED LINE INTENSITY IN 100 Å WAVELENGTH INTERVALS FOR TUNGSTEN I AND II AT A TEMPERATURE OF 7000 DEG K FOR TUNGSTEN TO ARGON MASS RATIO OF 1.0×10^{-7}

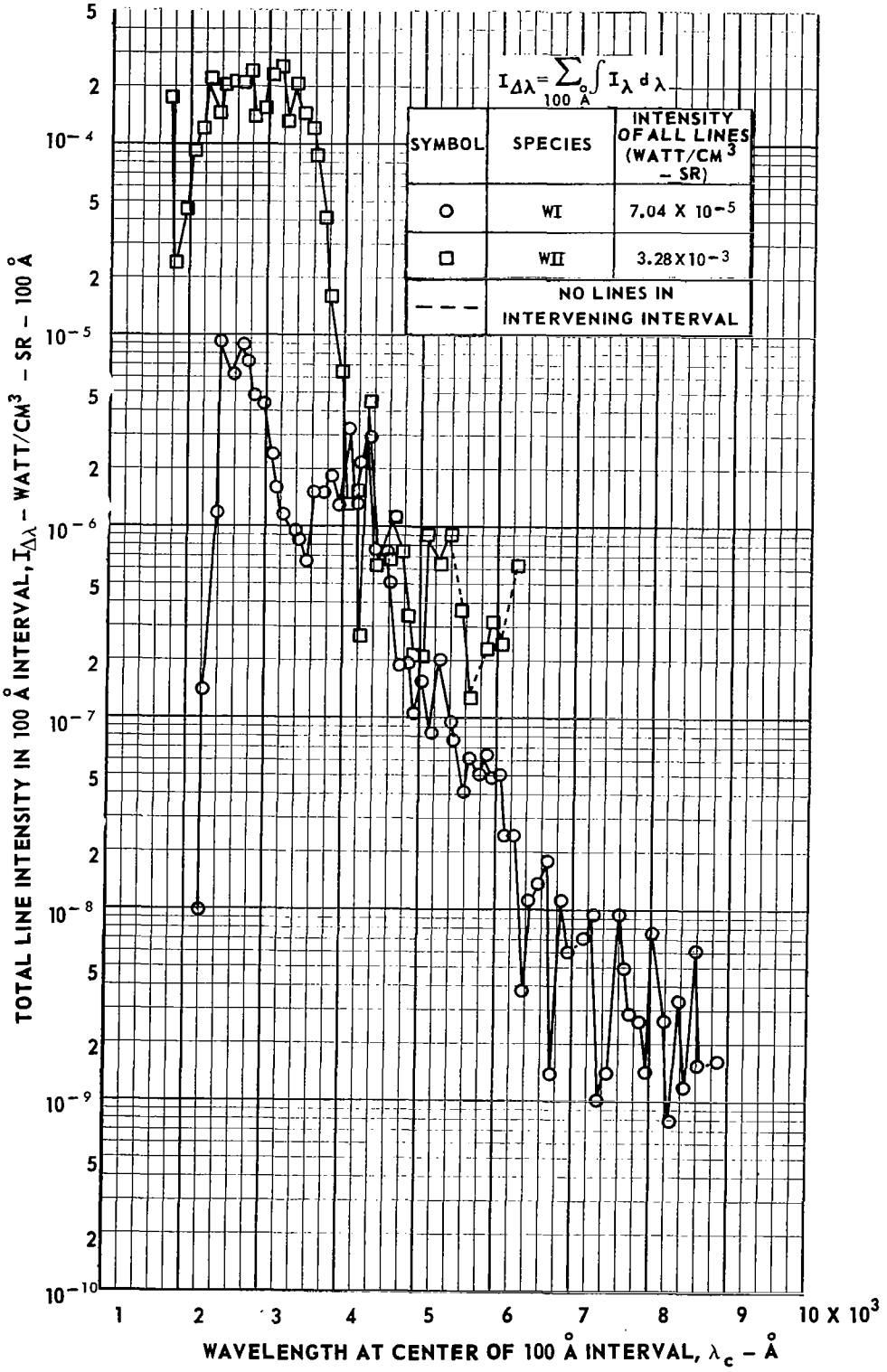

FIG. 32

TOTAL INTEGRATED LINE INTENSITY IN 100 Å WAVELENGTH INTERVALS FOR TUNGSTEN I AND II AT A TEMPERATURE OF 9000 DEG K FOR TUNGSTEN TO ARGON MASS RATIO OF 1.0×10^{-7}

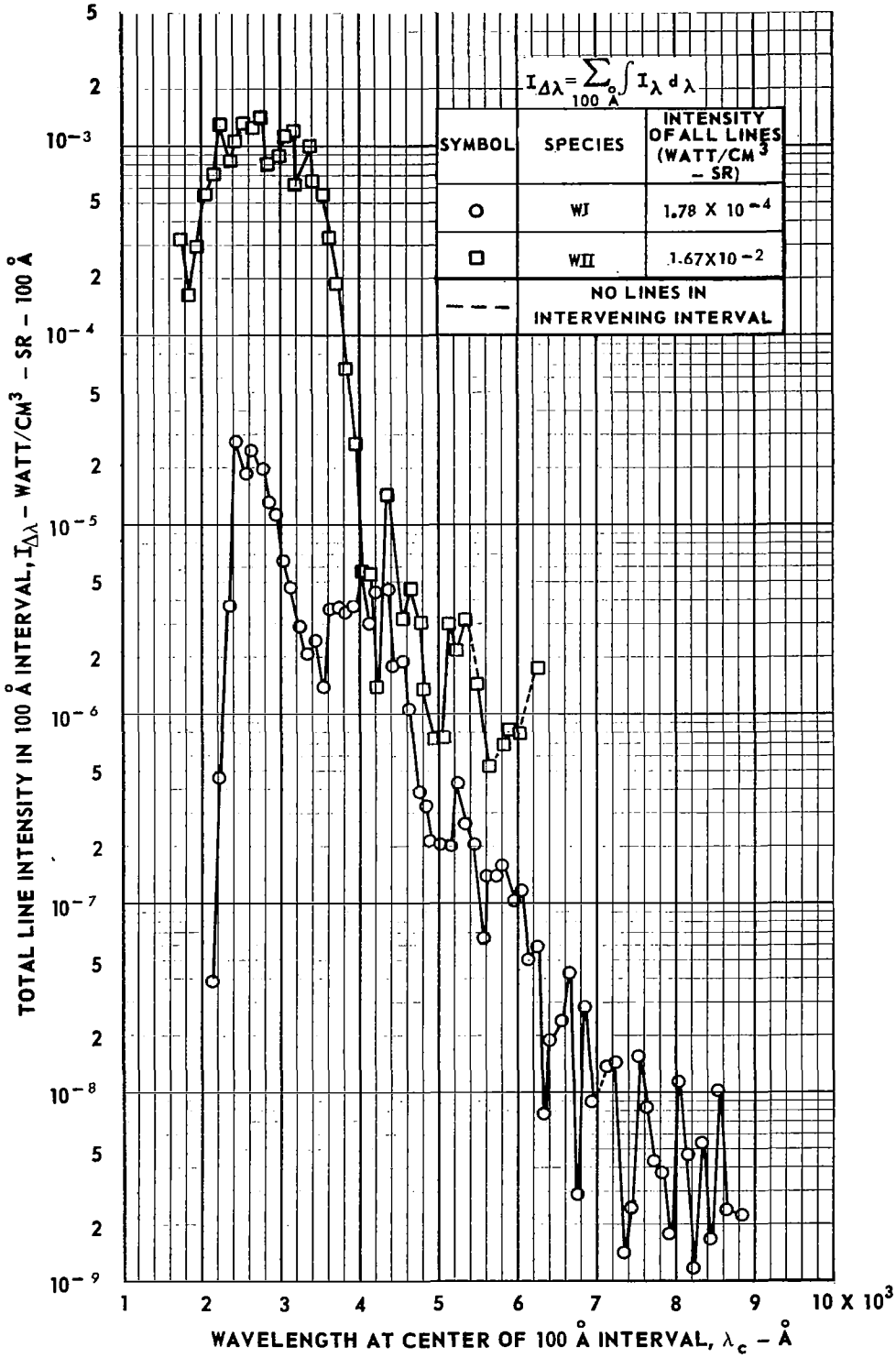

FIG. 33

TOTAL INTEGRATED LINE INTENSITY IN 100 Å WAVELENGTH INTERVALS FOR URANIUM I AND II AT A TEMPERATURE OF 5000 DEG K FOR URANIUM TO ARGON MASS RATIO OF 1.0×10^{-3}

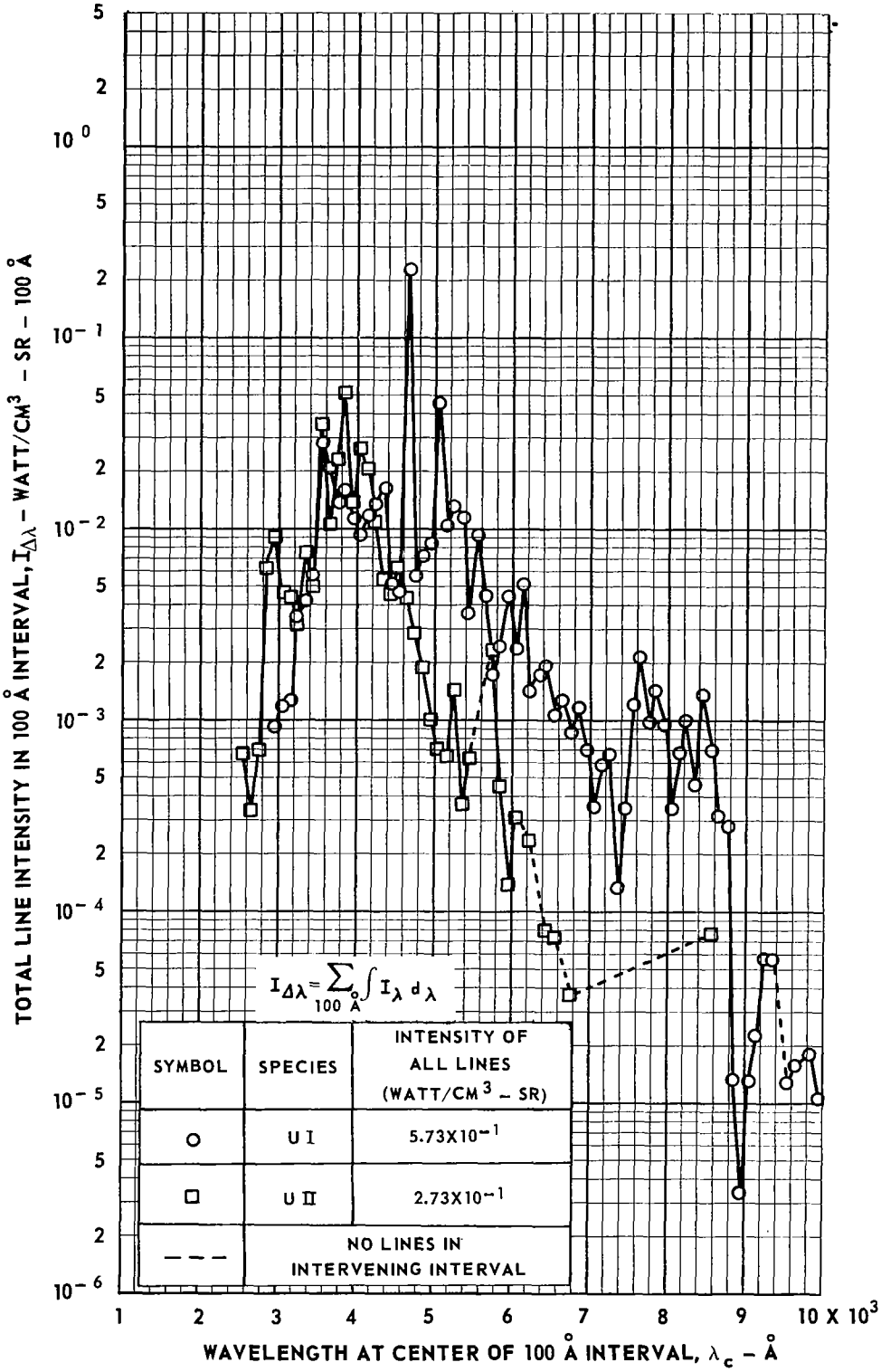

FIG. 34

TOTAL INTEGRATED LINE INTENSITY IN 100 Å WAVELENGTH INTERVALS FOR URANIUM I AND II AT A TEMPERATURE OF 7000 DEG K FOR URANIUM TO ARGON MASS RATIO OF 1.0×10^{-3}

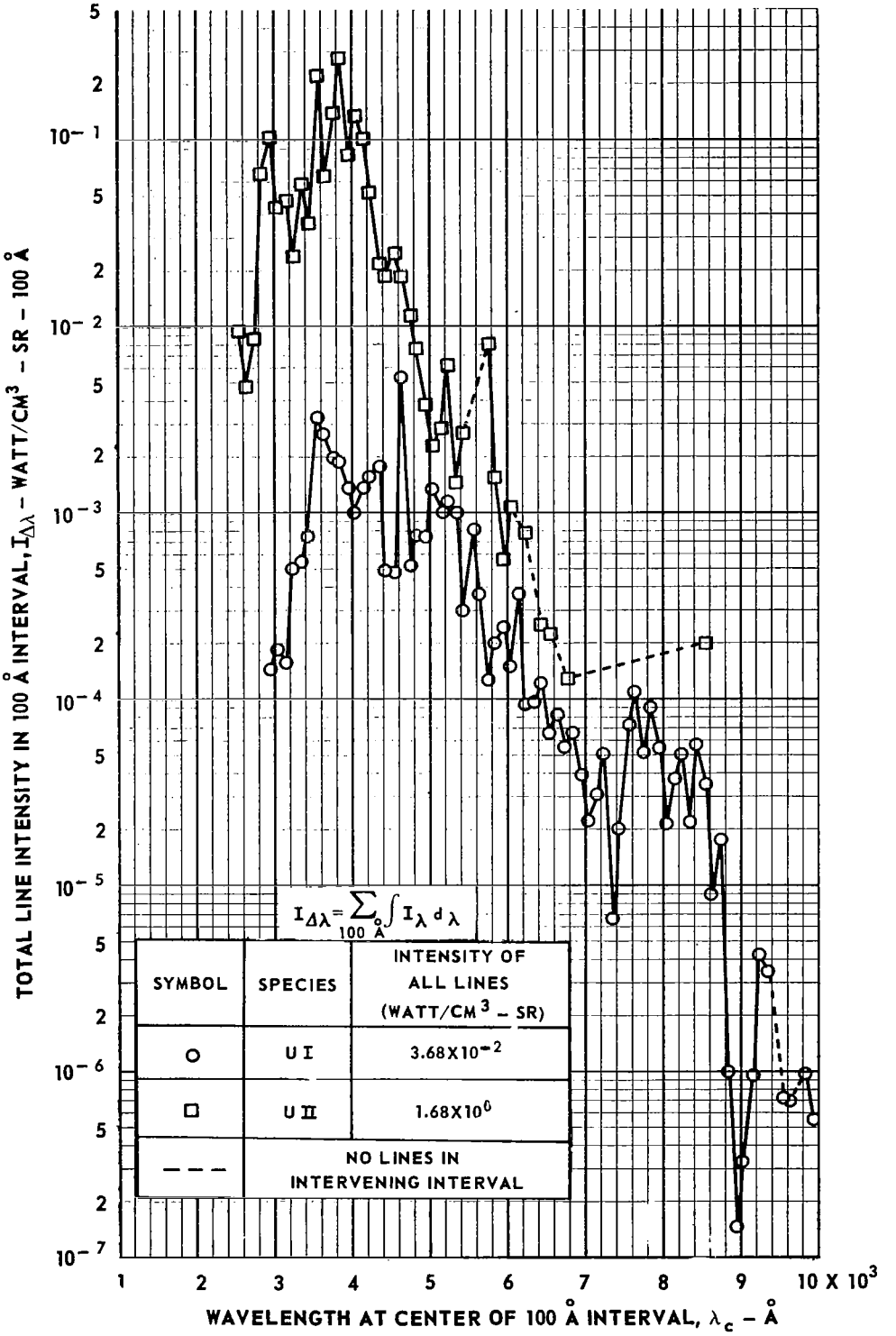

FIG. 35

TOTAL INTEGRATED LINE INTENSITY IN 100 Å WAVELENGTH INTERVALS FOR URANIUM I AND II AT A TEMPERATURE OF 9000 DEG K FOR URANIUM TO ARGON MASS RATIO OF 1.0×10^{-3}

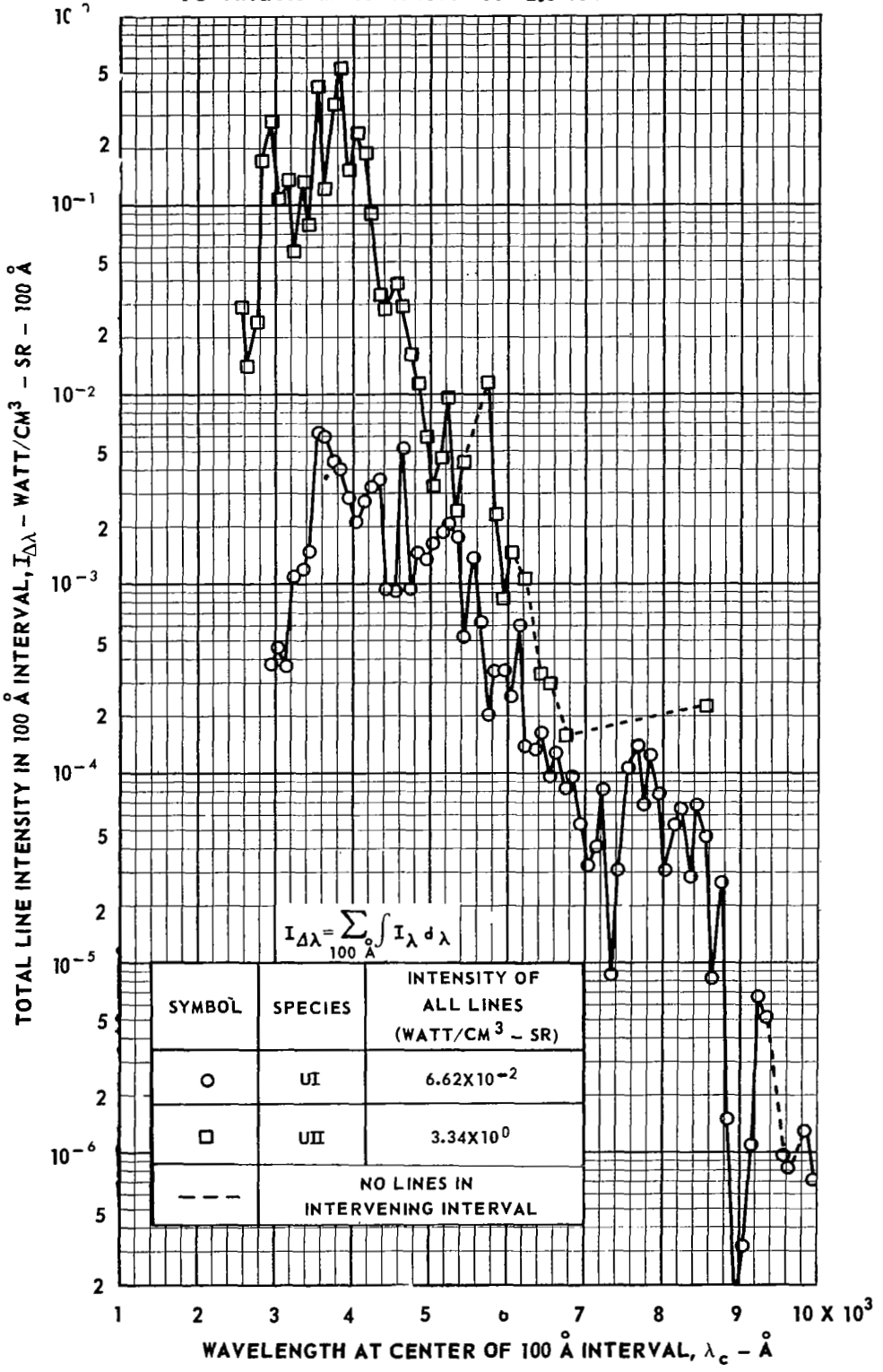

FIG. 36

TOTAL INTEGRATED LINE INTENSITY IN 100 Å WAVELENGTH INTERVALS FOR URANIUM I AND II AT A TEMPERATURE OF 5000 DEG K FOR URANIUM TO ARGON MASS RATIO OF 1.0×10^{-5}

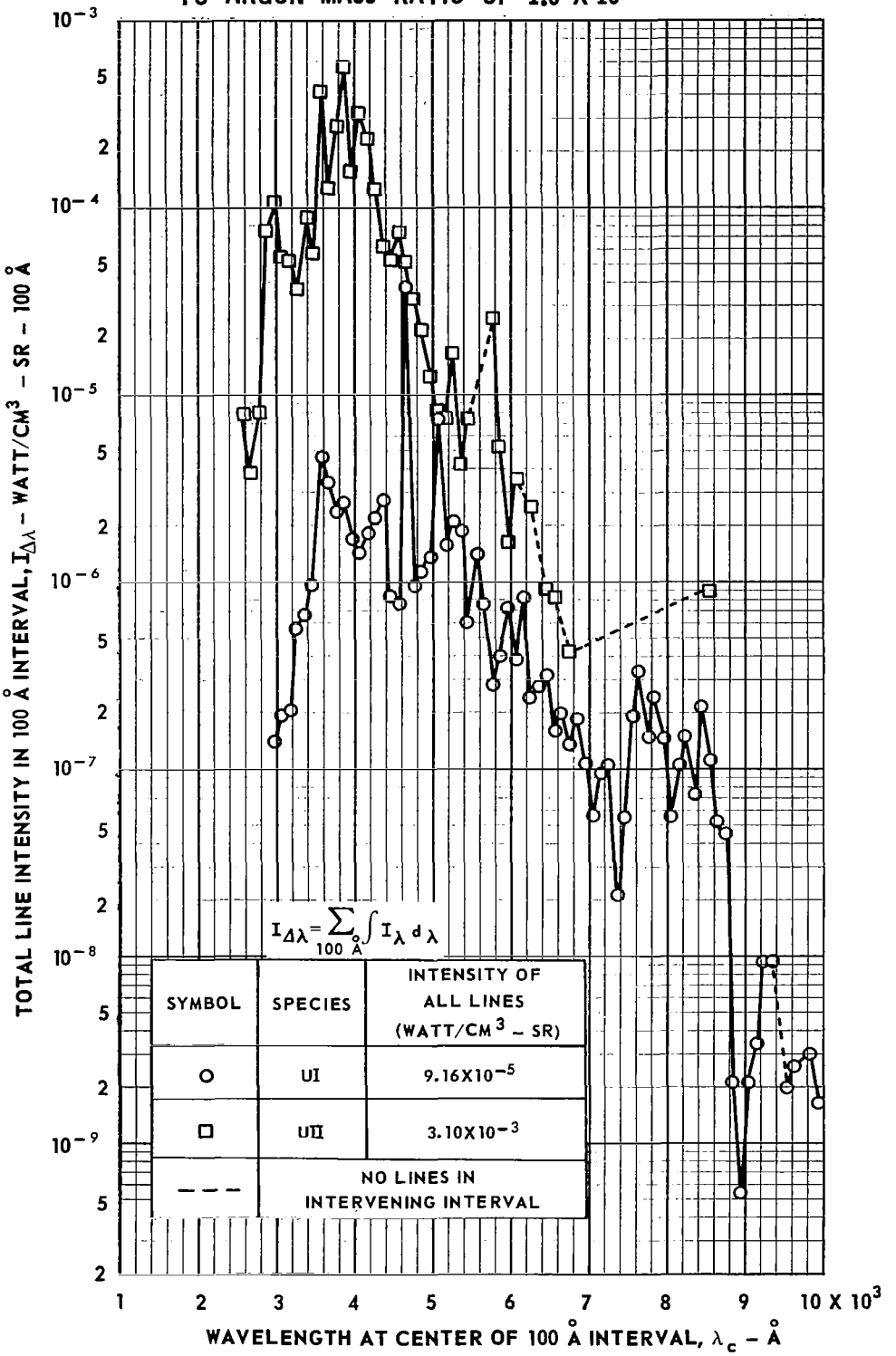

FIG. 37

TOTAL INTEGRATED LINE INTENSITY IN 100 Å WAVELENGTH INTERVALS FOR URANIUM I AND II AT A TEMPERATURE OF 7000 DEG K FOR URANIUM TO ARGON MASS RATIO OF 1.0×10^{-5}

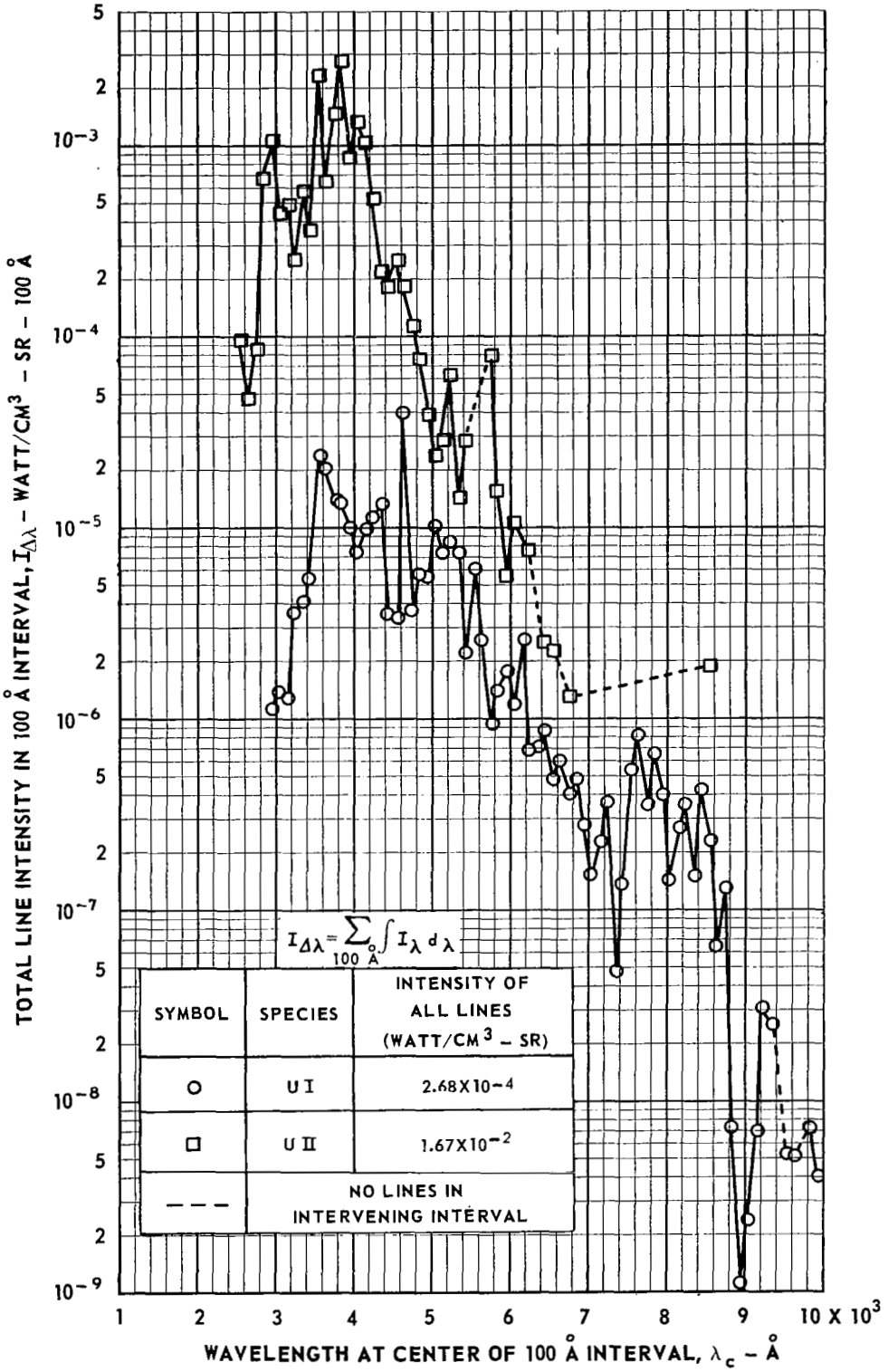

FIG. 38

TOTAL INTEGRATED LINE INTENSITY IN 100 Å WAVELENGTH INTERVALS FOR URANIUM I AND II AT A TEMPERATURE OF 9000 DEG K FOR URANIUM TO ARGON MASS RATIO OF 1.0×10^{-5}

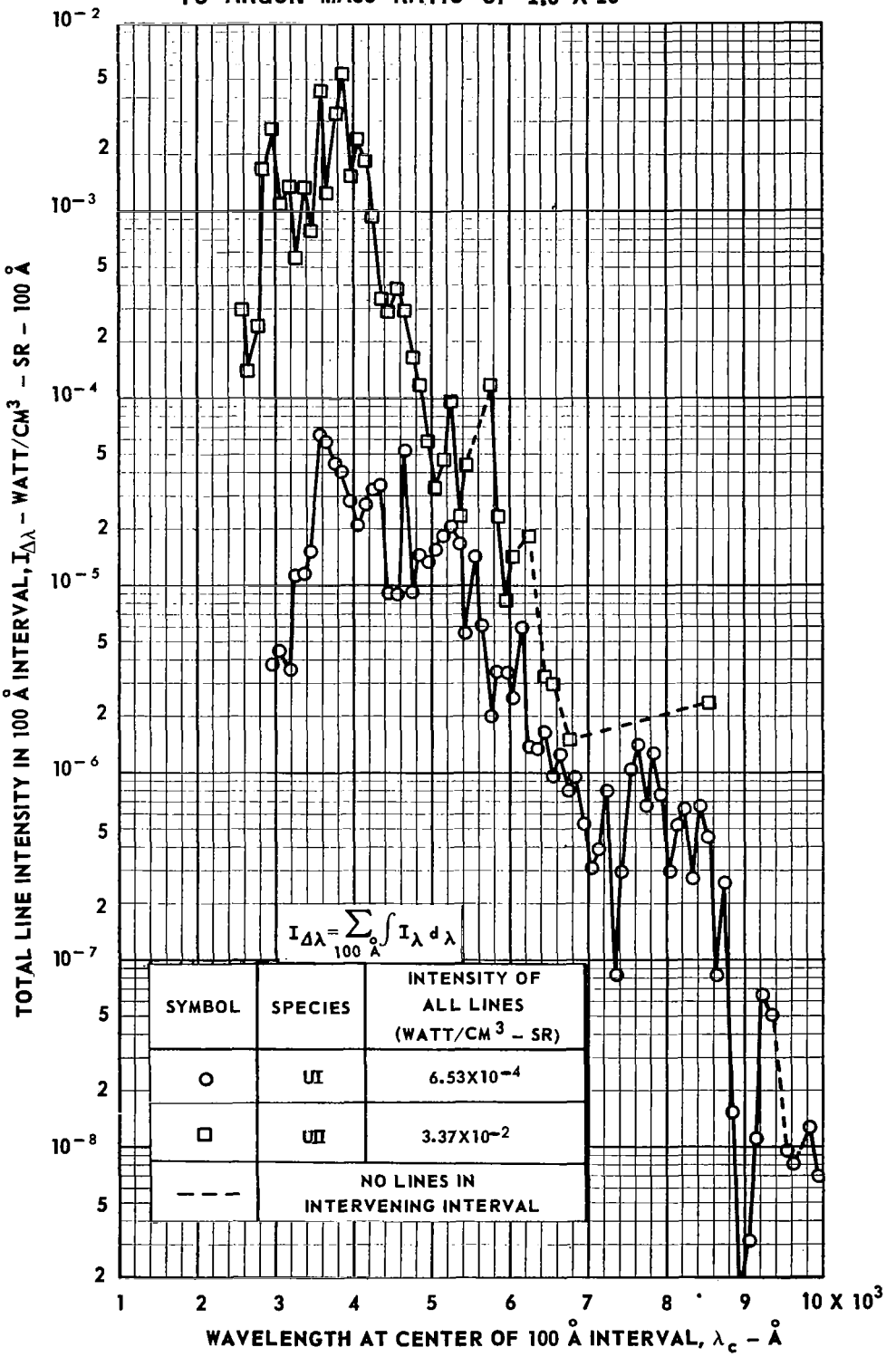

FIG. 39

TOTAL INTEGRATED LINE INTENSITY IN 100 Å WAVELENGTH INTERVALS FOR URANIUM I AND II AT A TEMPERATURE OF 5000 DEG K FOR URANIUM TO ARGON MASS RATIO OF 1.0×10^{-7}

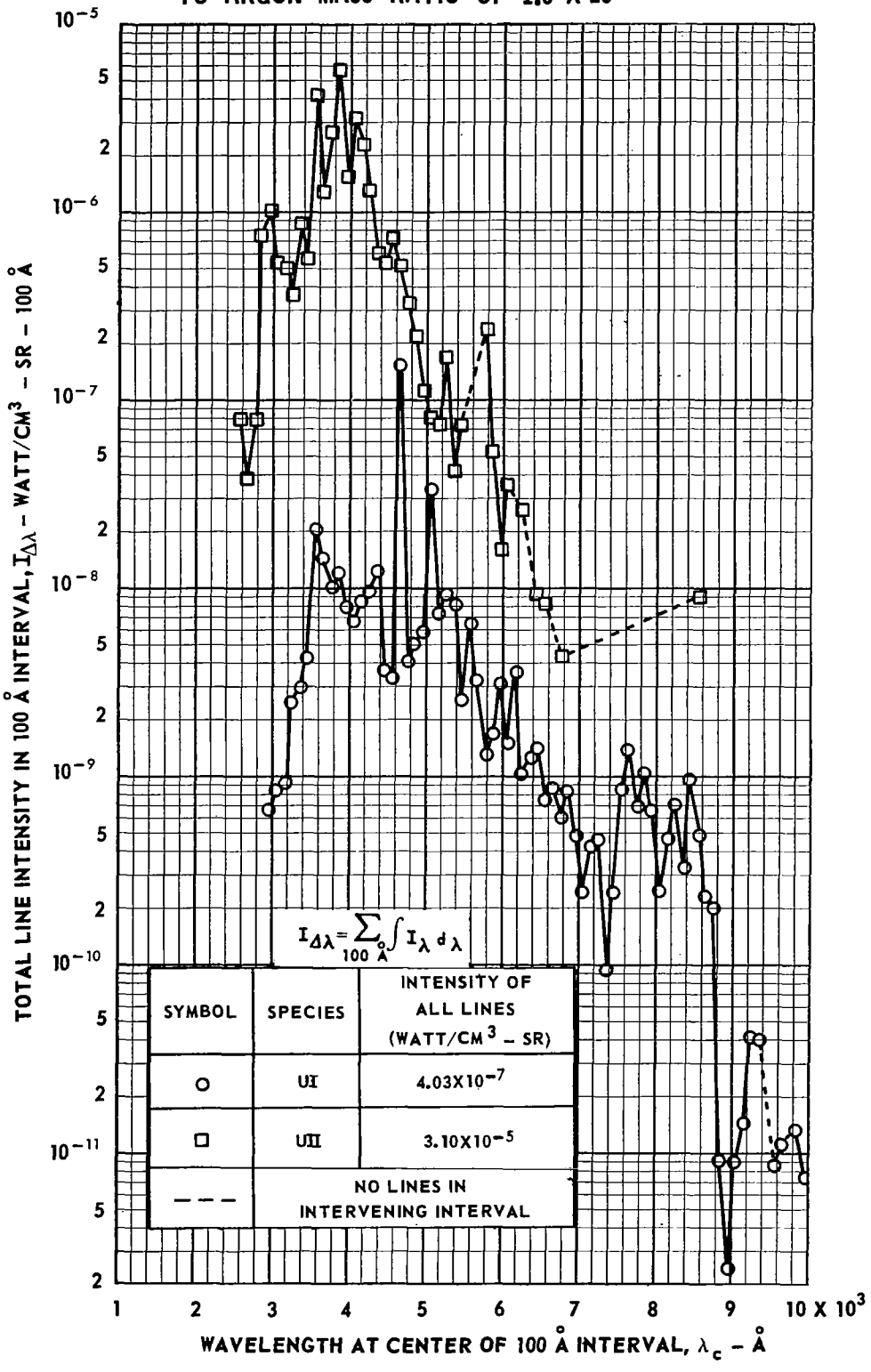

FIG. 40

TOTAL INTEGRATED LINE INTENSITY IN 100 Å WAVELENGTH INTERVALS FOR URANIUM I AND II AT A TEMPERATURE OF 7000 DEG K FOR URANIUM TO ARGON MASS RATIO OF 1.0×10^{-7}

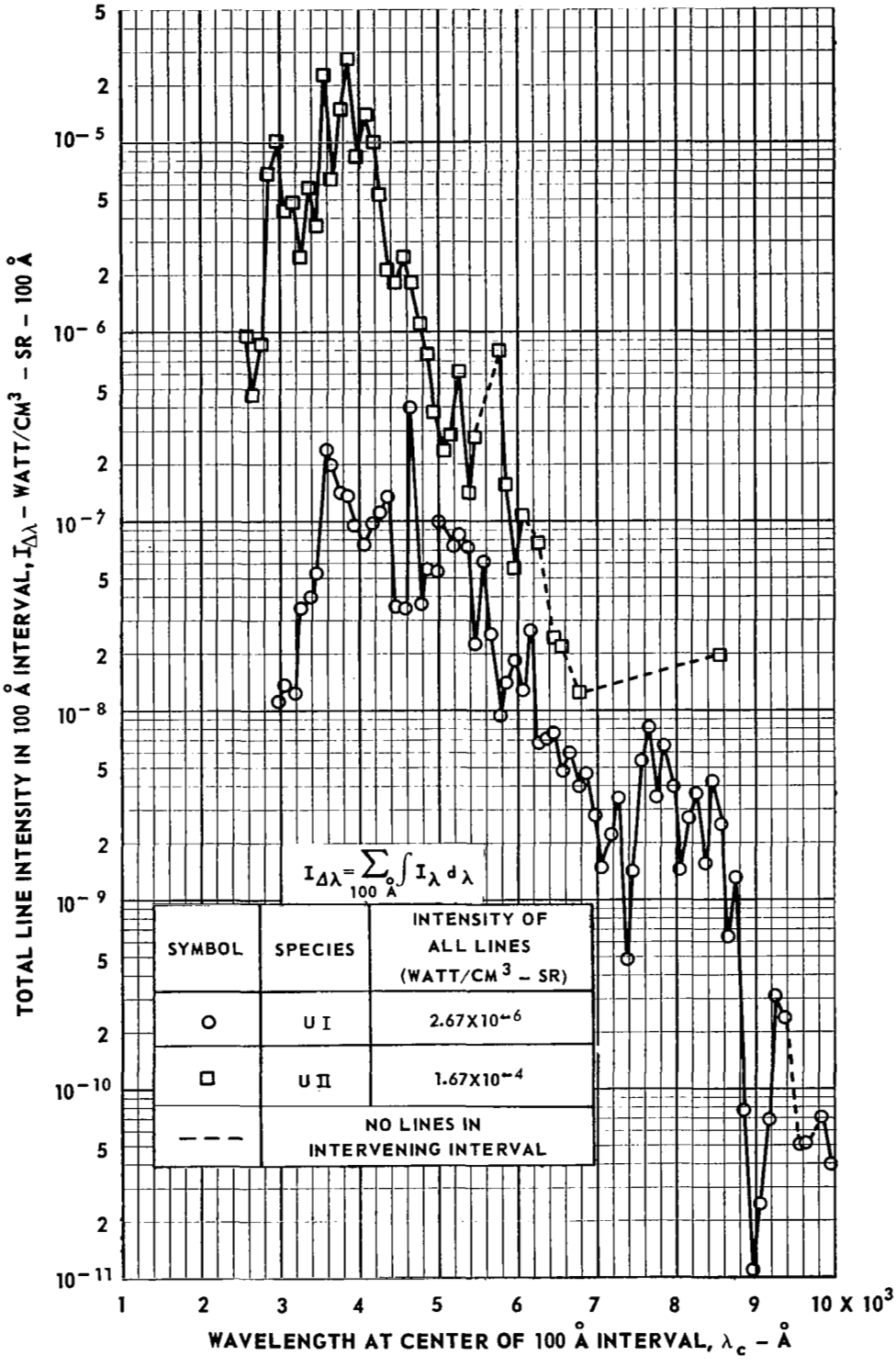

FIG. 41

TOTAL INTEGRATED LINE INTENSITY IN 100 Å WAVELENGTH INTERVALS FOR URANIUM I AND II AT A TEMPERATURE OF 9000 DEG K FOR URANIUM TO ARGON MASS RATIO OF 1.0×10^{-7}

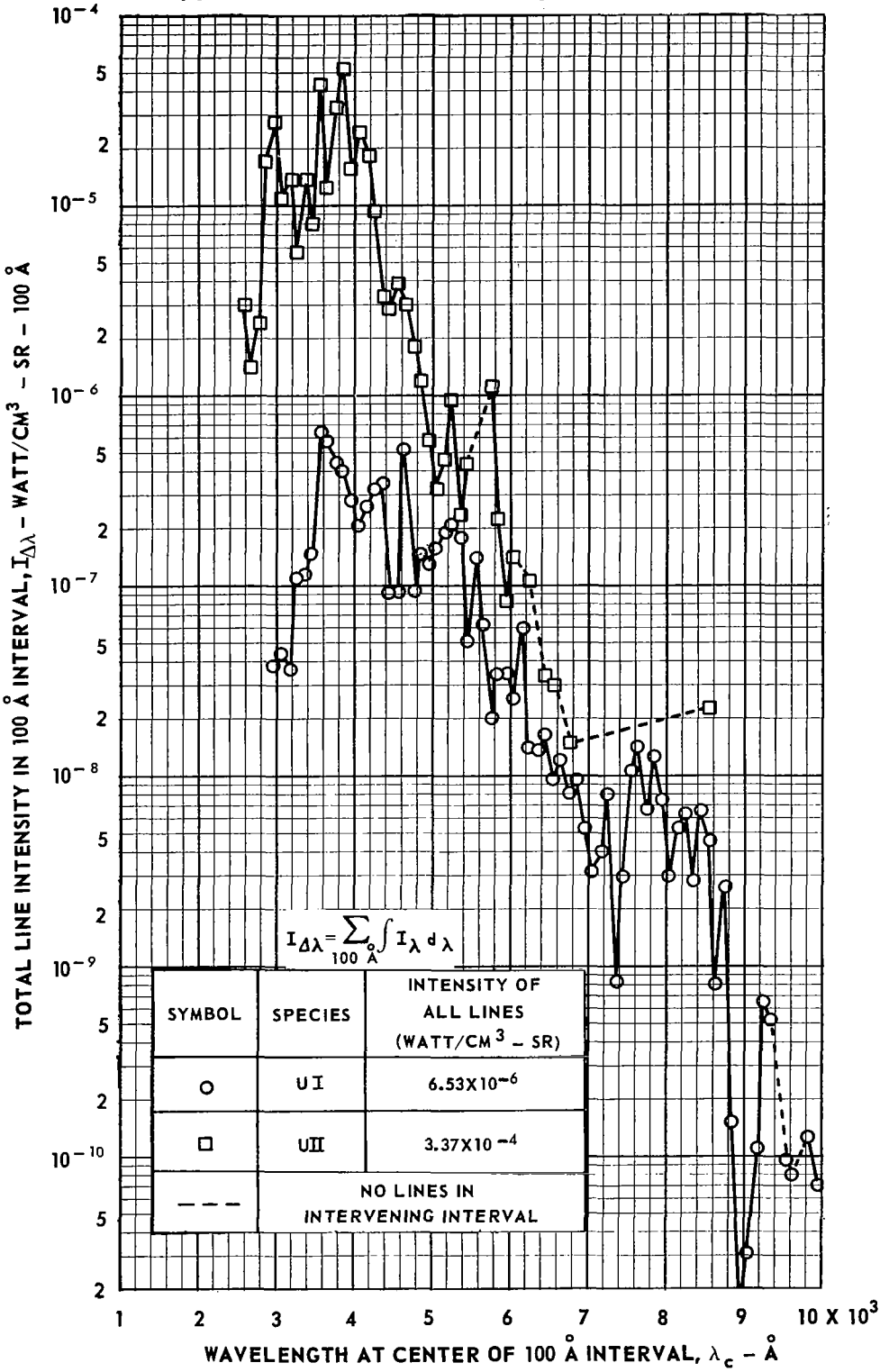

FIG. 42

SUM OF TUNGSTEN I AND II LINE INTENSITIES IN 100 Å INTERVALS AT TEMPERATURE OF 5000 DEG K FOR VARIOUS TUNGSTEN TO ARGON MASS RATIOS

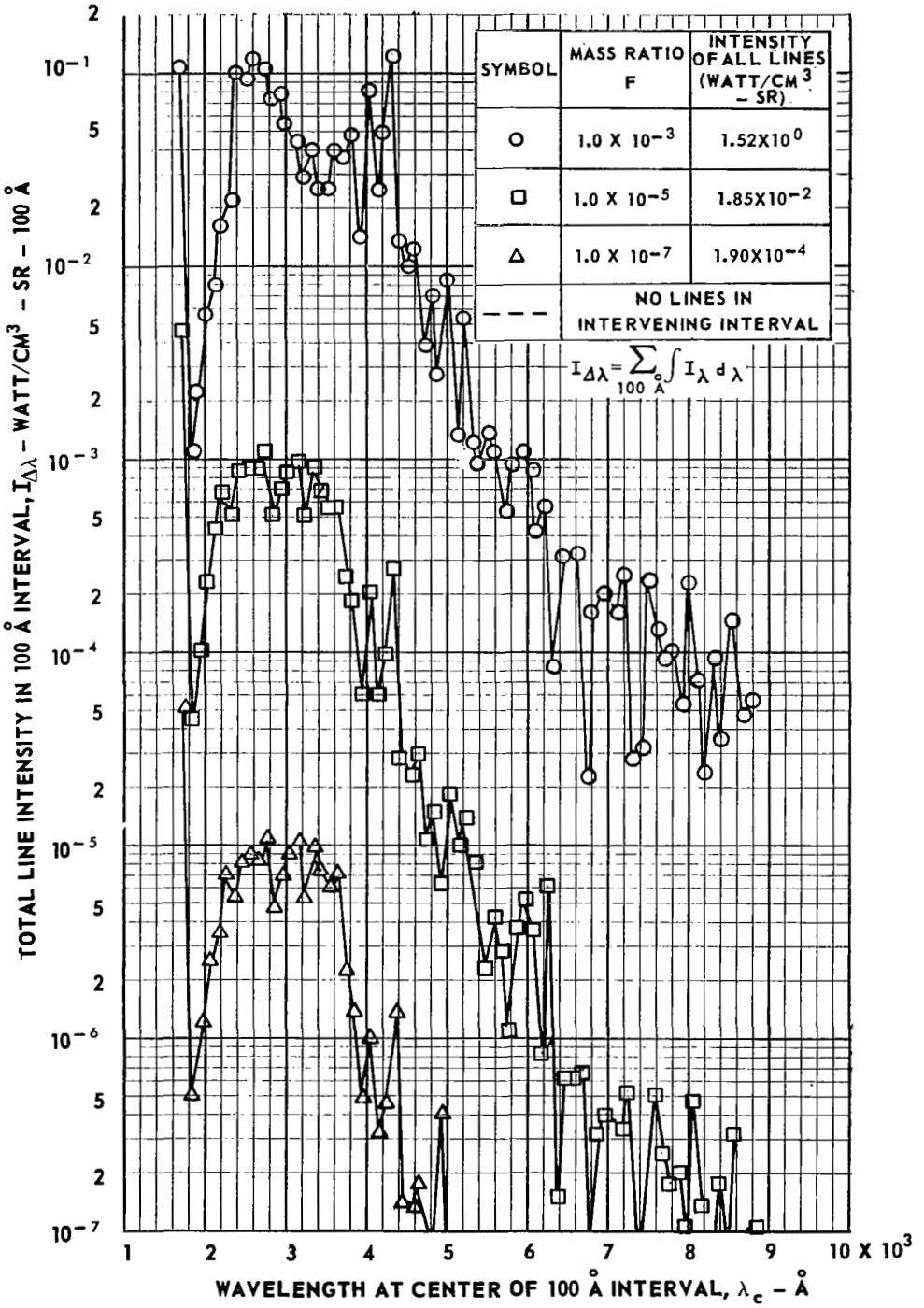

FIG. 43

SUM OF TUNGSTEN I AND II LINE INTENSITIES IN 100 Å INTERVALS AT TEMPERATURE OF 7000 DEG K FOR VARIOUS TUNGSTEN TO ARGON MASS RATIOS

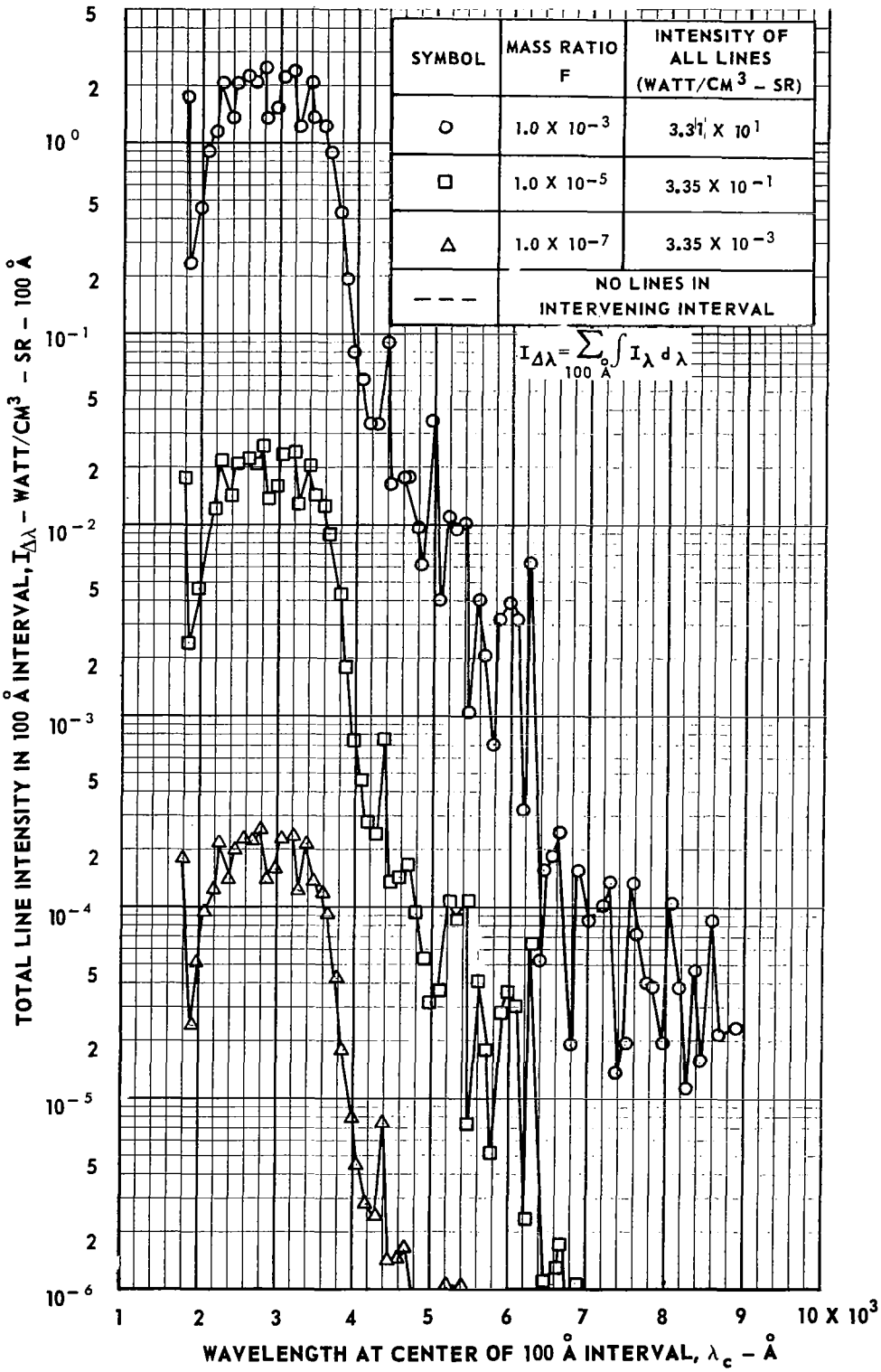

FIG. 44

SUM OF TUNGSTEN I AND II LINE INTENSITIES IN 100 Å INTERVALS AT TEMPERATURE OF 9000 DEG K FOR VARIOUS TUNGSTEN TO ARGON MASS RATIOS

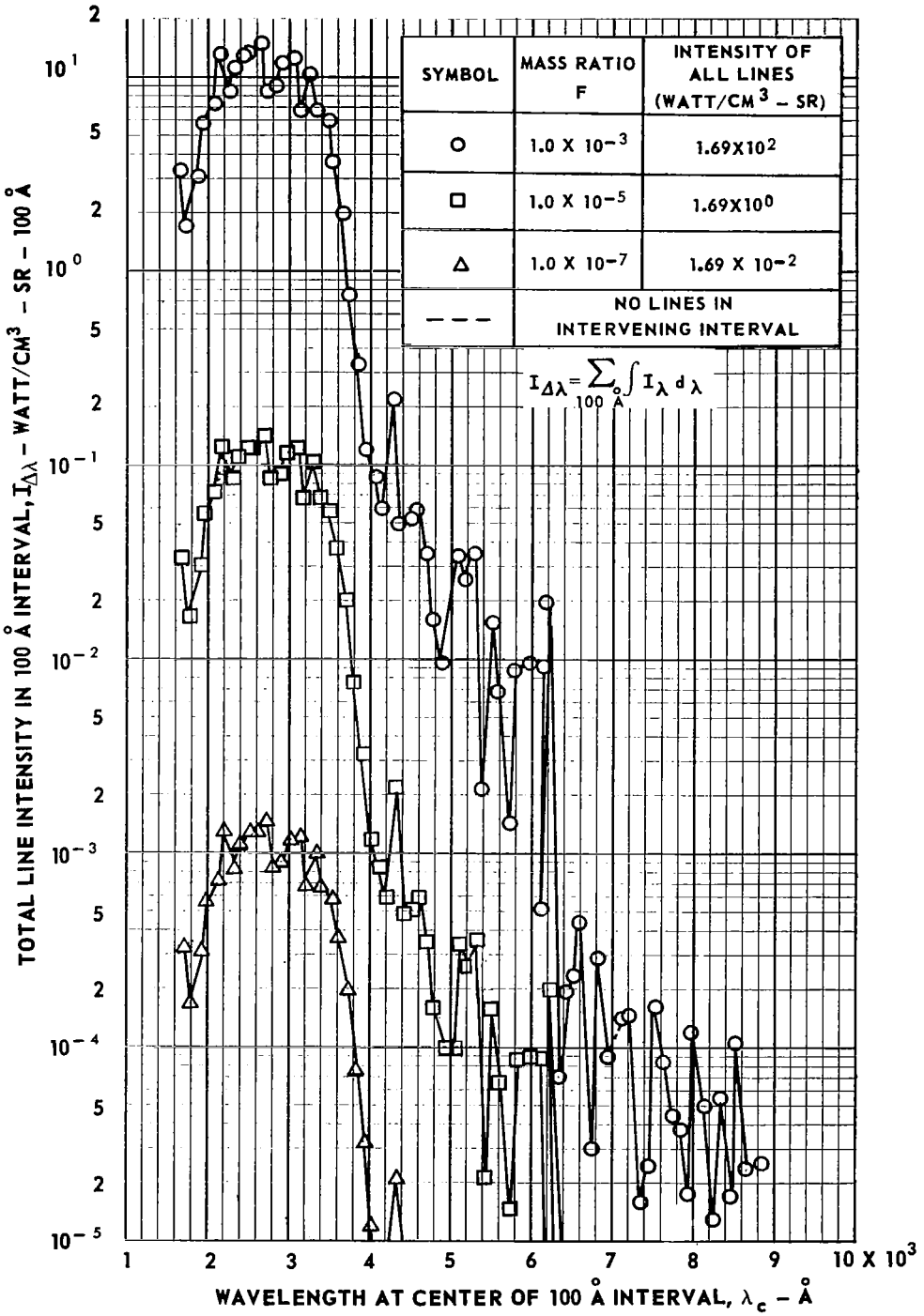

FIG. 45

SUM OF URANIUM I AND II LINE INTENSITIES IN 100 Å INTERVALS AT TEMPERATURE OF 5000 DEG K FOR VARIOUS URANIUM TO ARGON MASS RATIOS

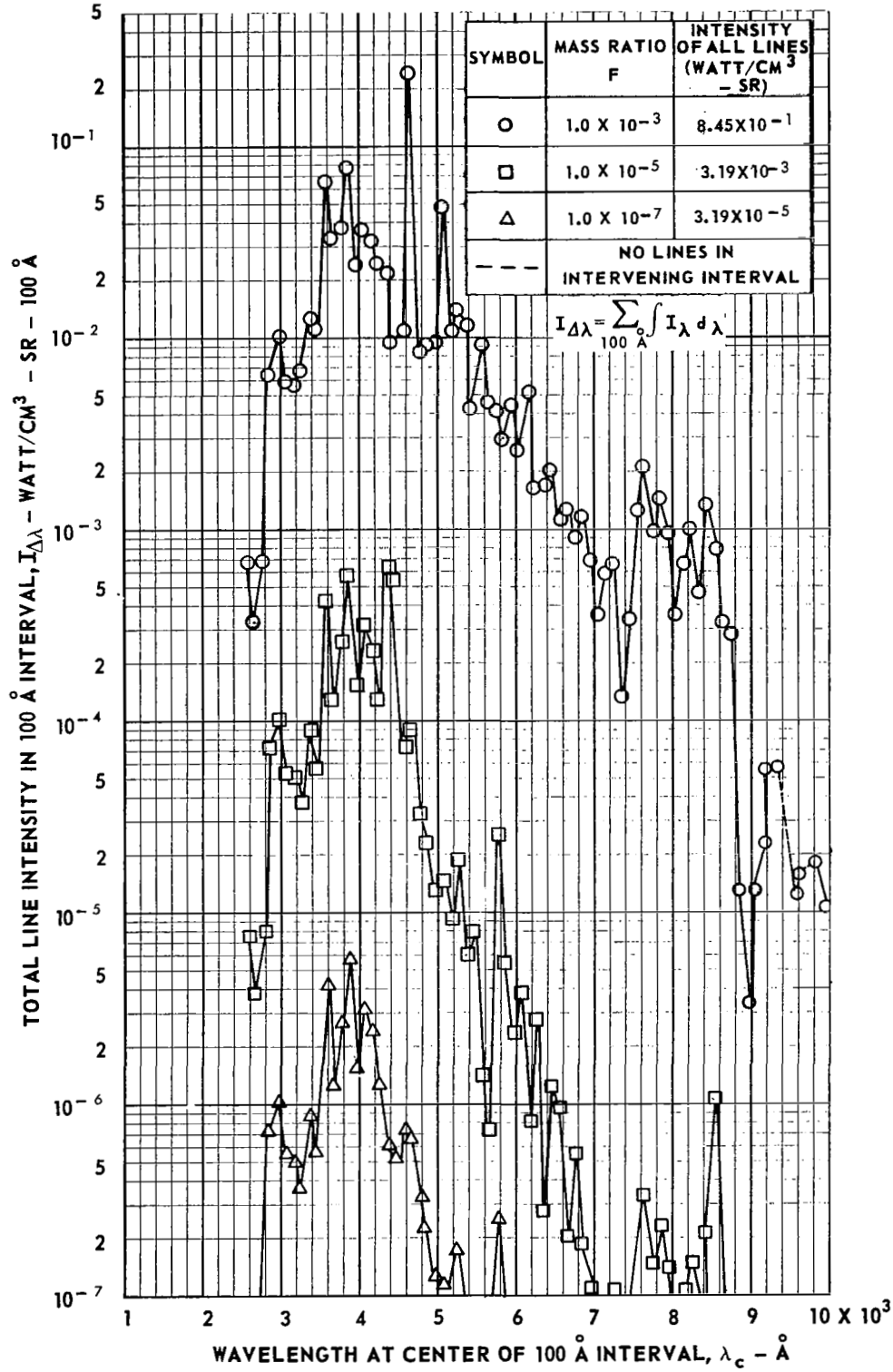

FIG. 46

SUM OF URANIUM I AND II LINE INTENSITIES IN 100 Å INTERVALS AT TEMPERATURE OF 7000 DEG K FOR VARIOUS URANIUM TO ARGON MASS RATIOS

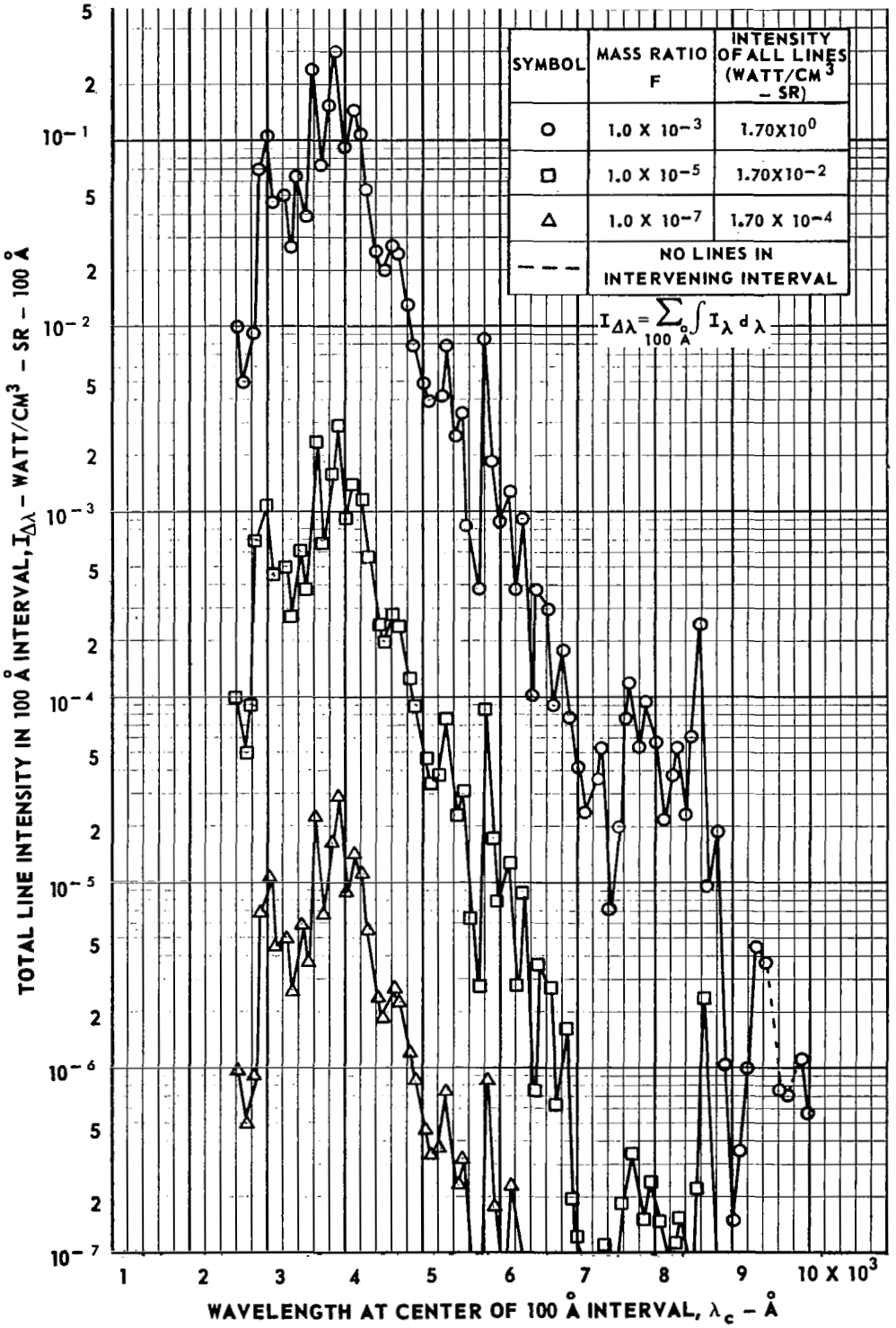

FIG. 47

SUM OF URANIUM I AND II LINE INTENSITIES IN 100 Å INTERVALS AT TEMPERATURE OF 9000 DEG K FOR VARIOUS URANIUM TO ARGON MASS RATIOS

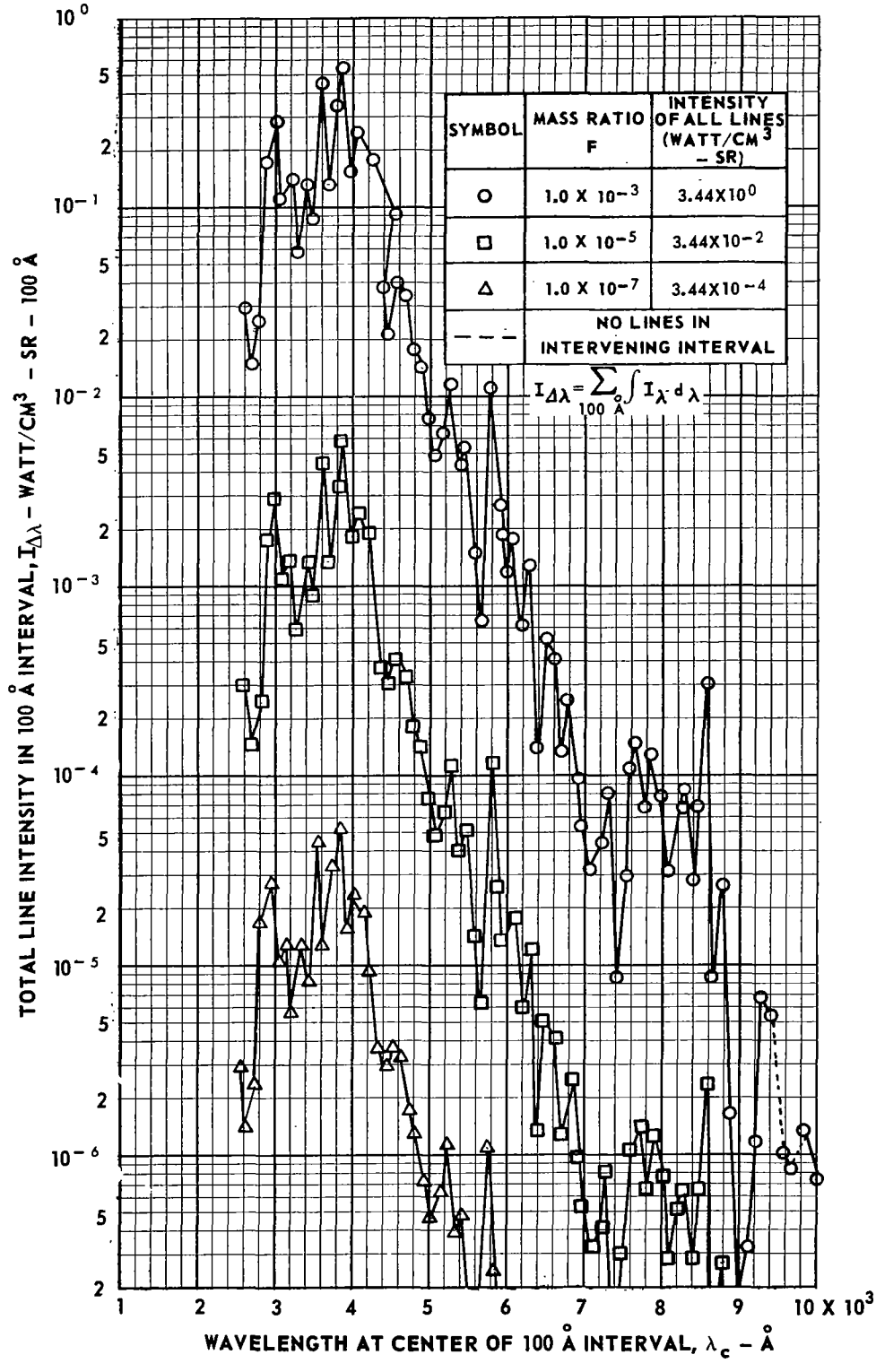

FIG. 48

TOTAL AND COMBINED LINE INTENSITY OF ARGON AND GASEOUS METALS IN ARGON – METAL HEXAFLUORIDE PLASMAS AS A FUNCTION OF TEMPERATURE FOR METAL TO ARGON MASS RATIO OF 10×10^{-3}

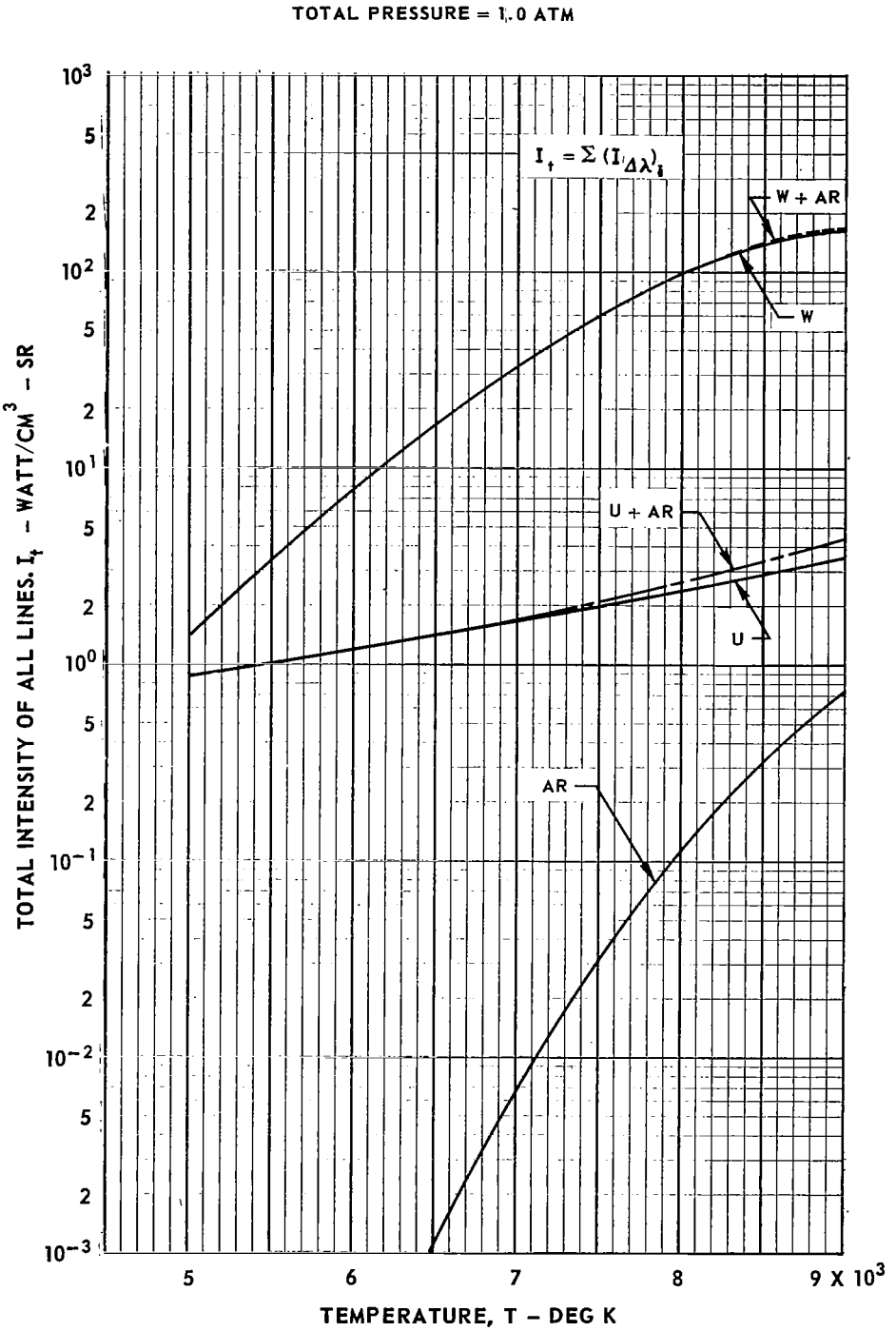

FIG. 49

TOTAL AND COMBINED LINE INTENSITY OF ARGON AND GASEOUS METALS IN ARGON – METAL HEXAFLUORIDE PLASMAS AS A FUNCTION OF TEMPERATURE FOR METAL TO ARGON MASS RATIO OF 1.0×10^{-5}

TOTAL PRESSURE = 1.0 ATM

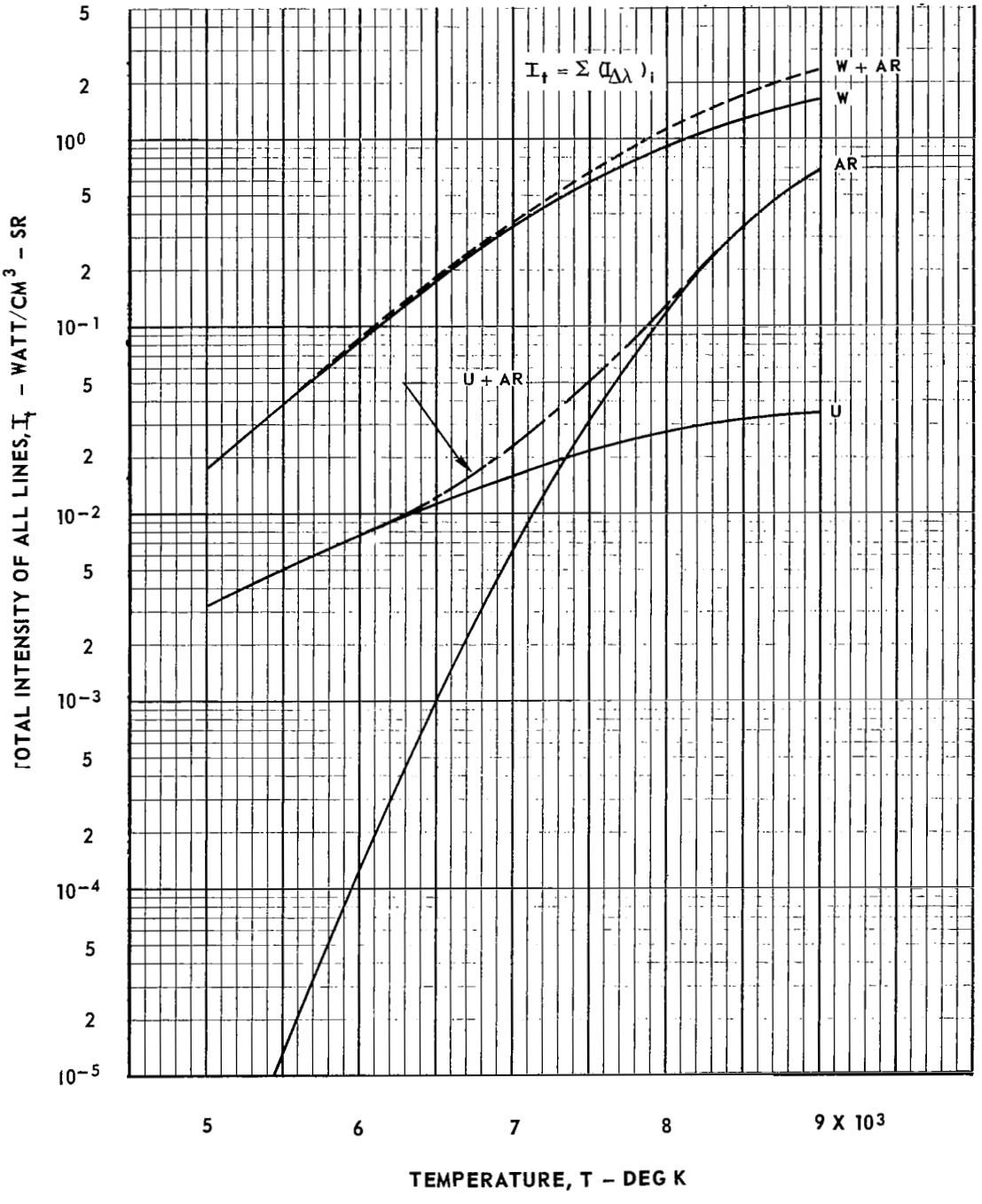

FIG. 50

TOTAL AND COMBINED LINE INTENSITY OF ARGON AND GASEOUS METALS IN ARGON – METAL HEXAFLUORIDE PLASMAS AS A FUNCTION OF TEMPERATURE FOR METAL TO ARGON MASS RATIO OF 1.0×10^{-7}

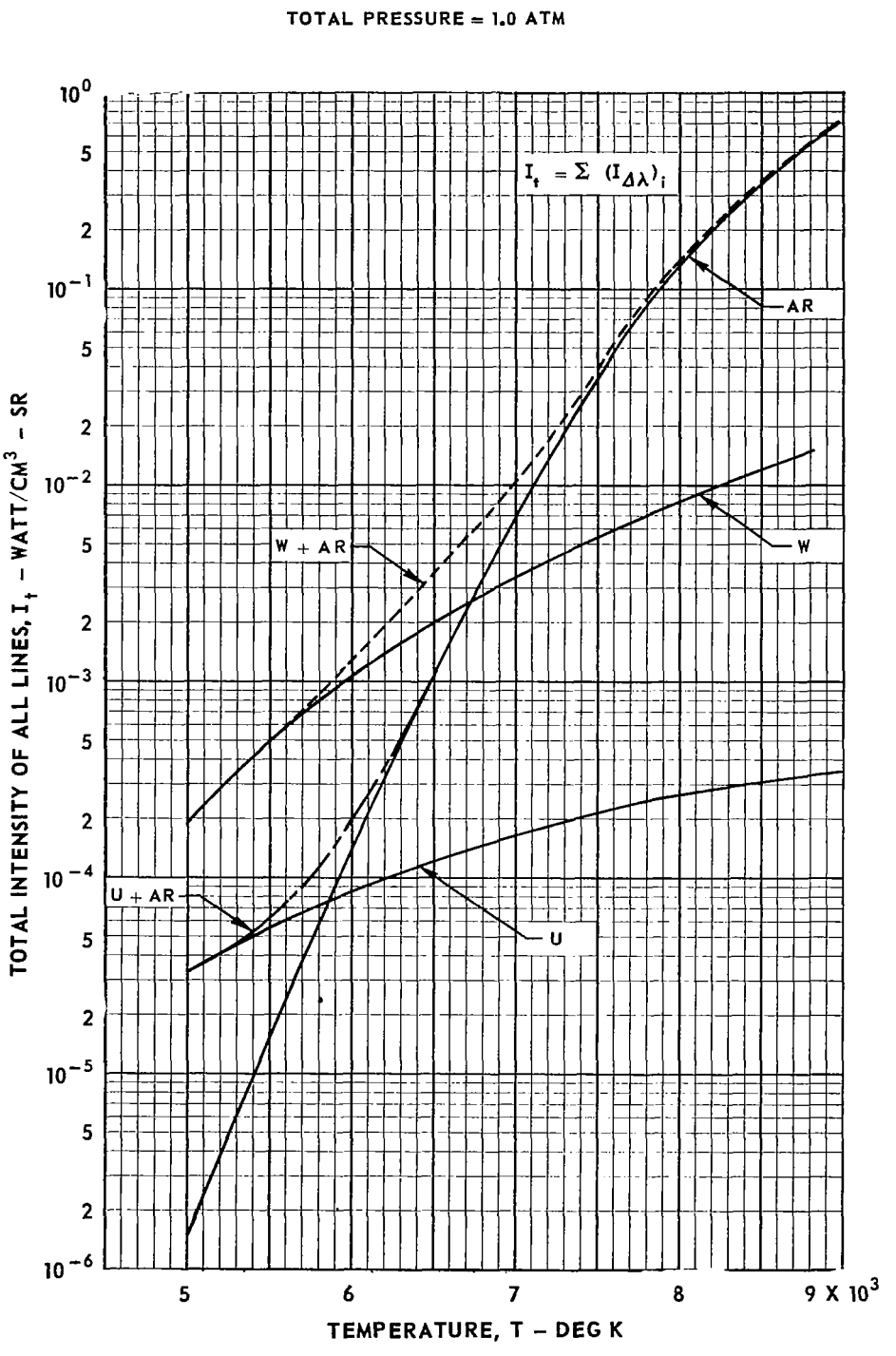

FIG. 51

INTENSITY OF A BLACK BODY IN WAVELENGTH INTERVALS OF 100 Å FOR VARIOUS TEMPERATURES

REF : 23

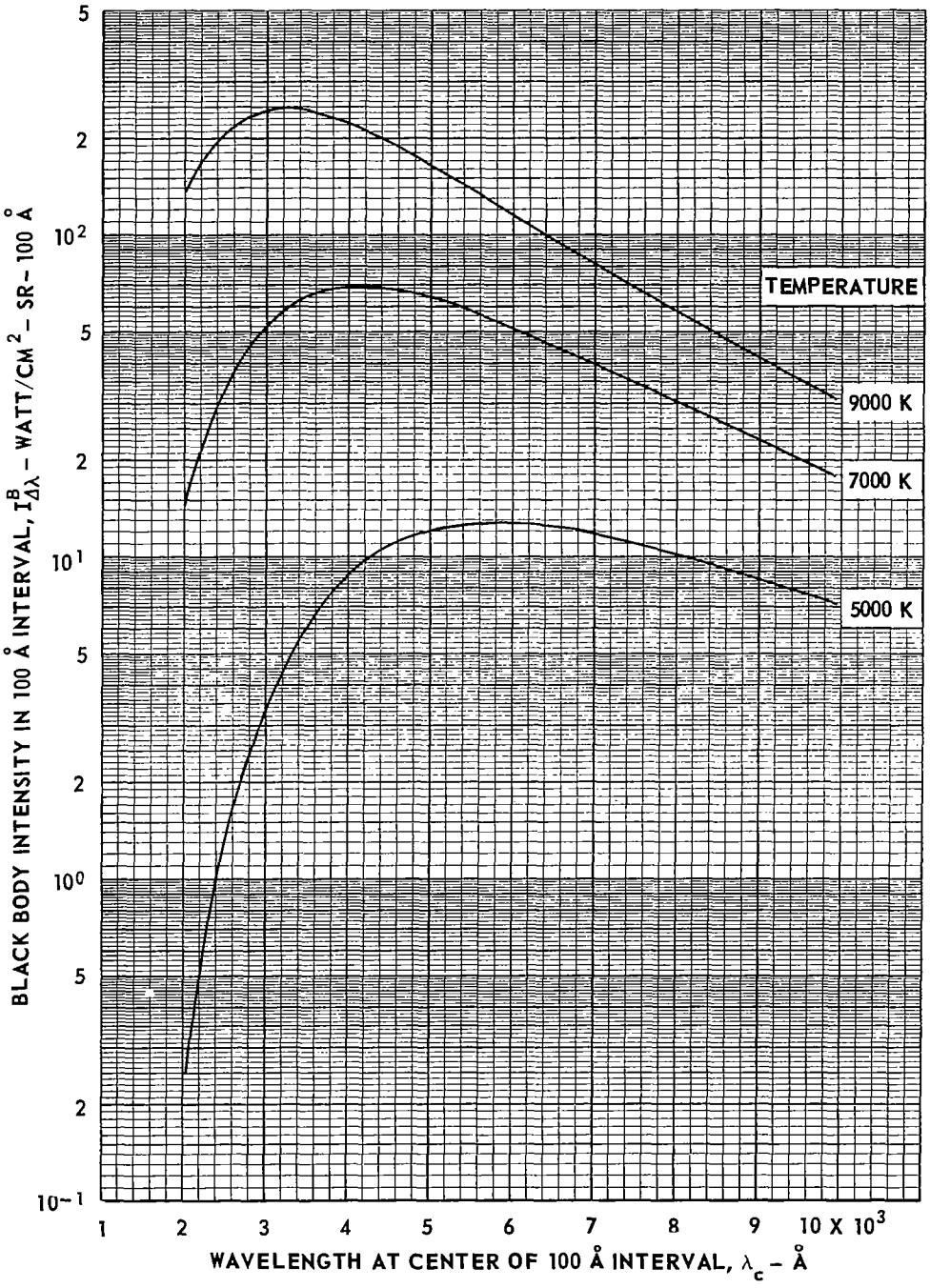

NASA-Langley, 1969 —— 25 CR-1313